Distributed Space-Time Coding including the Golden Code with Application in Cooperative Networks

by

Lu Ge

A doctoral thesis submitted in partial fulfilment of the requirements for the award of the degree of Doctor of Philosophy (PhD), at Loughborough University.

October 2014

Advanced Signal Processing Group,
School of Electronic, Electrical and Systems Engineering,
Loughborough University, Loughborough
Leicestershire, UK, LE11 3TU.

CERTIFICATE OF ORIGINALITY

This is to certify that I am responsible for the work submitted in this thesis, that the original work is my own except as specified in acknowledgements or in footnotes, and that neither the thesis nor the original work contained therein has been submitted to this or any other institution for a degree.

..... (Signed)

..... (candidate)

I dedicate this thesis to my loving parents.

Abstract

This thesis presents new methodologies to improve performance of wireless cooperative networks using the Golden Code. As a form of space-time coding, the Golden Code can achieve diversity-multiplexing tradeoff and the data rate can be twice that of the Alamouti code. In practice, however, asynchronism between relay nodes may reduce performance and channel quality can be degraded from certain antennas.

Firstly, a simple offset transmission scheme, which employs full interference cancellation (FIC) and orthogonal frequency division multiplexing (OFDM), is enhanced through the use of four relay nodes and receiver processing to mitigate asynchronism. Then, the potential reduction in diversity gain due to the dependent channel matrix elements in the distributed Golden Code transmission, and the rate penalty of multihop transmission, are mitigated by relay selection based on two-way transmission. The Golden Code is also implemented in an asynchronous one-way relay network over frequency flat and selective channels, and a simple approach to overcome asynchronism is proposed. In one-way communication with computationally efficient sphere decoding, the maximum of the channel parameter means is shown to achieve the best performance for the relay selection through bit error rate simulations.

Secondly, to reduce the cost of hardware when multiple antennas are available in a cooperative network, multi-antenna selection is exploited. In this context, maximum-sum transmit antenna selection is proposed. End-to-end signal-to-noise ratio (SNR) is calculated and outage probability analysis is performed when the links are modelled as Rayleigh fading frequency flat channels. The numerical results support the analysis and for a MIMO system

maximum-sum selection is shown to outperform maximum-minimum selection. Additionally, pairwise error probability (PEP) analysis is performed for maximum-sum transmit antenna selection with the Golden Code and the diversity order is obtained.

Finally, with the assumption of fibre-connected multiple antennas with finite buffers, multiple-antenna selection is implemented on the basis of maximum-sum antenna selection. Frequency flat Rayleigh fading channels are assumed together with a decode and forward transmission scheme. Outage probability analysis is performed by exploiting the steady-state stationarity of a Markov Chain model.

Contents

1 INTRODUCTION **1**

1.1 Multi-antenna Communications 1

1.2 Wireless Cooperative Networks 6

1.2.1 Relay Selection 8

1.2.2 Antenna Selection 8

1.3 Aim and Objectives of the Thesis 9

1.4 Thesis Outline 10

2 BACKGROUND **12**

2.1 Introduction 12

2.2 Point-to-point MIMO Wireless Networks 14

2.2.1 Alamouti Code in MIMO Systems 14

2.2.2 The Golden Code in MIMO Systems 17

2.2.3 Space-Time Coding in MIMO-OFDM Systems 19

2.2.4 Antenna Selection 24

2.3 Distributed MIMO systems in Cooperative Networks 27

2.3.1 Cooperative Strategies in Relay Networks 29

2.3.2 Distributed Relay Selection 34

2.4 Performance Analysis of Wireless Cooperative Networks 37

2.4.1 Pairwise Error Probability 37

2.4.2 Outage Probability 42

2.5 Summary 46

3 INCREASING DATA RATE IN ASYNCHRONOUS ONE-WAY AND TWO-WAY RELAY NETWORKS 48

3.1 Introduction 49

3.2 STBC Scheme with FIC for an Asynchronous Cooperative Four Relay Network 50

3.2.1 Interference Cancellation Scheme 55

3.2.2 Simulation Results 59

3.3 Two-way Distributed Relay Transmission Using the Golden Code 62

3.3.1 Overview of the Golden Code 62

3.3.2 Two-way Fixed Relay Scheme for the Golden Code 64

3.3.3 Discussion of Relay Selection for Two-Way Transmission of the Golden Code 68

3.3.4 Discussion of the DMT of the Golden Code 69

3.3.5 Simulation Results 70

3.4 Summary 73

4 RELAY SELECTION IN A DISTRIBUTED RELAY NETWORK USING THE GOLDEN CODE 75

4.1 Introduction 76

4.2 Relay Selection Based on the Golden Code in Synchronous Wireless Networks 80

4.2.1 Fixed Relay Scheme with the Golden Code 80

4.2.2 Maximum-likelihood Decoding and Sphere Decoding 82

4.2.3 Relay Selection with the Golden Code 85

4.2.4 Simulation Results 87

4.3 Transmission strategy of the Golden Code in coded MIMO-OFDM System 92

4.3.1 Channel Models 92

4.3.2 System Model 94
4.3.3 Channel Coding - Convolutional Code 98
4.3.4 Simulation Results 99
4.4 Relay Selection over Asynchronous Two-hop MIMO Relay Channels 100
4.4.1 System Model 100
4.4.2 A Relay Selection Scheme in Asynchronous Distribution System 106
4.4.3 Simulation Results 108
4.5 Summary 112

5 MULTI-ANTENNA SELECTION POLICIES USING THE GOLDEN CODE IN MIMO SYSTEMS 114
5.1 Introduction 114
5.2 System Model 116
5.3 Multi-antenna Selection with Outage Probability Analysis 118
5.3.1 Maximum-Minimum Selection 119
5.3.2 Maximum-Sum Selection 122
5.4 PEP Analysis of the Maximum-Sum Multi-Antenna Selection with the Golden Code 124
5.5 Simulation Results 127
5.6 Summary 130

6 BUFFER-AIDED DISTRIBUTED MULTI-ANTENNA SELECTION FOR COOPERATIVE NETWORKS 132
6.1 Introduction 133
6.2 System Model and Maximum-Sum DMA selection 136
6.2.1 System Model 136
6.2.2 Buffering Max-Sum Antenna Selection 137

6.3 Outage Performance Analysis Based Markov Chain Stationary Distribution 140
6.4 Simulation Results 146
6.5 Summary 148

7 CONCLUSIONS AND FUTURE WORK 150
7.1 Conclusions 150
7.2 Future Work 153

Statement of Originality

The contributions of this thesis are mainly on application of the Golden Code in cooperative networks. The novelty of the contributions is supported by the following international journal and conference papers.

In Chapter 3, a simple full interference cancellation (FIC) scheme and orthogonal frequency-division multiplexing (OFDM) are used in a two-hop cooperative four relay network with asynchronism in the second stage. Moreover, the Golden Code is used in two-way transmission over a wireless relay network in the fixed and selected relay cases. The results have been published in:

1. G. J. Chen, L. Ge and J. A. Chambers, 'Offset transmission scheme with full interference cancellation for an asynchronous cooperative four relay network', IEEE WiAd, London, UK, pp. 21 - 25, June 2011.

2. L. Ge, G. J. Chen, Y. Gong and J. A. Chambers, 'Two-way distributed transmission based on the Golden Code for application in wireless relay networks', 20th International Conference on Telecommunications (ICT), Casablanca, Morocco, pp. 1 - 5, May 2013.

In Chapter 4, the Golden Code is again exploited, and a strategy for relay selection, called the maximum-mean selection policy, is introduced. In addition, an effective scheme is proposed to achieve asynchronous distributed transmission with the Golden Code over a two-hop MIMO relay channel. The results have been published in:

3. L. Ge, G. J. Chen and J. A. Chambers, 'Relay selection in distributed transmission based on the Golden Code in wireless networks', 5th International Conference on Next Generation Mobile Applications, Services and Technologies (NGMAST), Cardiff, U.K., pp. 196 - 199, September 2011.

4. L. Ge, G. J. Chen and J. A. Chambers, 'Relay selection in distributed transmission based on the Golden Code using ML and sphere decoding in wireless networks', International Journal of Information Technology and Web Engineering (IJITWE), Vol. 6, No. 4, pp. 63 - 75, October-December 2011.

5. L. Ge, G. J. Chen and J. A. Chambers, 'The Golden Code in asynchronous distributed networks with relay selection', 2012 International Symposium on Wireless Communication Systems (ISWCS), Paris, France, pp. 701 - 705, August 2012.

In Chapter 5, transmit antenna selection and performance analysis for MIMO systems with the Golden Code are investigated. The results of this scheme are presented in:

6. L. Ge, G. J. Chen, Y. Gong, and J. A. Chambers, 'Performance analysis of multi-antenna selection policies using the Golden Code in MIMO systems', IET Communications, Vol. 8, No. 12, pp. 2147 - 2152, August 2014.

In Chapter 6, relay station with fiber-connected distributed multi-antenna (DMA) selection is investigated for reception and transmission with buffers in cooperative decode-and-forward (DF) MIMO systems. The results are published in:

7. L. Ge, G. J. Chen, Y. Gong, and J. A. Chambers, 'Max-sum buffer-aided distributed multi-antenna selection for cooperative diversity systems', in preparation.

Acknowledgements

This thesis would not have been possible were it not for the invaluable support of a group of people who have given far more support than I could possibly have asked for.

First and foremost, I would like to convey my utmost thanks to my supervisor, Prof. Jonathon Chambers, for his invaluable guidance, cordial advice and continuous encouragement throughout this research. His innovative ideas and engineering experience inspired me exceptionally as a young researcher. Also, I would particularly like to thank him for being so kind to me and making a friendly and comfortable environment during this entire research period.

I also would like to express my sincere gratitude to Professor Sangarapillai Lambotharan and my second supervisor Dr. Yu Gong for his assistance and invaluable support. Their passion in both research and life encouraged and inspired me. Again, I would like to thank them for their patience and kindness towards me.

I would also like to take this opportunity to thank my colleagues Dr Gaojie Chen, Yanfeng Liang and Zhao Tian in the Advanced Signal Processing Group for providing a stable and cooperative environment.

Most importantly, the biggest thanks of all go to my parents for their limitless love and never ending spiritual support, which motivated me to do my best throughout the period of my research abroad. I love you both very much.

Finally, I would like to thank everyone else who helped me to successfully realise this thesis.

List of Acronyms

AF	Amplify-and-Forward
AS	Antenna Selection
AWGN	Additive White Gaussian Noise
BER	Bit Error Rate
BS	Base Station
BPSK	Binary Phase Shift Keying
BRS	Best Relay Selection
CCU	Central Control Unit
CDF	Cumulative Distribution Function
CP	Cyclic Prefix
CSI	Channel State Information
DA	Distributed Antenna
DF	Decode-and-Forward
DFT	Discrete Fourier Transform
DMA	Distributed Multi-Antenna
DMT	Diversity and Multiplexing Tradeoff

DSTC	Distributed Space-Time Coding
FER	Frame Error Rate
FIC	Full Interference Cancellation
IDFT	Inverse Discrete Fourier Transform
IEEE	Institute of Electrical and Electronics Engineers
IFFT	Inverse Fast Fourier Transform
i.i.d.	independent and identically distributed
IRI	Inter-Relay Interference
MIMO	Multi-Input Multi-Output
ML	Maximum Likelihood
MMRS	Max-Max Relay Selection
MRC	Maximum Ratio Combiner
NAF	Non-orthogonal Amplify-and-Forward
ODSTC	Orthogonal Distributed Space-Time Code
OFDM	Orthogonal Frequency Division Multiplexing
PDF	Probability Density Function
PEP	Pairwise Error Probability
QAM	Quadrature Amplitude Modulation
QPSK	Quadrature Phase Shift Keying
QoS	Quality of Service
RF	Radio Frequency

RoF	Radio-over-Fibre
SD	Sphere Decoding
SIMO	Single-Input Multiple-Output
SISO	Single-Input Single-Output
SNR	Signal-to-Noise Ratio
STBC	Space-Time Block Coding
UE	User Equipment
WiFi	Wireless Fidelity
WiMax	Worldwide Interoperability for Microwave Access
ZF	Zero Forcing

List of Symbols

Scalar variables are denoted by plain lower-case letters, (i.e., x), vectors by bold-face lower-case letters, (i.e., $\mathbf{x}$), and matrices by upper-case bold-face letters, (i.e., $\mathbf{X}$). Some frequently used notations are as follows:

$\|.\|$	Absolute value
$\|\|.\|\|_2$	Euclidean norm
$\|\|.\|\|_F$	Frobenius norm
$(.)^T$	Transpose operator
$(.)^H$	Hermitian transpose operator
$(.)^\dagger$	Pseudo-inverse
Λ	Diagonal matrix
$diag(\mathbf{d})$	Diagonal matrix with the elements of vector $\boldsymbol{d}$ on its main diagonal
$E\{\cdot\}$	Statistical expectation operator
$\mathbf{I}$	Identity matrix
DFT(.)	Discrete Fourier Transform
IDFT(.)	Inverse Discrete Fourier Transform

List of Figures

1.1 Simplified block diagram of an $M \times N$ single stage MIMO system [1]. 2

1.2 The benefits of multi-antenna techniques for wireless communications [1]. 3

2.1 A 2×2 MIMO system showing the implementation of the Alamouti Code and maximum likelihood decoding [2]. 14

2.2 Alamouti Code v.s. Golden Code. 18

2.3 The basic baseband block diagram of a 2×2 MIMO-OFDM transceiver. 21

2.4 Bit error rate versus SNR of SISO-OFDM and MIMO-OFDM systems. 23

2.5 Frame error rate versus SNR of SISO-OFDM and MIMO-OFDM systems. 24

2.6 Receive antenna selection [3]. 26

2.7 Transmit antenna selection [3]. 26

2.8 Distributed MIMO system concept with mobile nodes cooperating to provide the link to the base station. 27

2.9 The model of source-relay-destination two-hop links in a DF relaying protocol. [4] 29

2.10 The model of source-relay-destination two-hop links in a AF relaying protocol. [4] 30

2.11 Example two-stage co-operative relay network [5]. 32

2.12 A basic wireless cooperative network with a direct link and single relay node. 43

3.1 An offset transmission model for a four relay network with asynchronism. 51

3.2 Architecture of the offset transmission relay network. 53

3.3 BER performance for no FIC and FIC approaches 60

3.4 End-to-end transmission rate 61

3.5 BER performance of the four relay with offset transmission and FIC and varying uncertainty in Assumption 1. 62

3.6 The transmitted rotated constellation of the Golden Code (4QAM) 63

3.7 The system model for the use of the Golden Code over a two-way distributed wireless network. (The solid line is the downlink from BS to UE and the dashed line is the uplink from UE to BS.) 65

3.8 Comparison of BER performances of uncoded and coded distributed Golden Code for one-way and two-way cases without relay selection. 71

3.9 Comparison of BER performances of coded distributed Golden Code for two-way transmission with max-minimum relay selection. 72

3.10 Comparison of BER performances of coded distributed Golden Code for two-way transmission with max-mean relay selection. 73

4.1 The two-input two-output relay network transmission structure for the Golden Code. 80

4.2 Relay selection scheme with the Golden Code in distributed wireless networks. 85

4.3 Bit error rate performances of the Golden Code in the MIMO system with the maximum-likelihood detection, the sphere detection and zero-forcing detection. 88

4.4 Bit error rate performances of the Golden Code in the distributed MIMO system with the different radii of the sphere decoding. 89

4.5 Bit error rate performances of maximum-minimum relay selection with Golden Code based transmission. 90

4.6 Bit error rate performances of maximum-mean relay selection with Golden Code based transmission. 91

4.7 Bit error rate performances of maximum-minimum strategy and maximum-mean strategy with Golden Code based transmission. 92

4.8 The coded MIMO-OFDM transceiver structure within the Golden Code. 95

4.9 Block diagram for a simple convolutional encoder. 98

4.10 The BER and FER performances of the Golden Code in uncoded and coded MIMO-OFDM. 99

4.11 Relay selection with the Golden Code in an asynchronous two-hop MIMO wireless network. 101

4.12 Block diagram of the transmission of the Golden Code in an asynchronous wireless network. 103

4.13 End-to-end BER performances of the Golden Code in the asynchronous distributed system with the maximum-likelihood detection and the sphere detection. 109

4.14 End-to-end bit error rate performances of no selection, maximum-minimum,maximum-mean relay selections and to deal with time delay without OFDM in asynchronous distributed system with the sphere detection. 110

4.15 End-to-end bit error rate performances of no selection, maximum-minimum and maximum-mean relay selections in asynchronous distributed system over frequency selective fading channel with the sphere detection. 111

4.16 Bit error rate performances of relay selections in asynchronous distributed system over flat fading channel and sparse frequency selective channel with the sphere detection. 112

5.1 The system model of antenna selection at the transmitter, i.e. the ith and jth Antenna are selected. 117

5.2 The outage probability for the maximum-minimum antenna selection in the Golden Code system. 128

5.3 The outage probability for the maximum-sum antenna selection in the Golden Code system. 129

5.4 The PEP for the maximum-sum antenna selection in the Golden Code system. 130

6.1 The system model of the distributed multi-antenna selection with buffers, i.e. the i-th and j-th antenna, are selected namely the best and the second best for reception and re-transmission. The fiber-connected DMAs use RoF to connect to the CCU. 136

6.2 State diagram of MC representing the states of the buffers and the transitions between them for a case with L =4, N=3. 142

6.3 The outage probability for a simulation with and without buffers, and theory of target rate R=1, 2 and 3bits/sec/Hz. 147

6.4 The outage probability for a simulation and theory of buffer size L=4, 10, 30 and 50. 148

6.5 The outage probability for a simulation and theory of participating available antennas N=3, 4 and 5. 149

List of Tables

6.1 Operation of the Max-Sum strategy for a given sequence with four distributed antennas $N = 4$. 139

Chapter 1

INTRODUCTION

1.1 Multi-antenna Communications

Conventional single-antenna transmission techniques operate in the time domain and/or in the frequency domain. Channel coding is typically employed, to overcome the detrimental effects of multipath fading. With the growing number of wireless services and concomitant demands on channel capacity, the antenna part of a radio system, and associated spatial processing is a topic of increasing importance. The great potential of using multiple antennas for wireless communications has become apparent during the last two decades. At the end of the 1990s multiple-antenna techniques were shown to provide a novel means to achieve both higher bit rates and smaller error rates. Altogether, multiple-antenna techniques thus constitute a key technology for modern wireless communications.

The general notion of a multiple-input multiple-output (MIMO) system or a MIMO network refers to an entire wireless system or network that contains a single or multiple MIMO links. MIMO wireless communications increases spectrum efficiency by spatial multiplexing and improves link reliability by antenna diversity [2] and [6]. A MIMO system has M transmit and N receive antennas. Its simplified block diagram is shown in Fig. 1.1. The input information bit sequence can be decomposed into block of M symbols represented by $\mathbf{s} = [s_1, s_2, \cdots, s_M]^T$ which are transmitted from M antennas. At the receiver the detection is over N receive antennas. Because the signals

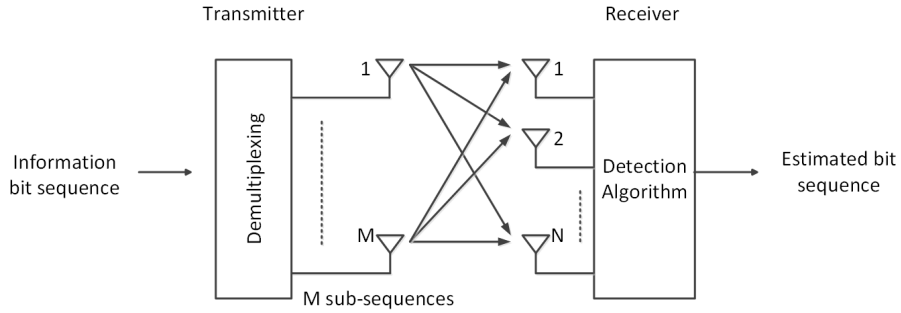

Figure 1.1. Simplified block diagram of an $M \times N$ single stage MIMO system [1].

go through the matrix channel, by adding the space dimension processing, a MIMO system can potentially improve the performance of past communication systems by exploiting the diversity introduced by the multiple spatial paths. Such point-to-point MIMO technology can provide spatial multiplexing gain, array gain and diversity technology within a system, each of which is described below.

The benefits of multiple antennas for wireless communication systems are summarized in Fig. 1.2.

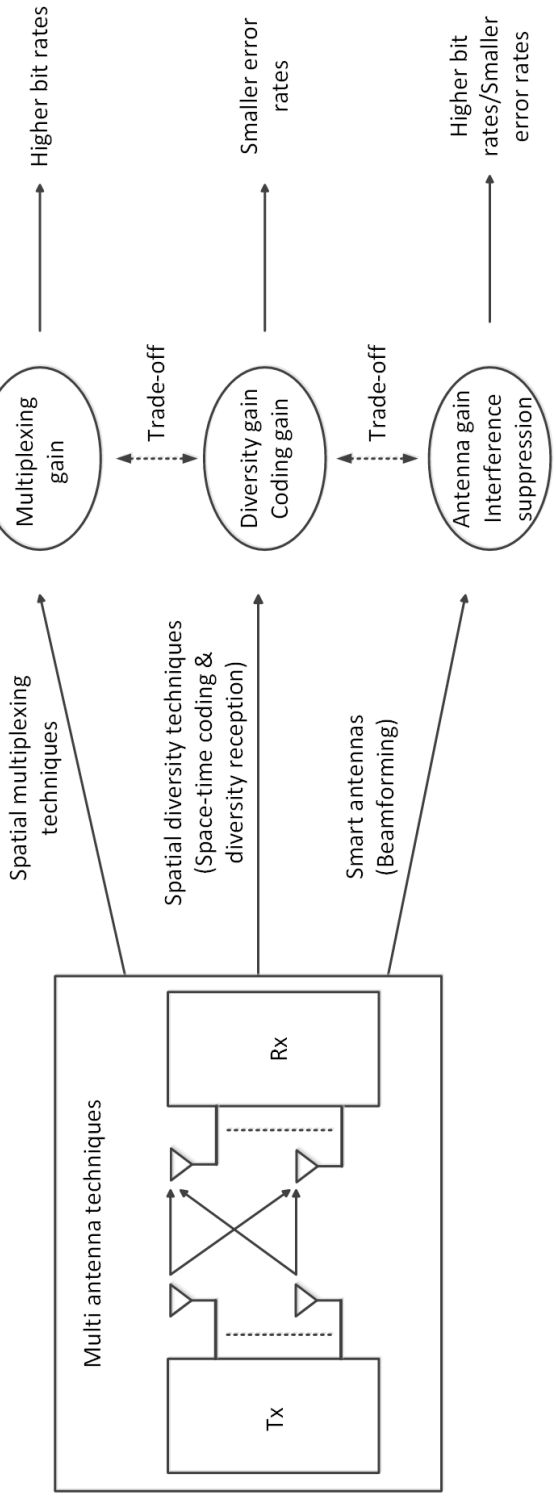

Figure 1.2. The benefits of multi-antenna techniques for wireless communications [1].

- **Spatial Diversity**

Multiple antennas can be used to improve the error rate of a system by transmitting and/or receiving redundant signals representing the same information sequence. This is similar to channel coding, and is achieved, by means of two-dimensional coding in time and space, commonly referred to as space-time coding, whereby the information sequence is spread out over multiple transmit antennas. At the receiver, combining of the redundant signals has to be performed to obtain diversity gain. As such, the diversity coding gain can be achieved as compared to single-antenna transmission. Example spatial diversity techniques for multi-transmit antenna systems are the Alamouti transmit diversity scheme [2] and the space-time trellis codes [7]. However, in this thesis space-time trellis codes will not be considered due to their increased complexity.

- **Spatial Multiplexing**

This consist of transmitting independent information sequences over multiple antennas. By using M transmit antennas, it boosts transmission rate by a factor of M, as compared with a single antenna scheme, and the transmit power per transmit antenna is lowered by a factor of 1/M. Spatial multiplexing gain can be realized by simply transmitting data layers from each of the transmit antennas, thus maximizing the average data rate over the MIMO system. It is an approach to increase throughput for high rate system operating at relatively high SNR. The zero-forcing (ZF) or minimum mean squared error (MMSE) decoding method is typically used at the receiver.

Foschini proposed the Bell-Labs layered space-time architecture (BLAST) and built a BLAST Multiuser MIMO system [8]. Assuming the same total transmitted power and the same bandwidth, the most striking advantage is that multiple antennas could offer considerable potential increase of the transmission rate [9]. This system will transform the transmission rate according to the number of antennas, and independently code each data

stream, by modulating and sending data separately from each transmit antennas. This is called spatial multiplexing. Strictly speaking, it is not based on transmit diversity, as the transmitted data are on the same frequency band, and signals are mixed. On the basis of the quality of estimated channel state information, the receiver can estimate the symbols from the different streams. However, in practice, spatial multiplexing is limited by the number of transmit and receive antennas in the system.

- **Beamforming**

In addition to higher bit rates and smaller error rates, multiple-antenna techniques can also be utilized to improve the signal-to-noise ratio (SNR) at the receiver and to suppress co-channel interference in a multiuser scenario. Using beamforming techniques, the beam patterns of the transmit and receive antenna arrays can be steered in certain desired directions [1]. Beamforming can be interpreted as linear filtering in the spatial domain. The SNR gains achieved by means of beamforming are often called antenna gains or array gains. Array gain is a classical feature of multi-antenna systems. It is important to make a clear distinction between array gain and diversity gains. Array gain is achieved through the coherent combining of the received signals from each antenna to improve the SNR of the array output signal. It can be achieved at the transmiter or receiver. Diversity gain on the other hand is increased average SNR due to transmission of the same signals over independently fading channel paths, and will be described in more detail in the next section.

- **Diversity-Multiplexing Trade-off**

Multi-antenna arrays have an important role to play in both improving the robustness of wireless transmission through spatial diversity and increasing the bit rate through spatial multiplexing. In recent years, there has been focus upon the trade-off between these two gains in the high SNR regime. The scaling behaviour of this diversity-multiplexing trade-off takes a particularly

simple form which will be described in detail in the next section.

In traditional communication networks data transmission directly occurs between the transmitter and the receiver. No user solicits the assistance of another one. However, in a general wireless communication network, there can be many intermediate nodes available to help in transmission.

1.2 Wireless Cooperative Networks

Cooperation relates to any architecture where a user's communication link is enhanced in a supportive way by relays or in a cooperative way by other users [10]. Compared with conventional MIMO systems, a cooperative network has different nodes which can share antennas, and thereby generate a virtual multiple antenna array (virtual MIMO) based on cooperation protocols [11] and [4]. For example in wireless networks, when one node broadcasts its messages, all nearby nodes overhear this transmission.

Cooperative communications yields several gains. In the following, three of them are introduced.

- **Diversity Gain**

Providing additional independent copies of the same information yields diversity gain. The gain is from the fact that with the amount of additional copies increasing, the probability of all of them being illegible decreases. The provision of such copies can be achieved, for example, by having a relay provide a copy in addition to the information received already via the direct link; or by having several relays provide copies in parallel. Diversity gain improves the performance of the system, such as the average error probability P_e or outage probability P_{out}. The diversity gain is defined as [10]

$$d = -\lim_{SNR\to\infty} \frac{\log P_{out}(R, SNR)}{\log SNR} \tag{1.2.1}$$

where $P_{out}(R, SNR)$ is in the Shannon sense at a given average SNR and

required rate R, and d is the diversity gain.

- **Multiplexing Gain**

The achievable transmission data rate R is known to be proportional to the logarithm of the SNR, that is [12]

$$r = \lim_{SNR \to \infty} \frac{R(SNR)}{\log SNR}, \tag{1.2.2}$$

where r is multiplexing gain and is equal to the degrees of freedom of the channel. It shows the actual rate changed of the system increases with SNR. In a system with M transmit and N receive antennas, the maximum number of independent channels under favorable propagation conditions is $r = \min(M, N)$.

- **Diversity-Multiplexing Trade-off**

The diversity-multiplexing trade-off (DMT) was first quantified in [13]. It describes the speed the probability of outage decreases and the communication rate increases with an increase in SNR. The DMT is applicable to any real world system operating over slow or fast fading channels, which allows one to trade reliability against rate. DMT is established for point-to-point multiple antenna slow fading channels in [12]. An important notion in wireless communications is determining whether the channel is slow or fast fading by related to the symbol duration T_s and the channel is coherence time T_c [14]. If $T_s < T_c$, the system undergoes slow fading. In the high SNR regime, it is equivalent to the gradient of the capacity or rate curves. Inserting (1.2.2) into equation (1.2.1) yields

$$d(r) = -\lim_{SNR \to \infty} \frac{\log P_{out}(r \log_2 SNR)}{\log SNR}. \tag{1.2.3}$$

This is the general DMT expression, which implies that increasing the rate multiplexing capabilities inherently requires the reliability of these rates to be decreased.

In this thesis, the Golden Code can achieve the DMT, therefore, in the next chapters, performance of cooperative multi-antenna system with the Golden Code will be particularly described.

1.2.1 Relay Selection

In cooperative wireless networks, using all the relays may not obtain the optimal end-to-end performance of a relay network because all the relays may compound practical problems such as synchronization between the relays. Improved performance can be potentially achieved by selecting the cooperating relays to employ. In particular, selection can aim to find the best relay for solving the problem of multiple relay transmission by requesting only a single relay forwards the information from the source [15]. Such relay selection must be repeated as the channel conditions will generally change in a wireless system. In [16], an example scheme was proposed for opportunistic relaying to exploit cooperative diversity. The scheme relies on distributed path selection considering the instantaneous end-to-end wireless channel conditions, and employs the maximum-minimum selection strategy.

1.2.2 Antenna Selection

Multiple antenna systems, however, need multiple radio-frequency (RF) chains associated with each antenna. A MIMO system, with M transmit and N receive antennas, requires M and N RF chains respectively. Each RF chain includes an analog-to-digital converter, down converters and low-noise amplifiers [17]. This leads to a considerable increase in the cost and complexity of implementing such systems and represents a major practical drawback. Receive antenna selection, therefore, selects a subset of antennas to feed to the RF chains. The selection algorithm is based on the SNR of the received signals. It benefits diversity but not spatial multiplexing. Both single transmit and single receive antenna selection are examined in [18].

The work in [19] proposed two joint relay-and-antenna selection schemes which combine opportunistic relaying and selection cooperation with a DF transmission policy.

1.3 Aim and Objectives of the Thesis

The overall aim of the study is to enhance the end-to-end performance of a wireless cooperative network. The particular objectives are:

- Objective 1: to increase the transmission rate when using the Golden Code

In Chapter 3, the Golden Code is used in two-way transmission over a wireless relay network in the fixed and selected relay cases. One of the properties of the Golden Code is the doubling of data rate as compared with early space-time coding based on the Alamouti code. Relay selection for the Golden Code is also presented to improve further the performance.

- Objective 2: to overcome asynchronism in the synchronous relay network when using the Golden Code

In Chapter 4, based on relay selection, orthogonal frequency division multiplexing is used to overcome a weakness of the Golden Code in losing its properties because of inter-symbol interference in frequency selective channel environments. Moreover, a simple approach to overcome asynchronism is used.

- Objective 3: to exploit multi-antenna selection in a multi-source multi-destination system using the Golden Code and to derive and verify the performance of Golden Code transmission when multi-antenna selection is employed

In Chapter 5, multi-antenna selection with Golden Code transmission is proposed, and a new max-sum multi-antenna selection policy is designed.

The PEP and outage probability of this system are derived.

- Objective 4: to propose Golden Code transmission with distributed multi-antenna selection

In Chapter 6, based on Chapter 5, a distributed multi-antenna system with the Golden Code is constructed. The max-sum multi-antenna selection is used on the two sides of the relay station. To enhance performance, buffers are exploited in each antenna in the relay station.

1.4 Thesis Outline

The outline of this thesis is as follows:

Chapter 1 introduces briefly conventional multi-antenna systems and wireless cooperative networks. The recent developments of relay selection and antenna selection are mentioned.

Chapter 2 firstly briefly overviews space-time coding, including the Alamouti code and the Golden Code in a conventional MIMO system and MIMO-OFDM. Based on a point-to-point MIMO system, antenna selection is considered. To overcome the drawbacks of conventional MIMO, a distributed MIMO system as a cooperative network with corresponding distributed relay selection is introduced. Then, the performance analysis of wireless cooperative networks is also briefly introduced.

Chapter 3 proposes a simple offset transmission with FIC and OFDM scheme for a four path asynchronous cooperative relay system. In order to achieve asymptotically full data rate the source and one group of relays transmits on even transmission steps, whilst on odd transmission steps, a different group of relays transmit and the first group receive. In order to mitigate the potential reduction in diversity gain due to dependent channel matrix elements in the distributed Golden Code transmission, and the rate penalty of multihop transmission, relay selection based on two-way trans-

mission is proposed.

In Chapter 4, distributed transmission by using the Golden Code in wireless relay networks, and a new multiple relay selection strategy, are proposed. The maximum of the channel parameter means selection is shown to achieve the best performance. On the other hand, the Golden Code is also implemented in an asynchronous wireless relay network over frequency flat and selective channels, and a simple approach to overcome asynchronism is proposed.

Chapter 5 examines the best two transmit antenna selection for the Golden Code in a MIMO system with instantaneous channel conditions by using maximum-minimum and maximum-sum selection. The outage probability, based on the different participating transmit antennas, and the outage events of antenna selection for a MIMO system using maximum-sum selection is shown to outperform the maximum-minimum selection. The PEP analysis is performed for maximum-sum transmit antenna selection within the Golden Code and the diversity order is obtained.

Chapter 6 realises fibre-connected distributed multi-antenna selection with finite buffers for cooperative wireless networks. Max-sum antenna selection was used with a DF scheme over Rayleigh fading channels. The state stationary property of a Markov Chain is to used analyse the outage probability performance of the system.

In Chapter 7, conclusions are drawn, and ideas for future work are given.

Chapter 2

BACKGROUND

2.1 Introduction

When developing new wireless systems, researchers are facing several challenges. Since the radio frequency spectrum is a limited resource, reducing the effect of multipath fading and multi-user interference, and improving the spectrum efficiency and link reliability are extremely important. In recent years, MIMO wireless communications techniques have emerged to increase the spectrum efficiency by spatial multiplexing and ensure link reliability by antenna diversity. Weakness is in this sort of system are inevitable. In practice, traditional point-to-point MIMO needs increased space at the transmitter or receiver to achieve uncorrelated spatial channels. Therefore, a new technology, distributed MIMO has been proposed. This approach is better for transmitting signals over long distances than distributed MIMO since path loss is reduced. As such, in cooperative wireless networks exploiting distributed MIMO improves link quality and increases coverage area. When increasing the number of users, co-channel interference will affect the quality of links. Mitigating such interference with interference cancellation is a subject of on-going research.

In recent years there has been considerable effort in the development of cooperative diversity schemes. The most important cooperative diversity schemes are amplify-and-forward (AF) and decode-and-forward (DF) approaches. For AF schemes, every relay cooperates and just retransmits its

received signal scaled by its own transmitted power. For most DF schemes, every relay decodes the transmitted information before retransmitting it using its transmit power [20]. However, using all the relays may not obtain the optimal performance of the relay network, and presents practical problems such as asynchronism between the relays. Improved performance can be potentially achieved by selecting the cooperating relays to employ. In particular, selection can aim to find the best relay for solving the problem of multiple relay transmission by requesting only a single relay or a subset of relays to forward the information from the source [21]. Best relay selection must be repeated as the channel conditions can change for each symbol block.

Multiple antenna systems, however, need multiple radio-frequency (RF) chains associated with each antenna. Each RF chain includes an analog-to-digital converter, down converter and a low-noise amplifier [3]. This leads to a considerable increase in the cost and complexity of implementing such systems and represents a major practical drawback. Antenna selection selects a subset of antennas to feed to the RF chains. The selection algorithm is typically based on the SNR of the received signals.

In this chapter, a brief overview of traditional MIMO and MIMO-OFDM with space-time coding will be given. To overcome the drawback of traditional MIMO, distributed MIMO with distributed space-time coding will be introduced. Relay selection and antenna selection will be presented as the methodologies to improve the performance of distributed MIMO. Finally, the Golden Code, which achieves the diversity-multiplexing tradeoff, and is the focus of this thesis will be introduced in this chapter.

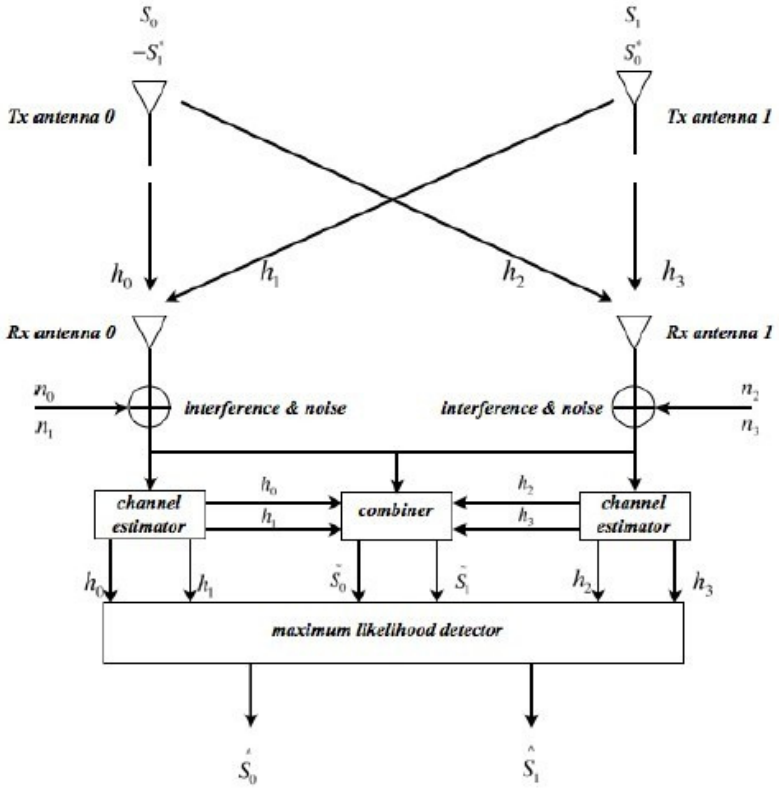

Figure 2.1. A 2×2 MIMO system showing the implementation of the Alamouti Code and maximum likelihood decoding [2].

2.2 Point-to-point MIMO Wireless Networks

2.2.1 Alamouti Code in MIMO Systems

Space-time block coding is a simple and smart coding scheme designed for transmit diversity in MIMO technology. The Alamouti space-time coding scheme is classical and important for understanding the principle of space-time block coding. It can be implemented with two transmit antennas and M receive antennas to provide a diversity order of 2M [2]. The core technique of the Alamouti scheme is providing full transmit diversity for the system.

The Alamouti transmit diversity scheme is next elaborated.

- **The encoding and transmission process**

In Fig.2.1, assuming that s_0 and s_1 are the generally complex modulated transmitted information symbols at the first time slot. Then $-s_1^*$ and s_0^* denote the complex signals transmitted at the second time slot. The matrix denoting the encoding is

$$\mathbf{S} = \begin{bmatrix} s_0 & s_1 \\ -s_1^* & s_0^* \end{bmatrix}, \tag{2.2.1}$$

where the rows denote the time slots and the columns the antennas. The channel parameters are denoted h_0, h_1, h_2 and h_3. Therefore, the received signals at two different antennas over two time periods are given by

$$\begin{cases} r_0 &= h_0 s_0 + h_1 s_1 + n_0 \\ r_1 &= -h_0 s_1^* + h_1 s_0^* + n_1 \\ r_2 &= h_2 s_0 + h_3 s_1 + n_2 \\ r_3 &= -h_2 s_1^* + h_3 s_0^* + n_3 \end{cases} \tag{2.2.2}$$

where n_0, n_1, n_2 and n_3 represent the additive white Gaussian noise (AWGN) and are independent and identically distributed (i.i.d.) complex Gaussian random variables with zero mean and power spectral density $N_0/2$ per dimension receiver noise. In practice, interference may be also included in n_0, n_1, n_2 and n_3. Equation (2.2.2) is rewritten in a matrix form as

$$\mathbf{y} = \mathbf{H}\mathbf{s} + \mathbf{n}. \tag{2.2.3}$$

where $\mathbf{n}$ is a complex Gaussian random vector with zero mean and covari-

ance matrix $N_0 \cdot \mathbf{I}_4$. The symbol vector $\mathbf{s} = [s_0 \;\; s_1]^T$ and $\mathbf{H} = \begin{bmatrix} h_0 & h_1 \\ h_1^* & -h_0^* \\ h_2 & h_3 \\ h_3^* & -h_2^* \end{bmatrix}$.

• **The combining scheme and maximum likelihood detector**

Because the channels h_0, h_1, h_2 and h_3 are assumed known, the received signals can be combined into two signals as $\widehat{s_0}$ and $\widehat{s_1}$ to be sent to the maximum likelihood detector:

$$\begin{aligned} \widehat{s_0} &= h_0^* r_0 + h_1 r_1^* + h_2^* r_2 + h_3 r_3^* \\ \widehat{s_1} &= h_1^* r_0 - h_0 r_1^* + h_3^* r_2 - h_2 r_3^*. \end{aligned} \tag{2.2.4}$$

To estimate the transmitted signals, the Alamouti scheme then uses the following maximum likelihood decision rule:

$$\widehat{\mathbf{s}} = \arg\min_{s \in S_c} \|\mathbf{y} - \mathbf{H}\mathbf{s}\|_2 \tag{2.2.5}$$

where $\|\cdot\|_2$ denotes the Euclidean norm and S_c is the set of all possible transmitted signal vectors from the source. The ML detection is therefore based on linear processing at the receiver. However, for space-time trellis coding, once the number of antennas is fixed, the decoding complexity (measured by the number of trellis states at the decoder) increases exponentially as a function of the diversity level and transmission rate [22]. The reduced computational cost of the Alamouti scheme explains why the scheme is so widely used, and why space time trellis coding is not considered further in the thesis.

2.2.2 The Golden Code in MIMO Systems

The Golden Code was proposed in 2004 [23], which is a full rate and full diversity 2×2 linear dispersion algebraic space-time block code that has a maximal coding gain for a two transmit antenna and two or more receive antenna MIMO system [23]. Due to the performance of the algebraic construction, the Golden Code outperforms the Alamouti code in flat fading channels. However, in frequency selective channels environment, the Golden Code loses its properties because of the inter-symbol interference (ISI) [24]. To overcome this weakness, orthogonal frequency division multiplexing (OFDM) modulation can be used and channel coding can also be adopted to improve the performance of the Golden Code in a MIMO system in the later Chapter 4.

The essence of the code is the Golden Number $\theta = \frac{1+\sqrt{5}}{2}$ which is used to generate the best performance [23]. The codeword is of the form

$$\mathbf{C} = \frac{1}{\sqrt{5}} \begin{bmatrix} \alpha(a+b\theta) & \alpha(c+d\theta) \\ \gamma\overline{\alpha}(c+d\overline{\theta}) & \overline{\alpha}(a+b\overline{\theta}) \end{bmatrix} = \frac{1}{\sqrt{5}} \begin{bmatrix} s_1 & s_2 \\ s_3 & s_4 \end{bmatrix}, \tag{2.2.6}$$

where a, b, c, d are drawn from the information symbol constellation from quadrature amplitude modulation (M-QAM); $\theta = \frac{1+\sqrt{5}}{2}$, $\overline{\theta} = \frac{1-\sqrt{5}}{2}$, $\alpha = 1 + i(1-\theta)$ and $\overline{\alpha} = 1 + i(1-\overline{\theta})$, where $i \triangleq \sqrt{-1}$. To avoid vanishing determinants, the factor $|\gamma|$ is set as unity, which guarantees that the same average power is transmitted from each antenna at each channel use [23]. The non-vanishing determinant can increase the rate. In this code matrix (2.2.6), the four degrees of freedom of the system are used, which allows four information symbols to be sent. The minimum determinant of the Golden Code is 1/5. The spectral efficiency is $2\log_2(M) bits/s/Hz$. For the Golden Code, the elements of the codeword matrix are from the information symbol constellation. The constellation of the Golden Code is

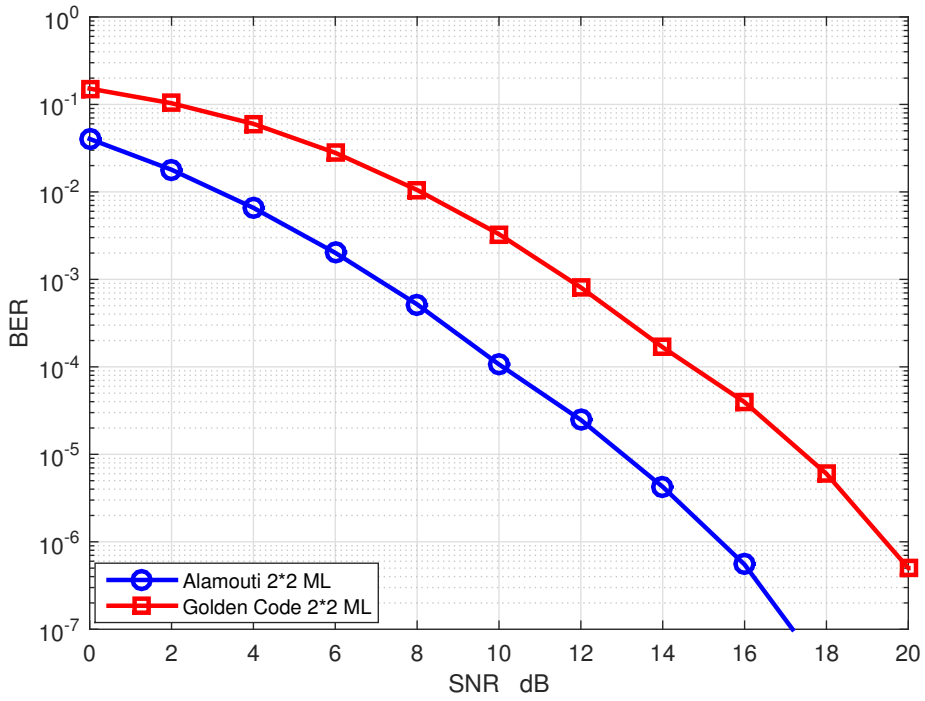

Figure 2.2. Alamouti Code v.s. Golden Code.

a rotated regular quadrature amplitude modulation (QAM) constellation. The diversity-multiplexing tradeoff is an essential tradeoff between the error probability and the data rate of a system. The Golden Code can achieve optimal diversity-multiplexing tradeoff for a 2×2 MIMO system [23]. Due to obtaining simultaneously both diversity and multiplexing gain, the Golden Code scheme is "Perfect". Several decoding strategies for Golden Codes have been studied, such as full maximum-likelihood and sphere decoding [25]. Fig. 2.2 shows the performances comparison of 2×2 Alamouti and the Golden Code with the maximum-likelihood detection. Although the bit error rate performance of the Golden Code is worse than Alamouti code, the transmit rate of the Golden Code is two times faster than Alamouti code. In Chapter 4, the sphere decoding will be introduced.

2.2.3 Space-Time Coding in MIMO-OFDM Systems

The orthogonal frequency-division multiplexing (OFDM) transmission scheme is another type of multichannel system and employs multiple subcarriers [26]. In OFDM, the entire channel is divided into many narrow parallel subchannels, thereby increasing the symbol duration in each sub-channel and eliminating inter-symbol interference (ISI) caused by the multipath. Therefore, OFDM has been used in digital audio and video broadcasting in Europe [27], and is a promising choice for future high-data-rate wireless systems. The multiple orthogonal subcarrier signals are overlapped in spectrum and can be produced by generalizing the single-carrier Nyquist criterion into the multicarrier criterion [26]. The discrete Fourier transform (DFT) and inverse DFT (IDFT) operations are useful for implementing these orthogonal signals. Combining with the characteristics of the MIMO channel, multiple transmit and receive antennas can be used with OFDM to further improve system performance, carrier frequency synchronization between the transmitter and receiver is very important. The main advantage of OFDM is that it converts a frequency-selective channel into a set of parallel flat fading subchannels, therefore, reducing the equalization and demodulation complexity at the receiver [28]. Consider an OFDM communication system using M transmit antennas and N receive antennas. Such a system could be implemented using a single space-time encoder employing a code for transmit antennas. In this case, the space-time encoder takes a single stream of binary input data and transforms it into parallel streams of baseband constellation symbols.

Fig.2.3 shows the block of 2×2 MIMO-OFDM transceiver. The frequency selective fading channel between the μ-th transmit antenna and the υ-th receive antenna is represented by the vector of impulse response coefficients $\mathbf{h}^{\nu,\mu} = [h_0^{\nu,\mu} \cdots h_L^{\nu,\mu}]^T$ with L denoting the channel order. The symbol transmitted on the p-th subcarrier from the μ-th transmit antenna during

the n-th OFDM symbol interval is represented as $x_n^{\mu}(p)$. These symbols are transmitted in parallel through the N_c subcarriers by N_t transmit antenna, where p is the frequency index of each transmitted symbol. Note that DFT and IDFT can be implemented efficiently by using fast Fourier transform (FFT) and inverse FFT (IFFT). The OFDM system inserts a guard interval cyclic prefix (CP) in the time domain to mitigate the inter-symbol interference (ISI) between adjacent OFDM symbols [26].

The received signal after CP removal and FFT processing at the v-th receive antenna can be expressed as

$$y_n^{\nu}(p) = \sum_{\mu=1}^{N_t} H^{(\nu,\mu)}(p) x_n^{\mu}(p) + \omega_n^{\nu}(p), \tag{2.2.7}$$

where $H^{(\nu,\mu)}$ is the subchannel transfer function from the μth transmit antenna to the vth receive antenna, and $\omega_n^{v}(p)$ is the AWGN which is assumed to be statistically independent across time, space and subcarriers.

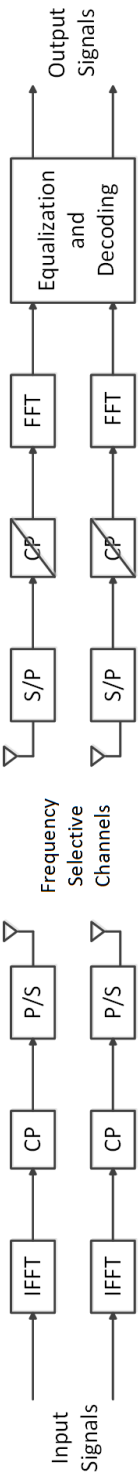

Figure 2.3. The basic baseband block diagram of a 2×2 MIMO-OFDM transceiver.

The MIMO-OFDM system operation in the frequency-domain can be expressed in vector form as:

$$\mathbf{y}_n^{\nu} = \sum_{\mu=1}^{N_t} \mathbf{D}^{(\nu,\mu)} \mathbf{x}_n^{\mu} + \mathbf{w}_n^{\nu}, \tag{2.2.8}$$

where $\mathbf{D}^{(\nu,\mu)} = diag[H^{(\nu,\mu)}(1) \cdots H^{(\nu,\mu)}(N_c)]$. According to (2.2.8), the received MIMO-OFDM blocks are expressed as the superposition of single antenna OFDM blocks.

At the receiver, the corresponding decoders developed for flat-fading channels are implemented again on a per subcarrier basis. Thus, the main advantage of the space-time OFDM transceiver with block-orthogonal ST codes per subcarrier is its low complexity and it can operate even for channels with large order L [28] although the transmission efficiency will be affected by the increased length of the CP. However, if there is no coding across subcarriers, the full diversity is not exploited [28]. In the following, the performance of MIMO-OFDM with the Alamouti code will be presented.

In Fig. 2.4, it shows the simulated performances of SISO-OFDM and 2×2MIMO-OFDM. The transmitter sends quadrature phase-shift keying (QPSK) symbols to the destination. The OFDM block length is $N = 64$, and the length of the cyclic prefix is 16. Moreover, the channel length is 4, and channel state information (CSI) is assumed to be perfectly known at the destination node. Full maximum-likelihood detection is used at the receiver. Obviously, the diversity gain is increasing and the slope of bit error rate (BER) curve is increasing. For the signal-noise ratio (SNR) region from 0 dB to 30 dB, each value of BER using MIMO-OFDM is smaller than using SISO-OFDM. i.e. when SNR equals to 15dB, the BER of SISO-OFDM is just at the value of $10^{-1.8}$. Comparing with MIMO-OFDM in the same case, the BER value approximately reach is 10^{-3}. Thus, at the same SNR, the performance of MIMO-OFDM outperforms SISO-OFDM. Therefore, diver-

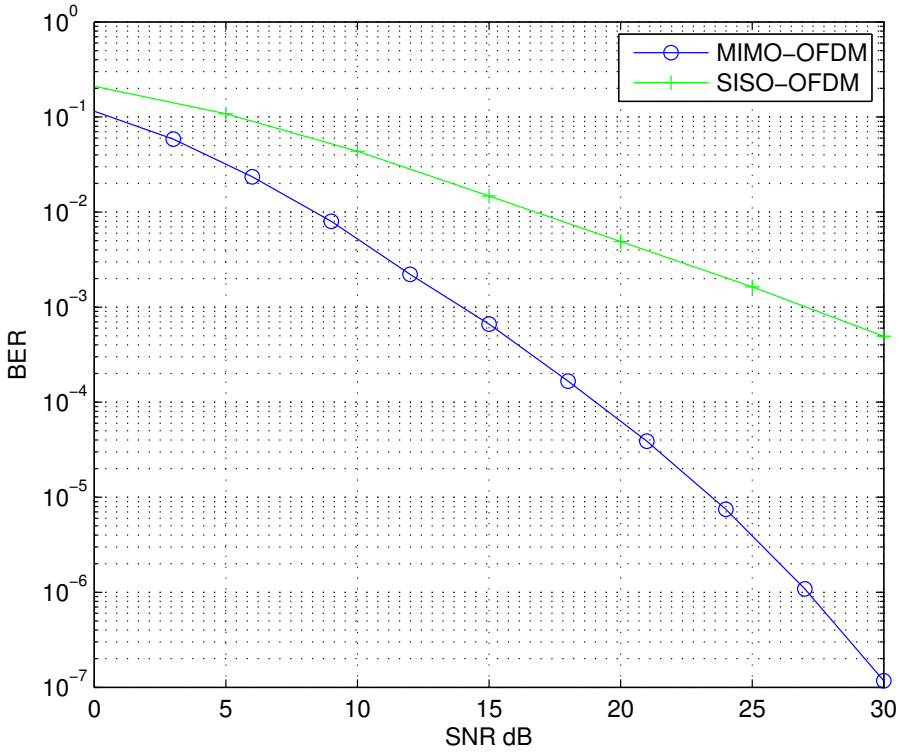

Figure 2.4. Bit error rate versus SNR of SISO-OFDM and MIMO-OFDM systems.

sity gain can mitigate the channel fading and increase the total resistance to co-channel interference, and thereby improve the effectiveness of the link.

Then, the same approach and same assumptions are applied to simulate the frame error rate (FER) of SISO-OFDM and MIMO-OFDM, results of which are shown in Fig. 2.5. The total frame number for both systems is 1500. It is easy to see the FER of SISO-OFDM is worse than for MIMO-OFDM with increasing SNR. Once there is one bit error in a frame, the frame is incorrect. The per frame error trend can be decided from the trend of BER in these two systems. Moreover, the number of error frames in SISO-OFDM is more than for MIMO-OFDM. For example, for the range 5 dB to approximately 14 dB SNR, the frame error rates of SISO-OFDM always equal to 1 and the curve decreases after 14 dB. From about 12 dB,

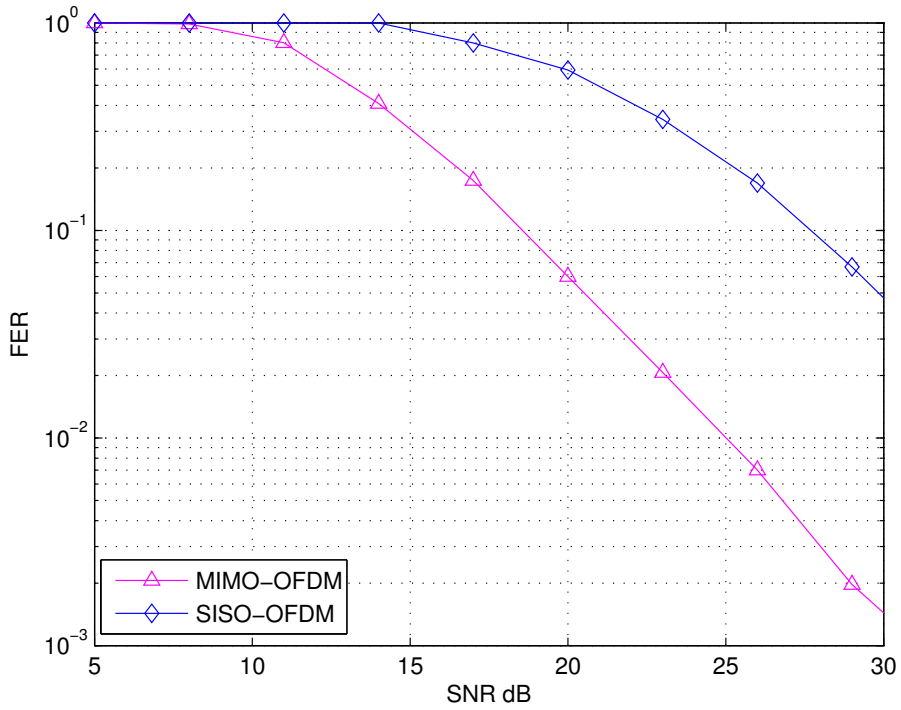

Figure 2.5. Frame error rate versus SNR of SISO-OFDM and MIMO-OFDM systems.

the curve of MIMO-OFDM starts to decrease and the slope is larger than for SISO-OFDM. Note, SNR could easily be replaced by E_s/N_0, and there would be a simple shift of 3 dB for QPSK.

2.2.4 Antenna Selection

Multiple-antenna systems, such as MIMO, can improve the capacity and reliability of radio communication. Although many benefits of multi-antenna systems have been verified, the deployment of multiple antennas requires multiple RF chains. These RF chains include multiple analog-digital converters, low noise amplifiers, and downconverters, whose high cost is undesirable especially for mobile handsets. Antenna sub-set selection where transmission is performed through a sub-set of the available antenna elements is a cost-effective solution [17], [29]. Thus employing a reduced number of RF

chains at the receiver and attempting to allocate optimally each chain to one of a larger number of receive antennas was proposed. In this case only the best set of antennas is used, while the remaining antennas are not employed, thus reducing the number of required RF chains. Thus, antenna selection is a low-cost low-complexity alternative to capture many of the advantages of MIMO systems. In antenna selection, a subset of the available antenna elements is adaptively chosen by a switch, and only signals from the chosen subset are processed further by the available RF chains [30]. Antenna selection has received considerable attention recently. It has been considered at the transmitter called transmit antenna selection (TAS), at the receiver it is called receive antenna selection (RAS), and at both the transmitter and the receiver is transmit and receive antenna selection (T-RAS). Its performance has been explored in terms of capacity and outage for spatial multiplexing systems, and diversity order and array gain for space-time coded systems [31]. The selection criteria of receive antenna selection or transmit antenna selection have been presented to minimise the error probability or maximise the capacity bounds based on the instantaneous CSI at the transmitter [32].

- **Receive Antenna Selection**

Diversity of multiple receive antennas is a direct extension of traditional receive diversity ideas. Selection diversity chooses the path with the highest SNR, and performs detection based on the signal from the selected path. Maximal ratio combining (MRC) makes decisions based on an optimal linear combination of the path signals. The application of the selection to receive antenna selection is shown in Fig. 2.6, in which a single receive antenna is chosen from among all available antennas. To know all SNRs simultaneously for optimal selection is based on the quasi-stationarity assumption for the channel gains. For example, one may use a training signal in a preamble to the information data. During this preamble, the receiver scans the antennas,

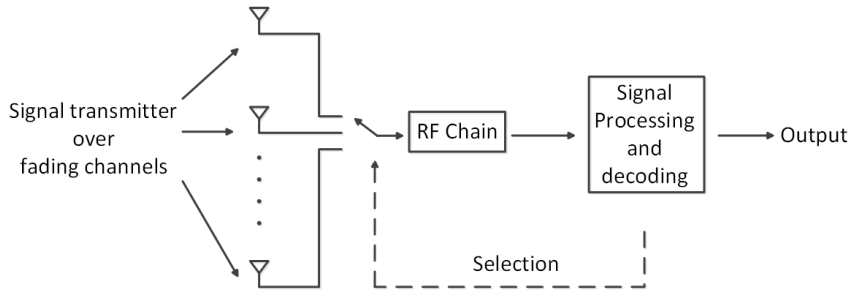

Figure 2.6. Receive antenna selection [3].

finds the antenna with the highest channel gain, and selects it for receiving the next data burst.

- **Transmit Antenna Selection**

Transmit antenna selection, unlike receive selection, requires a feedback

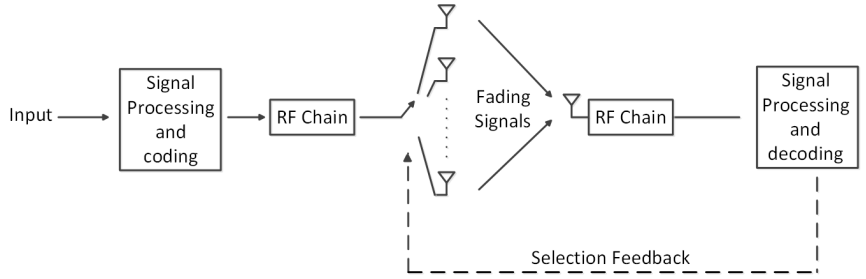

Figure 2.7. Transmit antenna selection [3].

path from the receiver to the transmitter as shown in Fig. 2.7. This feedback rate is rather small, especially for single antenna selection. It gives the transmitter some information about the state of the channel. Aside from that difference, however, transmit antenna selection is very similar to receive antenna selection; the antenna is selected that provides the highest equivalent receive SNR. In [33], the implementation of TAS is for secure transmission in the MIMO wiretap channel with low feedback which only selects only one antenna at the transmitter. In the thesis, the later Chapter

5 and Chapter 6 will consider multi-transmit antenna selection in distributed MIMO systems.

2.3 Distributed MIMO systems in Cooperative Networks

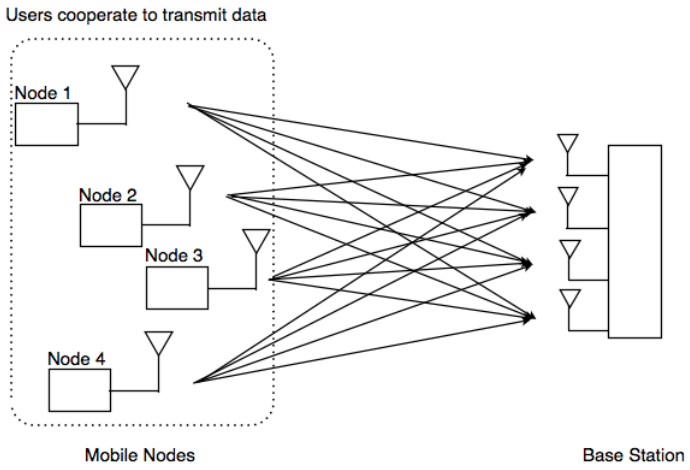

Figure 2.8. Distributed MIMO system concept with mobile nodes cooperating to provide the link to the base station.

MIMO wireless communications technologies can increase the spectrum efficiency by spatial multiplexing and ensure the reliability of the link by exploiting antenna diversity. Using diversity techniques for mitigating, even exploiting, multipath fading is central to improving the performance of wireless communication systems and networks [34]. The approach of distributed antennas can facilitate the applicability of MIMO techniques to a small terminal. In wireless telecommunication systems, large distances and obstacles in the practical environment cause path loss, and moving in a multipath environment can produce serious signal fading. There may be no direct link between the transmitter and receiver due to shadowing. The channels are typically modelled as Rayleigh flat fading and the channel parameters are

assumed not to change during transmitting one symbol, i.e. a quasi-static assumption. That is the transmitting method may be block-by-block. The channel parameters can therefore be changed after transmitting every block. A distributed MIMO scheme is therefore both useful and applicable. Cooperation is referred to as any architecture that deviates from the traditional point-to-point approach, that is a user's communication link is enhanced in a supportive way by relays or in a cooperative way by other users. For overcoming the space limitation of point-to-point MIMO, distributed MIMO systems have been proposed to realize point-to-point MIMO like performance in fading channels. The distributed MIMO system concept is represented in Fig.2.8. A mobile user is represented by a mobile node. The single antenna terminals act cooperatively to transmit data.

In recent years there has been considerable effort in the development of cooperative diversity schemes [4]. A variety of cooperative schemes has been proposed. Among these strategies, perhaps the most important are the amplify-and-forward (AF) and decode-and-forward (DF) approaches. For AF schemes, every relay cooperates and just retransmits its received signal scaled by its own transmitted power. For most DF schemes, every relay decodes the transmitted information before retransmitting it using its transmit power [20], and therefore provide increased complexity.

In previously proposed cooperative diversity schemes, it has been assumed that coordination among the relays allows for accurate symbol-level timing synchronization at the destination and orthogonal channel allocation, which can be quite costly in terms of signaling overhead in mobile ad hoc networks, which are often defined by their lack of a fixed infrastructure and the difficulty of centralized control [35]. While all full diversity achieving space-time codes for MIMO systems achieve full spatial diversity for synchronous cooperative systems, few of them do so for asynchronous cooperative systems [36]. There have been some studies on space-time coding to

achieve asynchronous cooperative diversity, for example, [35] and [37]. Most of them use the decode-and-forward approach. Distributed space-time coding in synchronous wireless networks is therefore extended to asynchronous wireless networks using an amplify-and-forward approach in this thesis.

The topic of the thesis on cooperative networks has also attracted a large amount of attention in industry. Cooperative relaying has been proposed in the IEEE 802.16j mobile multihop relay standard [38]. Meanwhile, many coordinated multicell space-frequency codes have been suggested in the third generation partnership project long term evolution (3GPP LTE) [38].

2.3.1 Cooperative Strategies in Relay Networks

Relay protocols affect the system performance in cooperative wireless networks. In this section, an overview of traditional relay protocols, decode-and-forward (DF) and amplify-and-forward (AF) is presented.

- **Decode-and-Forward Relay Protocol (DF)**

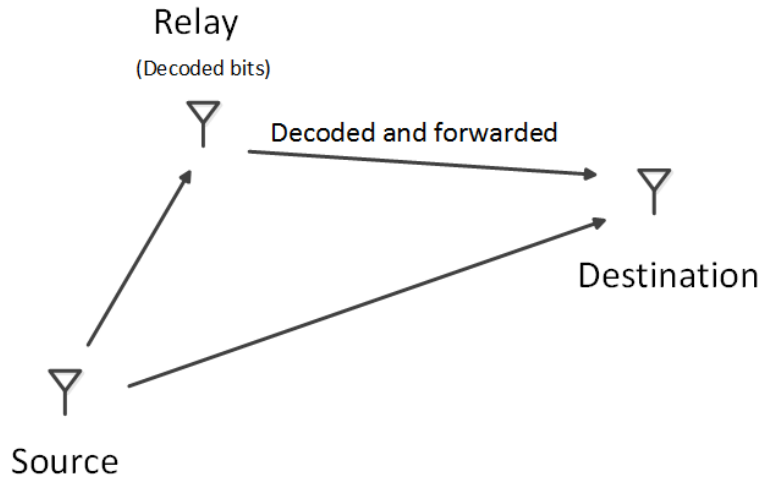

Figure 2.9. The model of source-relay-destination two-hop links in a DF relaying protocol. [4]

Fig. 2.9 is a simple representation of the decode-and-forward (DF) protocol. In this figure, the middle point is a mobile relay node which first decodes the received signals and then forwards the re-encoded signals to the destination. The decoding can be done fully at the bit level or partially at the symbol level. When the channel between the source and the relay is of good quality, DF provides error correlation capability and is then superior to amplify-and-forward (AF) [39]. However, when the channel link suffers from deep fading, the decoding could produce errors. On the other hands, although DF cannot provide full diversity by itself, it can achieve full diversity when complex codes are applied at the relays.

- **Amplify-and-Forward Relay Protocol (AF)**

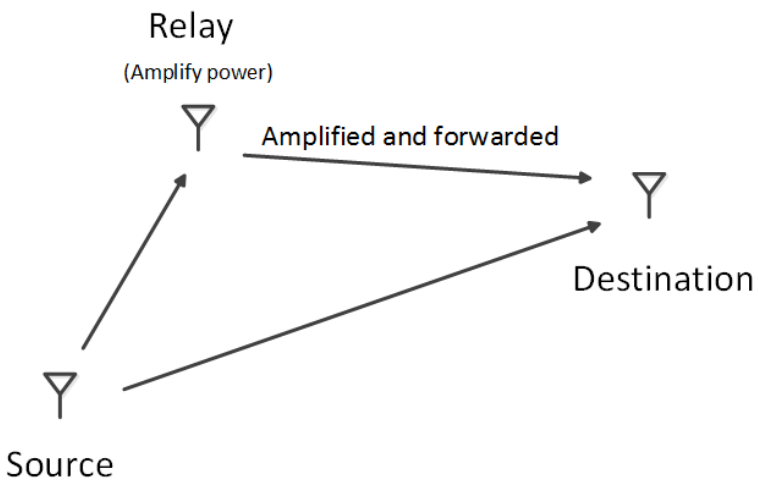

Figure 2.10. The model of source-relay-destination two-hop links in a AF relaying protocol. [4]

In the amplify-and-forward (AF) protocol, as represented in Fig. 2.10. The source broadcasts the signals to the relay and the destination. The relay amplifies the received noisy signals and forwards to the destination with transmitted power of the relay. In terms of details of the algorithm, the

source node sends the signal vector $\mathbf{x}_s$ and the relays receive signal $\mathbf{y}_r$. The relay will send the signal that is like:

$$\mathbf{x}_r = \beta_r \mathbf{y}_r \tag{2.3.1}$$

where β_r is the gain to amplify the relay given its power constraint

$$\beta_r \leq \sqrt{\frac{P_s}{|A_r|^2 P_r + N_0}}, \tag{2.3.2}$$

and the gain depends on A_r which is a channel fading coefficient between the source and relay.

After that, the destination node obtains the signal $\mathbf{y}_d$ from relays. However, the destination must know the channel coefficients to perform optimal coding with amplify and relay processing. Therefore, AF is a simple method that lends itself to analysis, and has been very useful in furthering understanding of a cooperative communication system [4].

• **Distributed Space-Time Coding**

Space-time coding can be applied to a relay network to achieve cooperative diversity [40]. This coding method is similar to a point-to-point MIMO system. In a distributed MIMO system, distributed space-time block coding (DSTBC) is extended to networks with multiple-antenna nodes. So, designing a DSTBC is the most important aspect for this system. It will successfully lead to realizing cooperation communication in wireless relay networks. As shown in Fig. 2.11, this is an R-relay wireless relay network model, which means the maximal diversity is R. One relay transmission procedure from source S to receiver X can be divided into two steps. In step one, the source broadcasts the signal to the relays, and in the second step relays the signals from the relays to the receiver. Through the use of R relays a linear space-time codeword is generated at the receiver.

The channels are assumed to be Rayleigh flat fading with coefficients

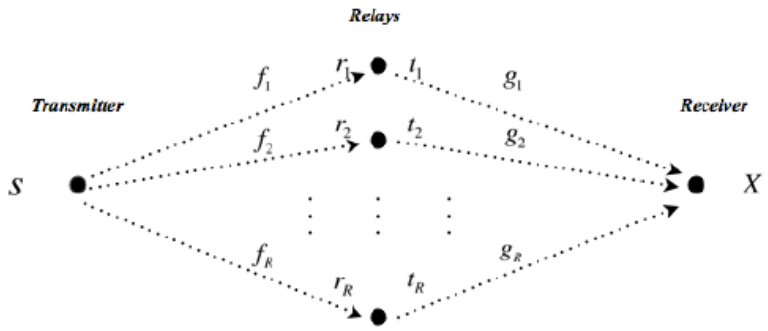

Figure 2.11. Example two-stage co-operative relay network [5].

f_i and g_i, which are complex Gaussian random variables independent and identically distributed (i.i.d.) with zero-mean and unit-variance. Assuming a block-fading model with coherence interval T, for which f_i and g_i remain constant during a block of T transmissions, and for the next block, the values are changed. In detail, a block of symbols to be transmitted is $\mathbf{s} = [s_1, \cdots, s_T]^T$ with the normalization $E\{\mathbf{s}^*\mathbf{s}\} = 1$. It means the power of the signal at the transmitter node is unity, where $(\cdot)^T$ denotes transpose and $(\cdot)^*$ conjugate transpose. In Fig. 2.11, the transmitter signal $\sqrt{P_1 T}\mathbf{s}$. P_1 is the average power per transmission at the transmitter. The received signal vector at the ith relay is denoted as $\mathbf{r}_i$. It includes the effect of f_i and the noise v_i. This is the broadcast step of the relay transmission. The received signal at the relays is given by

$$\mathbf{r}_i = \sqrt{P_1 T} f_i \mathbf{s} + \mathbf{v}_i \tag{2.3.3}$$

The next step is from relays to the receiver. The i-th relay transmits the signal vector $\mathbf{t}_i$ which corresponds to the received signal $\mathbf{r}_i$ multiplied by a scaled identity matrix. The transmitted signal from the ith relay node can

be generated from

$$\begin{aligned}\mathbf{t}_i &= \sqrt{\frac{P_2}{P_1+1}}(\mathbf{A}_i\mathbf{r}_i + \mathbf{B}_i\mathbf{r}_i^*) \\ &= \sqrt{\frac{P_1P_2T_s}{P_1+1}}(f_i\mathbf{A}_i\mathbf{s} + f_i^*\mathbf{B}_i\mathbf{s}^*) + \sqrt{\frac{P_2}{P_1+1}}(\mathbf{A}_i\mathbf{v}_i + \mathbf{B}_i\mathbf{v}_i^*)\end{aligned} \tag{2.3.4}$$

where $\mathbf{A}_i$ and $\mathbf{B}_i$ are $T \times T$ complex matrices used depending on the distributed space time code, 1 is the unity noise power, and P_2 is the average transmission power at every relay node. The received signal vector $\mathbf{y}$ at the receiver is given by

$$\mathbf{y} = \sum_{i=1}^{R} g_i\mathbf{t}_i + \mathbf{w}. \tag{2.3.5}$$

The special case that either $\mathbf{A}_i = \mathbf{0}_T$, $\mathbf{B}_i$ is unitary or $\mathbf{B}_i = \mathbf{0}_T$ and $\mathbf{A}_i$ is unitary is considered. $\mathbf{A}_i = \mathbf{0}_T$ means that the ith relay column of the code matrix contains the conjugates $s_1^*, ..., s_T^*$ only and $\mathbf{B}_i = \mathbf{0}_T$ means that the ith relay column contains the information symbols $s_1, \cdots, s_T$ only. Thus the following variables are defined as [5]

$$\begin{aligned}&\hat{\mathbf{A}}_i = \mathbf{A}_i, \quad \hat{f}_i = f_i, \quad \hat{\mathbf{v}}_\mathbf{i} = \mathbf{v}_\mathbf{i}, \quad \mathbf{s}^{(i)} = \mathbf{s}, \qquad \text{if } \mathbf{B}_i = \mathbf{0}_T \\ &\hat{\mathbf{A}}_i = \mathbf{B}_i, \quad \hat{f}_i = f_i^*, \quad \hat{\mathbf{v}}_\mathbf{i} = \mathbf{v}_i^*, \quad \mathbf{s}^{(i)} = \mathbf{s}^*, \qquad \text{if } \mathbf{A}_i = \mathbf{0}_T\end{aligned} \tag{2.3.6}$$

From (2.3.4),

$$\mathbf{t_i} = \sqrt{\frac{P_1P_2T}{P_1+1}}\hat{f}_i\hat{\mathbf{A}}_i\mathbf{s}^{(i)} + \sqrt{\frac{P_2}{P_1+1}}\hat{\mathbf{A}}_i\hat{\mathbf{v}}_\mathbf{i} \tag{2.3.7}$$

And then, the signal vector at the receiver is (considering noise $\mathbf{w}$):

$$\mathbf{y} = \sum_{i=1}^{R} g_i\mathbf{t}_i + \mathbf{w} = \sum_{i=1}^{R}\sqrt{\frac{P_1P_2T}{P_1+1}}\hat{f}_i g_i\hat{\mathbf{A}}_i\mathbf{s}^{(\mathbf{i})} + \sum_{i=1}^{R}\sqrt{\frac{P_2}{P_1+1}}g_i\hat{\mathbf{A}}_i\hat{\mathbf{v}}_\mathbf{i} + \mathbf{w}. \tag{2.3.8}$$

Thus, the general equation of the received signal vector at the destination can be obtained:

$$\mathbf{x} = \sqrt{\frac{P_1P_2T}{P_1+1}}\mathbf{S}\mathbf{h} + \mathbf{w} \tag{2.3.9}$$

where

$$\mathbf{S} = [\hat{\mathbf{A}}_1\mathbf{s}^{(1)} \ ... \ \hat{\mathbf{A}}_R\mathbf{s}^{(R)}] \quad , \quad \mathbf{h} = [\hat{f}_1 g_1 \ ... \ \hat{f}_R g_R]^T \tag{2.3.10}$$

and

$$\mathbf{w} = \sqrt{\frac{P_2}{P_1 + 1}} \sum_{i=1}^{R} g_i \hat{\mathbf{A}}_i \hat{\mathbf{v}}_i + \mathbf{w}_d$$

$\mathbf{S}$ is space-time coding matrix formed at the receiver by relays. The vector $\mathbf{h}$ is the equivalent channel and $\mathbf{w}_d$ is the equivalent noise. Maximum-likelihood decoding is defined by

$$\arg\min_{\mathbf{S}} \|\mathbf{x} - \sqrt{\frac{P_1 P_2 T}{P_1 + 1}}\mathbf{S}\mathbf{h}\|_2, \tag{2.3.11}$$

where $\|\cdot\|_2$ denotes the Euclidean norm, and all possible $\mathbf{S}$ formed as in (2.3.10) from the source signal vectors $\mathbf{s}$ defined by the source constellation. If the total power is fixed as P per symbol transmission within this network, then the optimal power allocation, which maximizes the expected receive SNR, is [5]

$$P_1 = \frac{P}{2} \text{ and } P_2 = \frac{P}{2R} \tag{2.3.12}$$

So far the transmission process of a distributed MIMO system, and distributed space-time coding design have been discussed. Note that in a practical application, neither $\mathbf{A}_i$ nor $\mathbf{B}_i$ are zero.

2.3.2 Distributed Relay Selection

In the previous sections, all relays participate in the relayed transmission which they transmit over orthogonal channels. Although the orthogonality assumption reduces the system implementation complexity, it limits the system throughput. It can however lead to a further capacity increase, but system implementation complexity is also increased, such as the CSI of the forward channels from the relays to the destination needs to be found. To

overcome these problems, in this section, a simple relay selection algorithm based on an AF relay protocol to facilitate the system design for two-hop multiple relay networks is introduced. The relay selection improves the system performance and capacity compared to the all participation orthogonal AF relay schemes.

This section considers the same two-hop relay network Fig. 2.11, which consists of one source, n relays and one destination, and assuming that there is no direct link. Let $\gamma_f^i = |f_i|^2\bar{\gamma}_f^i$ and $\gamma_g^i = |g_i|^2\bar{\gamma}_g^i$ denote the instantaneously received SNR in the link from the source to the relay i and that from the relay i to the destination, where $\bar{\gamma}_f^i = \frac{p_s(f_i)^2}{N_0}$ and $\bar{\gamma}_g^i = \frac{p_r^i(g_i)^2}{N_0}$ are the average SNRs in the link from the source to the relay i and from the relay i to the destination, and p_s is the source transmission power and p_r^i is the relay transmission power.

Assuming $\bar{\gamma}_f^i = \bar{\gamma}_f$ and $\bar{\gamma}_g^i = \bar{\gamma}_g$ for all $i = 1, 2, \cdots, n$. Using the same calculation as for the AF protocol, let γ_{fg}^i be the destination received SNR [10],

$$\gamma_{fg}^i = \frac{\gamma_f^i \gamma_g^i}{\gamma_f^i + \gamma_g^i + 1}. \tag{2.3.13}$$

In the AF relay selection scheme, a single relay, which has the maximum source-relay-destination link SNR is selected to forward the information symbols from the source to the destination. Therefore, the mathematical expression is determined by

$$i = \arg \max_{1 \le i \le n} \{\gamma_{fg}^i\}. \tag{2.3.14}$$

To analyze the performance of AF relay selection schemes, order statistics are also useful. In this section, some basic order statistical tools are introduced [41], which will be used later for the performance analysis.

Assuming j independent and identically distributed random variables, $X_1, \cdots, X_j$, each with a CDF F(x). Arranging the variables $X_1, \cdots, X_n$ in

an increasing order of magnitude, denoted by:

$$X_{(1)} \leq X_{(2)} \leq \cdots \leq X_{(j)}, \tag{2.3.15}$$

where $X_{(\omega)}$ is the wth order statistic. Then the CDF of the ωth order statistic $X_{(\omega)}$ is given by [41]

$$F_{(w)}(x) = P(X_{(w)} \leq x) = \sum_{k=1}^{j} \binom{j}{w} F^w(x)[1 - F(x)]^{j-w}. \tag{2.3.16}$$

If $w = 1$ and $w = j$, the above equation can become

$$\begin{aligned} F_{(j)}(x) &= F^j(x) \\ F_{(1)}(x) &= 1 - [1 - F(x)]^j. \end{aligned} \tag{2.3.17}$$

The PDFs of $X_{(1)}$ and $X_{(j)}$ are obtained by differentiating their respective CDFs

$$\begin{aligned} f_{(j)}(x) &= \frac{\partial F_{(j)(x)}}{\partial x} = jf(x)F^{j-1}(x) \\ F_{(1)}(x) &= \frac{\partial F_{(1)(x)}}{\partial x} = jf(x)1 - [1 - F(x)]^{j-1}. \end{aligned} \tag{2.3.18}$$

Therefore, the joint PDF of $X_{(j_1)}, \cdots, X_{(j_k)} (1 \leq j_1 \leq j_2 \leq j_k \leq j)$ can be achieved

$$\begin{aligned} f_{(j_1),\cdots,(j_k)}(x_1, \cdots, x_k) = \frac{j!}{(j_1 - 1)!(j_2 - j_1 - 1)! \cdots (j - j_k)!} \\ F^{j_1-1}(x_1)f(x_1)[F(x_2) - F(x_1)]^{j_2-j_1-1}f(x_2) \cdots [1 - F(x_k)]^{j-j_k}f(x_k) \end{aligned} \tag{2.3.19}$$

In particular, the joint PDF of all j order statistics is given by

$$j!f(x_1)f(x_2) \cdots f(x_j), \qquad x_1 \leq \cdots \leq x_j. \tag{2.3.20}$$

2.4 Performance Analysis of Wireless Cooperative Networks

In wireless cooperative networks, signal fading arising from multipath propagation is a particularly severe channel impairment that can be mitigated through the application of diversity. When compared with the pairwise error probability (PEP) of a traditional MIMO system, the diversity gain for the cooperative system is no longer just a simple exponential function of the signal-to-noise ratio (SNR), rather, it involves the logarithm of the SNR. The term diversity gain function is used to designate this characteristic of the PEP. Diversity gain and coding gain can be achieved in a wireless relay network by having the relays cooperate distributively. The coding gain is the improvement in the PEP obtained by the code design [42]. Therefore, PEP analysis is an important method to analyze the cooperative diversity and will be described in this section. Moreover, performance characterization in terms of outage events is also an important evaluation of robustness of transmission to fading, typically performed as outage probability analysis. Therefore, the outage probability analysis will be presented after the PEP analysis in this section.

2.4.1 Pairwise Error Probability

• Chernoff Bound of General Communication System

Pairwise error probability (PEP) is an error measure that is related to system error performance via the union bound [43]. The upper PEP bound in the chapter is the Chernoff bound. Chernoff bound provides a very tight upper bound in PEP [14]. Chernoff bound has been widely used in various cases in approximating the PEP [44] and [45]. The Chernoff bound for a general communication network is briefly described. A random variable k is

assumed together with function $f(k)$, which satisfies

$$f(k) \geq \begin{cases} 1 & k \geq 0 \\ 0 & k < 0 \end{cases}, \tag{2.4.1}$$

If the various order statistics of k always exist, the Chernoff bound implies that the following inequality always exists:

$$P(k > 0) \leq E(f(k)). \tag{2.4.2}$$

where $E(\cdot)$ represents the statistical expectation operation. Setting $f(k) = \exp(\lambda k)$, then the Chernoff bound becomes:

$$P(k > 0) \leq E(\exp(\lambda k)). \tag{2.4.3}$$

where $\lambda > 0$. Then, a general point-to-point single antenna communication system is considered. The received signal is obtained as $y = hs + n$, where s is the transmission signal, h is the fading coefficient and n is a Gaussian random noise with the spectrum density of N_0 per dimension. The maximum likelihood (ML) decoding is given by

$$\hat{s} = \arg\max_{s \in S_c} P(y|s) = \arg\min_{s \in S_c} |y - hs|^2. \tag{2.4.4}$$

The decoder always selects the symbol that has the minimum distance to the received signal. Therefore, the probability that the decoder chooses that a wrong symbol $\widetilde{s}$ is transmitted, denoted by $P(s \to \widetilde{s}|y, h)$, is given by:

$$P(s \to \tilde{s}|y, h) = P(|y - hs|^2 > |y - h\tilde{s}|^2) = P(|y - hs|^2 - |y - h\tilde{s}|^2) > 0). \tag{2.4.5}$$

Applying the Chernoff bound (2.4.3) to the equation (2.4.5), yields:

$$P(s \to \tilde{s}|y,h) \leq E(\exp(\lambda(|y-hs|^2 - |y-h\tilde{s}|^2))). \tag{2.4.6}$$

After some algebraic manipulation [7] and [46] , equation (2.4.7) can be obtained as

$$P(s \to \tilde{s}|y,h) = \exp(-\lambda h^2(1-N_0\lambda)|s-\tilde{s}|^2), \tag{2.4.7}$$

if $\lambda = 1/2N_0$, the above equation becomes

$$P(s \to \tilde{s}|y,h) \leq \exp(-\frac{1}{4N_0}h^2|s-\tilde{s}|^2). \tag{2.4.8}$$

Similarly, for a multiple antenna space-time coded system, the transmitted codeword, channel and noise terms become matrices, namely $\mathbf{S}$, $\mathbf{H}$ and $\mathbf{N}$, respectively. Thus, the received signal matrix can be represented as

$$\mathbf{Y} = \mathbf{HS} + \mathbf{N}. \tag{2.4.9}$$

Following the same calculation as in the single antenna system, the PEP of the decoder deciding in favour of another codeword $\mathbf{S}$ when actually $\tilde{\mathbf{S}}$ has been transmitted, can be upper bounded as

$$P(\mathbf{S} \to \tilde{\mathbf{S}}|\mathbf{Y},\mathbf{H}) \leq \exp(-\frac{1}{4N_0}\mathbf{H}^H(\mathbf{S}-\tilde{\mathbf{S}})^{\mathbf{H}}(\mathbf{S}-\tilde{\mathbf{S}})\mathbf{H}). \tag{2.4.10}$$

where $\mathbf{H}^H$ represents the Hermitian transpose of matrix $\mathbf{H}$.

- **PEP Upper Bound for a Distributed Space-Time Code**

This section employs the Chernoff bound to derive the PEP upper bound for an AF type DSTC network. Since A_i are unitary and w_j, $v_{i,j}$ in (2.3.6) are independent Gaussian random variables, $\mathbf{w}$ is a Gaussian random vector when the g_i are known. Assume that $\mathbf{s}_k$ is transmitted. Define $\mathbf{S}_k = [A_1\mathbf{s}_k \cdot$

$\cdots A_R \mathbf{s}_k]$. Therefore, $\mathbf{S}_k$ is an element in a distributed space-time code. As f_i and g_i are known, $\mathbf{x}|\mathbf{s}_k$ is also a Gaussian random vector with mean $\sqrt{\frac{P_1 P_2 T}{P_1+1}}\mathbf{S}_k\mathbf{h}$ and covariance matrix $(1+\frac{P_2}{P_1+1}\sum_{i=1}^{R}|g_i|^2)\mathbf{I}_T$. Therefore,

$$P(\mathbf{x}|\mathbf{s}_k) = \frac{e^{-\frac{(\mathbf{x}-\sqrt{\frac{P_1P_2T}{P_1+1}}\mathbf{S}_k\mathbf{h})^H(\mathbf{x}-\sqrt{\frac{P_1P_2T}{P_1+1}}\mathbf{S}_k\mathbf{h})}{1+\frac{P_2}{P_1+1}\sum_{i=1}^{R}|g_i|^2}}}{\pi^T(1+\frac{P_2}{P_1+1}\sum_{i=1}^{R}|g_i|^2)^T}. \tag{2.4.11}$$

Moreover, the maximum-likelihood (ML) decoding of the system can be easily seen to be

$$\arg\max_{\mathbf{S}_k\in\mathbf{S}_c} P(\mathbf{x}|\mathbf{s}_k) = \arg\min_{\mathbf{S}_k\in\mathbf{S}_c} \|\mathbf{x} - \sqrt{\frac{P_1P_2T}{P_1+1}}\mathbf{S}_k\mathbf{h}\|_2. \tag{2.4.12}$$

With the ML decoding in (2.4.12), the PEP, averaged over the channel coefficients, of mistaking $\mathbf{s}_k$ by $\mathbf{s}_l$ has the following Chernoff bound [42]:

$$P(\mathbf{S}\to\tilde{\mathbf{S}}\ |\mathbf{Y},\mathbf{h}) \le \exp\left(-\frac{P_1P_2T}{4(1+P_1+P_2\sum_{i=1}^{R}|g_i|^2)}\mathbf{h}^H(\mathbf{S}-\tilde{\mathbf{S}})^H(\mathbf{S}-\tilde{\mathbf{S}})\mathbf{h}\right) \tag{2.4.13}$$

Averaging the above equation with respect to the $|\hat{f}_i|^2$ yields

$$P(\mathbf{S}\to\tilde{\mathbf{S}}|\mathbf{Y},h_i,i=1,\cdots,R) \le \det{}^{-1}\left[\mathbf{I}_R + \frac{P_1P_2T}{4(1+P_1+P_2\sum_{i=1}^{R}|g_i|^2)}\mathbf{MG}\right] \tag{2.4.14}$$

where

$$\mathbf{M} = (\mathbf{S}-\tilde{\mathbf{S}})^H(\mathbf{S}-\tilde{\mathbf{S}}) \quad \text{and} \quad \mathbf{G} = diag\{|g_1|^2,\cdots,|g_R|^2\}, \tag{2.4.15}$$

and $det(\cdot)$ and $diag(\cdot)$ denote the matrix determinant and diagonal matrix respectively. Comparing with the PEP Chernoff bound of a multiple antenna system, the expressions are very similar. In order to derive the final PEP upper bound [44], to average equation (2.4.14) must be averaged over $|g_i|^2$. Unfortunately, the expectations over all $|g_i|^2$ are difficult to calculate in a

closed form, therefore, some approximation has to be considered. Setting $g = \sum_{i=1}^{R} |g_i|^2$ which has gamma distribution

$$f_g(x) = \frac{x^{R-1}e^{-x}}{(R-1)!}, \tag{2.4.16}$$

where R is both for mean and variance of g. For large R, the mean of $g \approx R$. Therefore,

$$P(\mathbf{S} \to \tilde{\mathbf{S}}|\mathbf{Y}, h_i, i = 1, \cdots, R) \leq \det{}^{-1}\left[\mathbf{I}_R + \frac{P_1 P_2 T}{4(1 + P_1 + P_2 R)}\mathbf{MG}\right] \tag{2.4.17}$$

When $\frac{P_1 P_2 T}{4(1+P_1+P_2 R}$) is maximised, the above equation is minimised. Letting $P = P_1 + P_2 R$ be the total transmission power at the source and all relays and according to the power allocation (2.3.12), the term in the above equation can be simplified as

$$\frac{P_1 P_2 T}{4(1 + P_1 + P_2 R)} = \frac{P_1(P - P_1)T}{4R(1 + P)} \leq \frac{P^2 T}{16R(1 + P)}. \tag{2.4.18}$$

Therefore,

$$P(\mathbf{S} \to \tilde{\mathbf{S}}|\mathbf{Y}, h_i, i = 1, \cdots, R) \leq \det{}^{-1}\left[\mathbf{I}_R + \frac{PT}{16R}\mathbf{MG}\right] \tag{2.4.19}$$

is obtained. Integrating the above equation with respect to $|g_i|^2$ and assuming $\mathbf{M}$ is a full rank matrix and $T \geq R$, the average PEP of the distributed space-time coding can be approximated as

$$P(\mathbf{S} \to \tilde{\mathbf{S}}|\mathbf{Y}) \leq \det{}^{-1}[\mathbf{M}] \left(\frac{8R}{T}\right)^R P^{-R(1-\frac{\log\log P}{\log P})}. \tag{2.4.20}$$

From the above equation, the diversity order is achieved $R(1 - \frac{\log\log P}{\log P})$. When P is very large, $\frac{\log\log P}{\log P} \to 0$ and the asymptotic diversity order is R. In general, the rank of $\mathbf{M}$ will be $\min\{T, R\}$ instead of R. Thereby, the diversity order achieved by the DSTC is $\min\{T, R\}(1 - \frac{\log\log P}{\log P})$.

2.4.2 Outage Probability

Developing performance characterisations in terms of outage events and associated outage probabilities, which measure robustness of the transmissions to fading is typically performed in the high signal-to-noise ratio (SNR) regime. The outage is converted into an equivalent event defined in terms of the fading coefficients of the channel. Since the channel average mutual information I is a function of the fading coefficients of the channel, it is a random variable. The event $I < \mathrm{R}$ that is the mutual information random variable falls below some fixed spectral R, which is referred to as an outage event, because reliable communication is not possible for realizations in this event. The probability of an outage event, $P[I < \mathrm{R}]$ is referred to as the outage probability of the channel. The outage events are independent of the distribution of the underlying random variables, while outage probabilities are intimately tied to them. Several of the cooperation strategies have similar outage probabilities, but the structure of their outage events is sufficiently different [47]. As a result, both outage events and outage probabilities are useful for characterising the transmission protocols.

- **Direct Transmission**

This transmission protocol is a typical three-node transmission as shown in Fig. 2.12. Under direct transmission, the source terminal transmits the signal over the channel directly to the destination node, while at this time, the relay node does not work. The maximum average mutual information between input and output is given by

$$I_D = \log_2(1 + SNR|h_{sd}|^2). \tag{2.4.21}$$

The outage event for spectral efficiency R is given by $I_D < \mathrm{R}$ and is equivalent to the event

$$|h_{sd}|^2 < \frac{2^{\mathrm{R}} - 1}{SNR}. \tag{2.4.22}$$

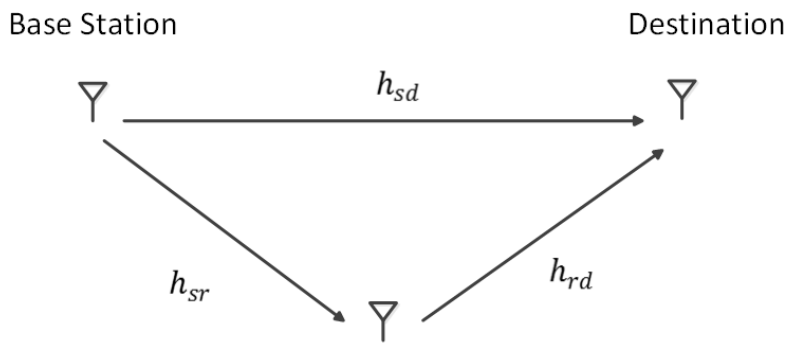

Figure 2.12. A basic wireless cooperative network with a direct link and single relay node.

For Rayleigh fading, i.e., $|h_{sd}|^2$ is exponentially distributed with parameter $|\sigma_{sd}|^{-2}$, the outage probability satisfies

$$\begin{aligned} P_D^{out}(SNR, \mathrm{R}) &= P(I_D < \mathrm{R}) = P(|h_{sd}|^2 < \frac{2^{\mathrm{R}} - 1}{SNR}) \\ &= 1 - \exp(-\frac{2^{\mathrm{R}} - 1}{SNR\sigma_{sd}^2}) \approx \frac{1}{\sigma_{sd}^2} \cdot \frac{2^{\mathrm{R}} - 1}{SNR}, \end{aligned} \tag{2.4.23}$$

where σ_{sd}^2 is the channel variance from the source to the destination. Therefore, to achieve low outage probability needs high SNR and channel variance σ_{sd}^2.

- **Fixed relay transmission**

Amplify-and-Forward Scheme

The AF transmission has a direct link and produces an equivalent one-input two-output, complex Gaussian noise channel with different noise levels in the outputs, and the maximum average mutual information between input and output is given by

$$I_{AF} = \frac{1}{2}\log(1 + SNR|h_{sd}|^2 + f(SNR|h_{sd}|^2, SNR|h_{rd}|^2)), \tag{2.4.24}$$

where $f(x, y) = \frac{xy}{x+y+1}$. The outage event for spectral efficiency R is given

by $I_D < \mathrm{R}$ and is equivalent to the event

$$|h_{sd}|^2 + \frac{1}{SNR} f(SNR|h_{sd}|^2, SNR|h_{rd}|^2)) < \frac{2^{2\mathrm{R}} - 1}{SNR}. \tag{2.4.25}$$

For Rayleigh fading, $|h_{ij}|^2$ is exponentially distributed with parameter σ_{ij}^{-2}, the outage probability can be approximated as

$$P_{AF}^{out} = P(I_{AF} < \mathrm{R}) \approx \left(\frac{\sigma_{sr}^2 \sigma_{rd}^2}{2\sigma_{sd}^2 \sigma_{sr}^2 \sigma_{rd}^2} \right) \left(\frac{2^{2\mathrm{R}} - 1}{SNR} \right)^2. \tag{2.4.26}$$

for high SNR, where σ_{ij}^2, $i \in (s, r)$ and $i \in (r, d)$ are the channel variances.

Decode-and-Forward Scheme

To establish decode-and-forward transmission, a particular decoding structure must be used at the relay. It is assumed the relay can fully decodes the source message and examine the symbol-by-symbol, and the destination also decode perfectly. The maximum average mutual information for repetition-coded DF can be shown to be [47]

$$I_{DF} = \frac{1}{2} \min\{\log_2(1 + SNR|h_{sr}|^2), \log_2(1 + SNR|h_{sd}|^2) + |h_{rd}|^2\}. \tag{2.4.27}$$

The first term of the above equation denotes the maximum rate at which the relay can reliably decode the source message, and the second term shows the maximum rate at which the destination can reliably decode the source message given repeated transmissions from the source and destination. The mutual information forms are typical of relay channels with full decoding at the relay [47]. The outage event for spectral efficiency R is given by $I_{DF} < \mathrm{R}$ and is equivalent to the event

$$\min\{|h_{sr}|^2, |h_{sd}|^2 + |h_{rd}|^2\} < \frac{2^{2\mathrm{R}} - 1}{SNR}. \tag{2.4.28}$$

For Rayleigh fading, the outage probability for repetition-coded DF can be computed as

$$P_{DF}^{out}(SNR,\mathrm{R}) = P(I_{DF} < \mathrm{R}) = P(|h_{sr}|^2 < \frac{2^{2\mathrm{R}}-1}{SNR}) + P(|h_{sr}|^2 \geq \frac{2^{2\mathrm{R}}-1}{SNR})P(|h_{sd}|^2 + |h_{rd}|^2 < \frac{2^{2\mathrm{R}}-1}{SNR}) \tag{2.4.29}$$

When SNR approaches infinity,

$$P_{DF}^{out}(SNR,\mathrm{R}) \approx \frac{2^{2\mathrm{R}}-1}{\sigma_{sr}^2 SNR} \tag{2.4.30}$$

where σ_{sr}^2 is channel variance from the source to the relay. Fixed DF transmission does not offer the diversity gain for large SNR, because the relays fully decode the source information which limits the performance of DF to that of direct transmission between the source and relay.

Selecting Relay Scheme

The task of relay selection is important to realise cooperative relaying in practice according to the measured SNR. When the relay cannot decode, direct transmission is implemented. Selection relaying can be applied to overcome the weakness of the DF transmission. This section introduces considering the performance of selection DF. In the case of repetition coding at the relay the mutual information can be shown to be

$$I_{ADF} = \begin{cases} \frac{1}{2}\log_2(1+2SNR|h_{sd}|^2) & |h_{sr}|^2 < \frac{2^{2\mathrm{R}}-1}{SNR} \\ \frac{1}{2}\log_2(1+SNR|h_{sd}|^2+SNR|h_{rd}|^2) & |h_{sr}|^2 \geq \frac{2^{2\mathrm{R}}-1}{SNR} \end{cases}, \tag{2.4.31}$$

The first case of the above equation represents the case when the relay is not available to decode and the source repeats its transmission so that the mutual information is that of repetition coding from the source to the destination, hence the extra factor of two in the SNR. For the second case, the relay

has the ability to decode and repeat the source transmission and the mutual information is that of repetition coding from the source and relay to the destination. The outage event for spectral efficiency R is given by $I_{SDF} < \mathrm{R}$ and is equivalent to the event

$$\begin{aligned}&\left(\{|h_{sr}|^2 < \frac{2^{2\mathrm{R}}-1}{SNR}\}\bigcap\{2|h_{sd}|^2 < \frac{2^{2\mathrm{R}}-1}{SNR}\}\right)\\ &\bigcup\left(\{|h_{sr}|^2 \geq \frac{2^{2\mathrm{R}}-1}{SNR}\}\bigcap\{|h_{sd}|^2+|h_{rd}|^2 < \frac{2^{2\mathrm{R}}-1}{SNR}\}\right)\end{aligned} \tag{2.4.32}$$

where $\bigcap$ and $\bigcup$ denote "OR" and "AND" operations. Because the events in the union of (2.4.32) are mutually exclusive, the outage probability becomes the sum

$$\begin{aligned}P_{SDF}^{out}(SNR,R) &= P(I_{SDF} < R)\\ &= P\left(|h_{sr}|^2 < \frac{2^{2\mathrm{R}}-1}{SNR}\right)P\left(2|h_{sd}|^2 < \frac{2^{2\mathrm{R}}-1}{SNR}\right)\\ &+ P\left(|h_{sr}|^2 \geq \frac{2^{2\mathrm{R}}-1}{SNR}\right)P\left(|h_{sd}|^2+|h_{rd}|^2 < \frac{2^{2\mathrm{R}}-1}{SNR}\right).\end{aligned} \tag{2.4.33}$$

When SNR$\rightarrow\infty$, the limit can be obtained from the above equation [47]

$$P_{SDF}^{out}(SNR,R) \approx \left(\frac{\sigma_{sr}^2\sigma_{rd}^2}{2\sigma_{sd}^2\sigma_{sr}^2\sigma_{rd}^2}\right) \tag{2.4.34}$$

Therefore, the performance of selection DF is identical to that of fixed AF for large SNR.

2.5 Summary

This chapter presented a brief overview of the space-time coding, including the Alamouti code and the Golden Code in a conventional MIMO system and MIMO-OFDM. OFDM offered the advantage of lower implementation complexity in systems with a large bandwidth-delay spread product. To

overcome the drawback of traditional MIMO, distributed MIMO with distributed space-time coding was discussed. Using all the relays may not obtain the optimal performance of the relay network, and may present practical problems such as asynchronism between the relays. Due to the high cost of a multi-antenna system, antenna selection was described. Improved performance was shown to be potentially achieved by selecting the cooperating relays and antennas employed. The next chapter considers methods for increasing data rate and mitigating asynchronism in relay networks.

Chapter 3

INCREASING DATA RATE IN ASYNCHRONOUS ONE-WAY AND TWO-WAY RELAY NETWORKS

In this chapter, firstly, a simple full interference cancellation (FIC) scheme and orthogonal frequency-division multiplexing (OFDM) are used in a two-hop cooperative four relay network with asynchronism in the second stage. This approach can achieve the full available diversity and asymptotically full rate with distributed space-time code (DSTC) scheme. This is followed by the description of an FIC scheme with offset transmission scheme for a more practical cooperative network with asynchronism in both stages. Then, the Golden Code is used in two-way transmission over a wireless relay network in the fixed and selected relay cases. The rate performance over one-way schemes is potentially improved by such two-way transmission. A four time slot amplify-and-forward (AF) protocol is exploited. Two policies are considered for relay selection, one based on a maximum-minimum strategy and a second using the maximum-mean approach. Finally, simulation results to demonstrate the behavior of the methods are presented.

3.1 Introduction

One of the key challenges to designing a high-performance distributed space-time code system is symbol-level synchronization among the relay nodes. In conventional point-to-point space time coded MIMO systems, co-located antennas obviate this issue. In cooperative systems, the antennas are separated by wireless links. Cooperative relays are an important physical layer concept for mobile wireless ad hoc networks. Moreover, as compared with conventional systems, relaying can provide high quality of service (QoS) for users at the cell edge or in shadowed areas [10]. One of the key challenges to designing high-performance distributed space-time code systems is symbol-level synchronisation among the relay nodes. For example, asynchronism results from the nodes being in different locations and mismatch between their individual oscillators [48]. The scheme in [36] achieves robustness to asynchronism with a simple space-time coding cooperative scheme through the use of OFDM type transmission and a cyclic prefix (CP). However, this scheme has weaknesses, firstly its end-to-end transmission rate is only one half. Therefore, an offset transmission scheme with FIC is applied in this chapter. The second disadvantage is that this network just considers the timing error from one relay node to the destination node and assumes perfect symbol level synchronisation in the transmission from the source to the relays, namely the signals are assumed to arrive at the relays at the same time. However, this assumption may not hold in practice. Therefore, in Section 3.2, two timing errors are considered in the channels, one from the source to a relay and a separate one from a relay to the destination. The timing errors are removed by exploiting the CP, and in order to decrease the complexity of decoding at the relay nodes, the CP removal is only implemented at the destination.

Initial work in the chapter focuses upon one-way transmission, as men-

tioned in Section 3.2. In one-way communication based on distributed space time coding an end-to-end transmission rate of a half is achieved when perfect channel state information is assumed to be available at the destination. Two-way communication on the other hand can make the system obtain full-rate. Such two-way communication without relay channels was first proposed by Shannon in 1961, and he derived the inner and outer bounds on the capacity region [49]. In two-way communication the destination (the other terminal) also has data to send to its source, i.e., the downlink and uplink need to exchange information [50]. This system was built based on single user transmission. Therefore, a multi-user two-way scheme is considered in Section 3.3. Such transmission is used to increase the sum-rate of two terminal users. On the other hand, using all the relays may not obtain the optimal performance. Improved performance can be achieved by selecting the cooperative relays. Selection can aim to find the best relays for solving the problem of multi-relay transmission by using a limited number of relays to forward the information from the source node [21].

3.2 STBC Scheme with FIC for an Asynchronous Cooperative Four Relay Network

The relay model for the four-path relay scheme is illustrated in Fig. 3.1. The f_i $(i = 1, ..., 4)$ denote the channels from the transmitter to the four relays and g_i $(i = 1, ..., 4)$ denote the channels from the four relays to the destination. The parameters τ_1 and τ_2 are delays from S to R1 and R2, and τ_3 and τ_4 are delays from R3 and R4 to D, respectively. There is no direct link between the source and the destination as path loss or shadowing is assumed to render it unusable. The inter-relay channels are reciprocal, i.e. the gains from R1 and R3 to R2 and R4 are the same as those from R2 and R4 to R1 and R3, which are denoted h_{12}, h_{23}, h_{34} and h_{14}. The channels are

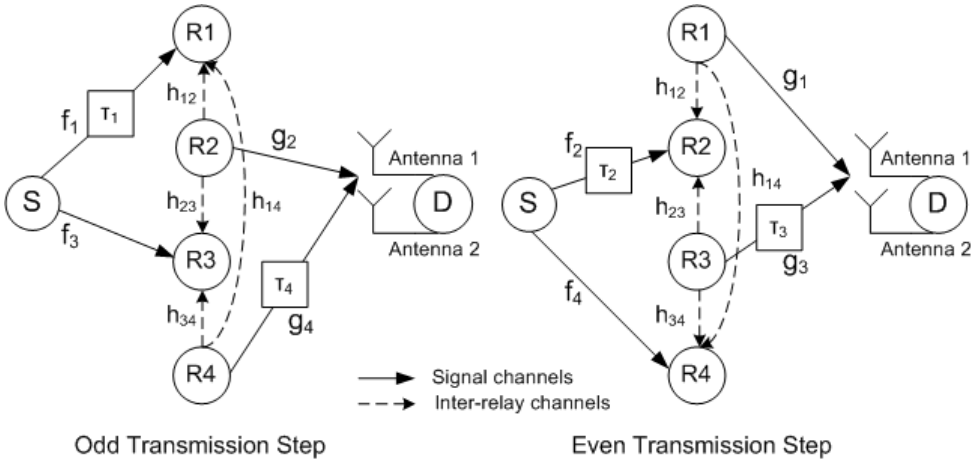

Figure 3.1. An offset transmission model for a four relay network with asynchronism.

quasi-static flat-fading: f_i and g_i are independent and identically distributed (i.i.d.) zero-mean and unit-variance complex Gaussian random variables. Two receive antennas 1 and 2 can be used to separate the signals from R1 (R2) and R3 (R4), respectively, since a beamforming technique can be applied at the destination node [51].

Implementation at the source node

At the source node, two consecutive OFDM blocks $\mathbf{x}_1 = [x_{0,1}, x_{1,1}, \ldots, x_{N-1,1}]^T$ and $\mathbf{x}_2 = [x_{0,2}, x_{1,2}, \ldots, x_{N-1,2}]^T$ are broadcast, which are composed of a set of N modulated complex symbols $x_{i,j}$, $i = 0, \cdots, N-1$ and $j = 1$ or 2, which are modulated into time domain samples using DFT operations. Therefore, $\mathbf{x}_{1_{dft}} = \mathrm{DFT}(\mathbf{x}_1)$ and $\mathbf{x}_{2_{dft}} = \mathrm{DFT}(\mathbf{x}_2)$. Then each block is preceded by a CP with length l_{cp}. Thus, each OFDM symbol consists of $L_s = N + l_{cp}$ samples. The length of the CP is not less than the maximum possible relative timing errors τ_{max} of the signals which arrive at the destination node from the relay nodes. The two OFDM symbols with their corresponding CPs are denoted as $\overline{\mathbf{x}}_1$ and $\overline{\mathbf{x}}_2$.

Implementation at the relay nodes

At the relay nodes, assume the channel coefficients are quasi-static over two OFDM symbol intervals. Then the received signals at the i^{th} $(i = 1, ..., 4)$ relay for two successive OFDM symbol durations can be written as

$$\mathbf{y}_{i1} = \overline{\mathbf{x}}_1 f_i + \mathbf{n}_{i1} \quad \text{and} \quad \mathbf{y}_{i2} = \overline{\mathbf{x}}_2 f_i + \mathbf{n}_{i2}, \tag{3.2.1}$$

where $\mathbf{n}_{i1}$ and $\mathbf{n}_{i2}$ are the corresponding AWGN vectors at the relay node i with zero-mean and identity-covariance matrix, in two successive OFDM symbol durations, respectively. Let P_s denote the transmission power at the source node, then the average power of the signal received at the relay node is $P_s + N_0$, where N_0 is the noise variances of the AWGN at the relay node. The optimum power allocation proposed in [42] is used in this scheme, where

$$P_s = RP_r = 0.5P \tag{3.2.2}$$

where P is the total transmission power in the whole scheme, P_r denotes the relay transmission power, and R is equal to 2 in this work. The relay nodes will process and transmit the received noisy signal according to the i^{th} column of the relay encoding matrix S,

$$S = \beta \begin{bmatrix} \zeta(\mathbf{y}_{11}) & -\mathbf{y}_{32}^* \\ \zeta(\mathbf{y}_{12}) & \mathbf{y}_{31}^* \end{bmatrix} \text{ or } \beta \begin{bmatrix} \zeta(\mathbf{y}_{21}) & -\mathbf{y}_{42}^* \\ \zeta(\mathbf{y}_{22}) & \mathbf{y}_{41}^* \end{bmatrix} \tag{3.2.3}$$

where $\beta = \sqrt{\frac{P_r}{P_s+1}}$, and $\zeta(.)$ represents the modulo L_s time-reversal of the signal, i.e., $\zeta(\mathbf{y}(n)) = \mathbf{y}(L_s - n)$, $n = 0, 1, \ldots, L_s - 1$, and $\mathbf{y}(L_s) = \mathbf{y}(0)$.

Implementation at the destination node

At the destination node, in order to separate out the individual relay transmitted signals, which arrive at the destination, a perfect beamforming tech-

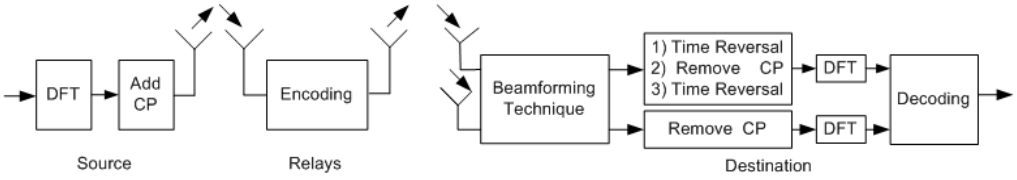

Figure 3.2. Architecture of the offset transmission relay network.

nique is assumed to be used. The effect of errors in this operation are considered in the simulation section. The CP only needs to be removed at the destination node thereby reducing complexity as compared to schemes which also remove the CP at the relays [52]. The destination processing consists of two paths for both sets of signals received from R1 and R3 and for the received signals from R2 and R4, as represented in Fig. 3.2. The first path consists of i) Time reversal; ii) Remove CP; and iii) Time reversal, and a second path in which only the CP is removed. After that, the two received signals are transformed by the N-point DFT. As mentioned before, because of timing errors, the signals from the source arrive at R1 or R2 τ_i $(i = 1, 2)$ samples later than the signals from the source to R3 or R4, respectively. And the signals from R3 or R4 arrive at the destination node τ_i $(i = 3, 4)$ samples later than the signals from R1 or R2, respectively. Since l_{cp} is not less than τ_{max}, the orthogonality between the subcarriers can be still maintained. The delay in the time domain corresponds to a phase change in the frequency domain,

$$\mathbf{u}_{\tau_i} = [u_{0,\tau_i}, u_{1,\tau_i}, \ldots, u_{N-1,\tau_i}]^T \tag{3.2.4}$$

where $u_{k,\tau_i} = \exp(-j2\pi k\tau_i/N)$ and $k = 0, 1, \cdots, N-1$.

Let $\mathbf{z}_1 = [z_{0,1}, z_{1,1}, \cdots, z_{N-1,1}]^T$ and $\mathbf{z}_2 = [z_{0,2}, z_{1,2}, \ldots, z_{N-1,2}]^T$ be the received signals for two successive OFDM blocks at the destination node

after the DFT transformation. In this DFT transformation,

$$F_1 = \mathrm{DFT}[\zeta(D(\mathrm{DFT}(\mathbf{x}_1)))]$$

$$F_2 = \mathrm{DFT}[D(-(\mathrm{DFT}(\mathbf{x}_2))^*)]$$

$$F_3 = \mathrm{DFT}[\zeta(D(\mathrm{DFT}(\mathbf{x}_2)))]$$

and

$$F_4 = \mathrm{DFT}[D((\mathrm{DFT}(\mathbf{x}_1))^*)]$$

where $D(\cdot)$ denotes the cyclic delay, the maximum delay is 15 in this work. Taking transmission step one as an example, $\mathbf{z}_1$ and $\mathbf{z}_2$ can be written as

$$\mathbf{z}_1 = \beta(F_1 f_1 g_1 + F_2 \circ \mathbf{u}_{\tau 1} f_3^* g_3 + \overline{\mathbf{n}}_{11} g_1 + \overline{\mathbf{n}}_{32} \circ \mathbf{u}_{\tau 3} g_3 + \mathbf{w}_1) \tag{3.2.5}$$

$$\mathbf{z}_2 = \beta(F_3 f_1 g_1 + F_4 \circ \mathbf{u}_{\tau 1} f_3^* g_3 + \overline{\mathbf{n}}_{12} g_1 + \overline{\mathbf{n}}_{31} \circ \mathbf{u}_{\tau 3} g_3 + \mathbf{w}_2) \tag{3.2.6}$$

where $\circ$ is the Hadamard product, $\overline{\mathbf{n}}_{ij}$ is the DFT of $\mathbf{n}_{ij}$ and $\mathbf{w}_j$, $j \in (1, 2)$, are AWGN vectors at the destination node with zero-mean and unit-variance elements in the j time slot. Using $\mathrm{DFT}[\zeta(D(\mathrm{DFT}(\mathbf{x})))] = \mathbf{x} \circ \mathbf{u}_\tau^*$, $\mathrm{DFT}[D(-(\mathrm{DFT}(\mathbf{x}))^*)] = -\mathbf{x}^* \circ \mathbf{u}_\tau$ and $\mathrm{DFT}[D((\mathrm{DFT}(\mathbf{x}))^*)] = \mathbf{x}^* \circ \mathbf{u}_\tau$, (3.2.5) and (3.2.6) can be rewritten as in the following Alamouti code at each subcarrier $k, 0 \leq k \leq N-1$

$$\begin{bmatrix} z_{k,1} \\ z_{k,2} \end{bmatrix} = \gamma \begin{bmatrix} x_{k,1} & -x_{k,2}^* \\ x_{k,2} & x_{k,1}^* \end{bmatrix} \begin{bmatrix} u_{k,\tau_1}^* f_1 g_1 \\ u_{k,\tau_3} f_3^* g_3 \end{bmatrix} + \begin{bmatrix} v_{k,1} \\ v_{k,2} \end{bmatrix} \tag{3.2.7}$$

where $v_{k,j} = \beta(\overline{n}_{k,1j} g_1 + \overline{n}_{k,3j} \circ u_{k,\tau_3} g_3) + w_{k,j}$. Then the Alamouti fast symbolwise ML decoding can be used at the destination node.

3.2.1 Interference Cancellation Scheme

In this part, the inter-relay inference from the other relays is removed completely by a full interference cancellation scheme. Similarly to that in [53], the relay nodes R1 and R3 are assumed to receive at the transmission step $n-1$, which corresponds to two time slots, and the relay nodes R2 and R4 send the signal to the destination node. And all of the channel information is known by the receiver.

Therefore, the received signals in the two time slots at the destination node at the transmission step $n-1$ can be written as

$$\begin{aligned}\mathbf{z}_{n-1,1} &= \beta\zeta(\mathbf{y}_{21})g_2(n-1) + \beta D((-\mathbf{y}_{42}^*)g_4(n-1)) + \mathbf{w}_1 \\ \mathbf{z}_{n-1,2} &= \beta\zeta(\mathbf{y}_{22})g_2(n-1) + \beta D(\mathbf{y}_{41}^* g_4(n-1)) + \mathbf{w}_2\end{aligned} \tag{3.2.8}$$

where $\beta = \sqrt{\frac{P_r}{P_s+1}}$, and $\mathbf{z}_{i,j}$ denote the received signals in the j^{th} $j \in (1,2)$ time slot at the i^{th} $(i = 1, 2, ..., n)$ transmission step, $\mathbf{y}_{21}$ and $\mathbf{y}_{42}$, $\mathbf{y}_{22}$ and $\mathbf{y}_{41}$ are the received signal vectors at R2 and R4 at transmission step $n-2$, respectively, and they are encoded by using (3.2.3), which are given by:

$$\begin{aligned}\mathbf{y}_{21} &= \sqrt{P_s}D(\overline{\mathbf{x}}_1 f_2(n-2)) + \overline{\mathbf{n}}_{21} + \beta(\zeta(\mathbf{y}_{11})h_{12} + (-\mathbf{y}_{32}^*)h_{32}) \\ \mathbf{y}_{41} &= \sqrt{P_s}\overline{\mathbf{x}}_1 f_4(n-2) + \overline{\mathbf{n}}_{41} + \beta(\zeta(\mathbf{y}_{11})h_{14} + (-\mathbf{y}_{32}^*)h_{34}) \\ \mathbf{y}_{22} &= \sqrt{P_s}D(\overline{\mathbf{x}}_2 f_2(n-2)) + \overline{\mathbf{n}}_{22} + \beta(\zeta(\mathbf{y}_{12})h_{12} + \mathbf{y}_{31}^* h_{32}) \\ \mathbf{y}_{42} &= \sqrt{P_s}\overline{\mathbf{x}}_2 f_4(n-2) + \overline{\mathbf{n}}_{42} + \beta(\zeta(\mathbf{y}_{12})h_{14} + \mathbf{y}_{31}^* h_{34})\end{aligned} \tag{3.2.9}$$

The received signals at the destination node at transmission step $n-2$ become

$$\begin{aligned}\mathbf{z}_{n-2,1} &= \beta\zeta(\mathbf{y}_{11})g_1(n-2) + \beta D((-\mathbf{y}_{32}^*)g_3(n-2)) + \mathbf{w}_1 \\ \mathbf{z}_{n-2,2} &= \beta\zeta(\mathbf{y}_{12})g_1(n-2) + \beta D((\mathbf{y}_{31}^*)g_3(n-2)) + \mathbf{w}_2\end{aligned} \tag{3.2.10}$$

Assumption 1: If multiple antennas are available at the destination node,

and given that the relays are sufficiently spatially separated by using a perfect beamforming technique, the assumption is that it is possible to separate out the individual relay components within

$$\mathbf{z}_{n-2,1} = \mathbf{z}_{n-2,1,1} + \mathbf{z}_{n-2,1,2} + \mathbf{w}_1$$
$$\mathbf{z}_{n-2,2} = \mathbf{z}_{n-2,2,1} + \mathbf{z}_{n-2,2,2} + \mathbf{w}_2,$$

as given by

$$\begin{aligned}
\mathbf{z}_{n-2,1,1} &= \beta\zeta(\mathbf{y}_{11})g_1(n-2) \\
\mathbf{z}_{n-2,1,2} &= \beta D((-\mathbf{y}_{32}^*)g_3(n-2)) \\
\mathbf{z}_{n-2,2,1} &= \beta\zeta(\mathbf{y}_{12})g_1(n-2) \\
\mathbf{z}_{n-2,2,2} &= \beta D((\mathbf{y}_{31}^*)g_3(n-2))
\end{aligned} \tag{3.2.11}$$

where the noise term is assumed to be insignificant in the current development however this issue and the validity of this assumption is addressed further in Section 3.2.2. Therefore,

$$\begin{aligned}
\zeta(\mathbf{y}_{11}) &= \frac{\mathbf{z}_{n-2,1,1}}{\beta g_1(n-2)} \qquad & D(-\mathbf{y}_{32}^*) &= \frac{\mathbf{z}_{n-2,1,2}}{\beta D(g_3(n-2))} \\
\zeta(\mathbf{y}_{12}) &= \frac{\mathbf{z}_{n-2,2,1}}{\beta g_1(n-2)} \qquad & D(\mathbf{y}_{31}^*) &= \frac{\mathbf{z}_{n-2,2,2}}{\beta D(g_3(n-2))}
\end{aligned} \tag{3.2.12}$$

Because the destination node knows the channel information and all of the delays, $-\mathbf{y}_{32}^*$ and $\mathbf{y}_{31}^*$ can be obtained at the destination node by using: i) CP removal; ii) shifting the first length of τ (l_τ) samples as the last samples; and iii) adding a CP. These processes can be denoted by $\psi(\cdot)$. Finally,

substituting (3.2.12) and (3.2.9) into (3.2.8) gives

$$\begin{aligned}\mathbf{z}_{n-1,1} = \beta g_2(n-1)[\zeta(\sqrt{P_s}D(\overline{\mathbf{x}}_1 f_2(n-2)) + \overline{\mathbf{n}}_{21} + \frac{\mathbf{z}_{n-2,1,1}}{g_1(n-2)}h_{12} \\ + \psi\left(\frac{\mathbf{z}_{n-2,1,2}}{g_3(n-2)}\right)h_{32})] - \beta D(g_4(n-1)(\sqrt{P_s}\overline{\mathbf{x}}_2^* f_4^*(n-2) + \overline{\mathbf{n}}_{42}^* \\ + \left(\frac{\mathbf{z}_{n-2,2,1}}{g_1(n-2)}h_{14}\right)^* + (\psi\left(\frac{\mathbf{z}_{n-2,2,2}}{g_3(n-2)}\right)h_{34})^*)) + \mathbf{w}_1\end{aligned} \tag{3.2.13}$$

$$\begin{aligned}\mathbf{z}_{n-1,2} = \beta g_2(n-1)[\zeta(\sqrt{P_s}D(\overline{\mathbf{x}}_2 f_2(n-2)) + \overline{\mathbf{n}}_{22} + \frac{\mathbf{z}_{n-2,2,1}}{g_1(n-2)}h_{12} \\ + \psi\left(\frac{\mathbf{z}_{n-2,2,2}}{g_3(n-2)}\right)h_{32})] + \beta D(g_4(n-1)(\sqrt{P_s}\overline{\mathbf{x}}_1^* f_4^*(n-2) + \overline{\mathbf{n}}_{41}^* \\ + \left(\frac{\mathbf{z}_{n-2,1,1}}{g_1(n-2)}h_{14}\right)^* + (\psi\left(\frac{\mathbf{z}_{n-2,1,2}}{g_3(n-2)}\right)h_{34})^*)) + \mathbf{w}_2\end{aligned} \tag{3.2.14}$$

From (3.2.13) and (3.2.14), the IRI is a recursive term in the received signal at the destination node. For example, (3.2.15), (3.2.16), (3.2.17) and (3.2.18) are IRI terms, which are functions only of the previous output values.

$$\beta g_2(n-1)\zeta(\frac{\mathbf{z}_{n-2,1,1}}{g_1(n-2)}h_{12} + \psi\left(\frac{\mathbf{z}_{n-2,1,2}}{g_3(n-2)}\right)h_{32}) \tag{3.2.15}$$

$$\beta D(g_4(n-1)(\frac{\mathbf{z}_{n-2,2,1}}{g_1(n-2)}h_{14} + \psi\left(\frac{\mathbf{z}_{n-2,2,2}}{g_3(n-2)}\right)h_{34})^* \tag{3.2.16}$$

$$\beta g_2(n-1)\zeta(\frac{\mathbf{z}_{n-2,1,1}}{g_1(n-2)}h_{12} + \psi\left(\frac{\mathbf{z}_{n-2,2,2}}{g_3(n-2)}\right)h_{32}) \tag{3.2.17}$$

$$\beta D(g_4(n-1)(\frac{\mathbf{z}_{n-2,2,1}}{g_1(n-2)}h_{14} + \psi\left(\frac{\mathbf{z}_{n-2,1,2}}{g_3(n-2)}\right)h_{34})^* \tag{3.2.18}$$

Therefore, these terms can be completely removed in order to cancel the IRI

at the receiver, which are given by

$$\begin{aligned}\mathbf{z}^{'}_{n-1,1} &= \beta g_2(n-1)[\zeta(\sqrt{P_s}D(\overline{\mathbf{x}}_1 f_2(n-2)) + \overline{\mathbf{n}}_{21})] \\ &\quad - \beta D(g_4(n-1)(\sqrt{P_s}\overline{\mathbf{x}}_2^* f_4^*(n-2) + \overline{\mathbf{n}}_{42}^*)) + \mathbf{w}_1 \\ \mathbf{z}^{'}_{n-1,2} &= \beta g_2(n-1)[\zeta(\sqrt{P_s}D(\overline{\mathbf{x}}_2 f_2(n-2)) + \overline{\mathbf{n}}_{22})] \\ &\quad + \beta D(g_4(n-1)(\sqrt{P_s}\overline{\mathbf{x}}_1^* f_4^*(n-2) + \overline{\mathbf{n}}_{41}^*)) + \mathbf{w}_2\end{aligned} \tag{3.2.19}$$

As such, (3.2.19) has no IRI, only the desired signal and the noise. The same method to obtain the received signal at transmission step n at the destination node yields

$$\begin{aligned}\mathbf{z}_{n,1} &= \beta g_1(n)[\zeta(\sqrt{P_s}D(\overline{\mathbf{x}}_1 f_1(n-1)) + \overline{\mathbf{n}}_{11} + \frac{\mathbf{z}_{n-1,1,1}}{g_2(n-1)}h_{21} \\ &\quad + \psi(\frac{\mathbf{z}_{n-1,1,2}}{g_4(n-1)})h_{41})] - \beta D(g_3(n)(\sqrt{P_s}\overline{\mathbf{x}}_2^* f_3^*(n-1) + \overline{\mathbf{x}}_{32}^* \\ &\quad + (\frac{\mathbf{z}_{n-1,2,1}}{g_2(n-1)}h_{23})^* + (\psi(\frac{\mathbf{z}_{n-1,2,2}}{g_4(n-1)})h_{43})^*)) + \mathbf{w}_1\end{aligned} \tag{3.2.20}$$

$$\begin{aligned}\mathbf{z}_{n,2} &= \beta g_1(n)[\zeta(\sqrt{P_s}D(\overline{\mathbf{x}}_2 f_1(n-1)) + \overline{\mathbf{n}}_{12} + \frac{\mathbf{z}_{n-1,2,1}}{g_2(n-1)}h_{21} \\ &\quad + \psi(\frac{\mathbf{z}_{n-1,2,2}}{g_4(n-1)})h_{41})] + \beta D(g_3(n)(\sqrt{P_s}\overline{\mathbf{X}}_1^* f_3^*(n-1) + \mathbf{N}_{31}^* \\ &\quad + (\frac{\mathbf{z}_{n-1,1,1}}{g_2(n-1)}h_{23})^* + (\psi(\frac{\mathbf{z}_{n-1,1,2}}{g_4(n-1)})h_{43})^*)) + \mathbf{w}_2\end{aligned} \tag{3.2.21}$$

From (3.2.20) and (3.2.21), the IRI is a recursive term in the received signal at the destination node. For example, (3.2.22), (3.2.23), (3.2.24) and (3.2.25) are IRI terms.

$$\beta g_1(n)\zeta(\frac{\mathbf{z}_{n-1,1,1}}{g_2(n-1)}h_{21} + \psi(\frac{\mathbf{z}_{n-1,1,2}}{g_4(n-1)})h_{41}) \tag{3.2.22}$$

$$\beta D(g_3(n)(\frac{\mathbf{z}_{n-1,2,1}}{g_2(n-1)}h_{23} + \psi(\frac{\mathbf{z}_{n-1,2,2}}{g_4(n-1)})h_{43})^* \tag{3.2.23}$$

$$\beta g_1(n)\zeta(\frac{\mathbf{z}_{n-1,1,1}}{g_2(n-1)}h_{21} + \psi(\frac{\mathbf{z}_{n-1,2,2}}{g_4(n-1)})h_{41}) \tag{3.2.24}$$

$$\beta D(g_3(n)(\frac{\mathbf{z}_{n-1,2,1}}{g_2(n-1)}h_{23} + \psi(\frac{\mathbf{z}_{n-1,1,2}}{g_4(n-1)})h_{43})^* \tag{3.2.25}$$

Therefore, these terms are completely removed from (3.2.20) and (3.2.21) by using the same method, which are given by:

$$\begin{aligned}
\mathbf{z}^{'}_{n,1} &= \beta g_1(n-1)[\zeta(\sqrt{P_s}D(\overline{\mathbf{x}}_1 f_1(n-1)) + \overline{\mathbf{n}}_{11})] - \\
&\quad \beta D(g_3(n)(\sqrt{P_s}\overline{\mathbf{x}}_2^* f_3^*(n-1) + \overline{\mathbf{n}}_{32}^*)) + \mathbf{w}_1 \\
\mathbf{z}^{'}_{n,2} &= \beta g_1(n)[\zeta(\sqrt{P_s}D(\overline{\mathbf{x}}_2 f_1(n-1)) + \overline{\mathbf{n}}_{12})] + \\
&\quad \beta D(g_3(n-1)(\sqrt{P_s}\overline{\mathbf{x}}_1^* f_3^*(n-1) + \overline{\mathbf{n}}_{31}^*)) + \mathbf{w}_2
\end{aligned} \tag{3.2.26}$$

Comparing (3.2.19) with (3.2.26), they have the same structure. However, according to the different offset transmission steps, the alternate channels are switched regularly. Therefore, the transmission symbols can be easily detected by the fast symbol-wise ML decoding.

3.2.2 Simulation Results

In this section, the simulated performance of the asynchronous relay network will be shown using the offset transmission with FIC and OFDM approaches. The performance is shown by the end-to-end BER using BPSK symbols. $N = 64$ and $CP = 16$ are assumed. The delays τ_i $i \in (1, 2, 3, 4)$ are chosen randomly from 0 to 15 with the uniform distribution. The total power per symbol transmission is fixed as P.

Fig. 3.3 compares, firstly, the BER performance without FIC and with FIC. The advantage of using the FIC scheme is clear, the BER performance is significantly better than without the FIC approach. In fact, without using FIC the scheme is unusable. The IRI considerably corrupts the transmission signal, thereby leading to the performance degradation. Secondly, the performance of Alamouti in an asynchronous two relay network without IRI is contrasted with that of the FIC Alamouti in an asynchronous four relay network with IRI. For the cooperative four relay network, the FIC scheme is used to completely remove the IRI, the performance closely matches the

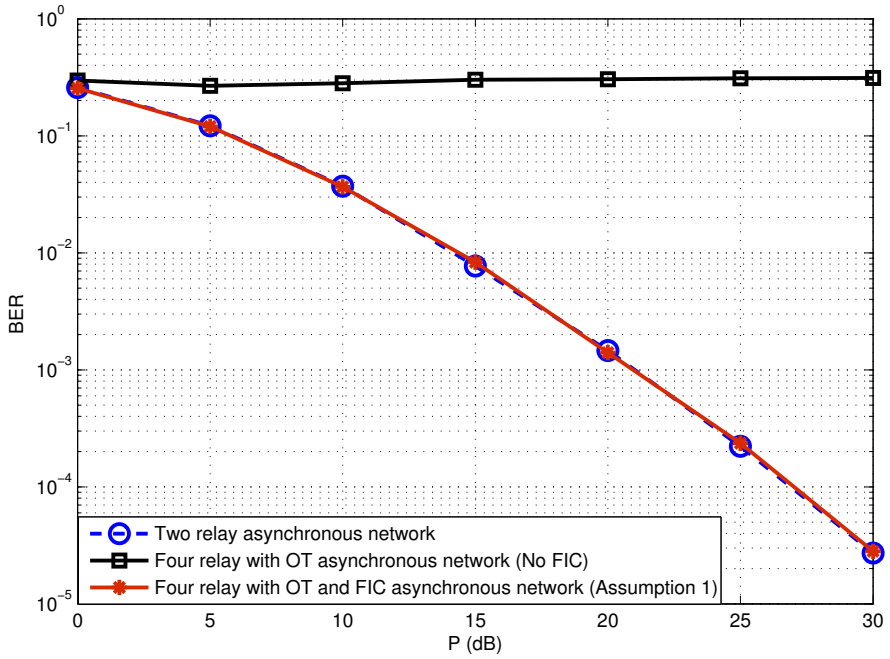

Figure 3.3. BER performance for no FIC and FIC approaches

Alamouti type scheme without IRI.

In Fig. 3.4, however, for the Alamouti type scheme with two relay networks, every transmission time slot is divided into two sub-slots: firstly, the source transmits to the relay nodes; secondly, the relay node sends the data to the destination. Therefore, the rate and bandwidth efficiency of this scheme is a half of the direct transmission. On the contrary, the proposed method uses the two group relay nodes in order to retain the successive transmission signal from the source node, so the full unity data rate can be obtained when the number of symbols is large.

In the next simulation result the effect of ASSUMPTION 1, which multiple antennas are used at the destination and using beam forming technique, is considered. To model the effect that even with multiple antennas at the destination node there will be uncertainties in the values of $\mathbf{z}_{n-2,1,1}$, $\mathbf{z}_{n-2,1,2}$, $\mathbf{z}_{n-2,2,1}$ and $\mathbf{z}_{n-2,2,2}$ in (3.2.11), due for example to estimation errors in

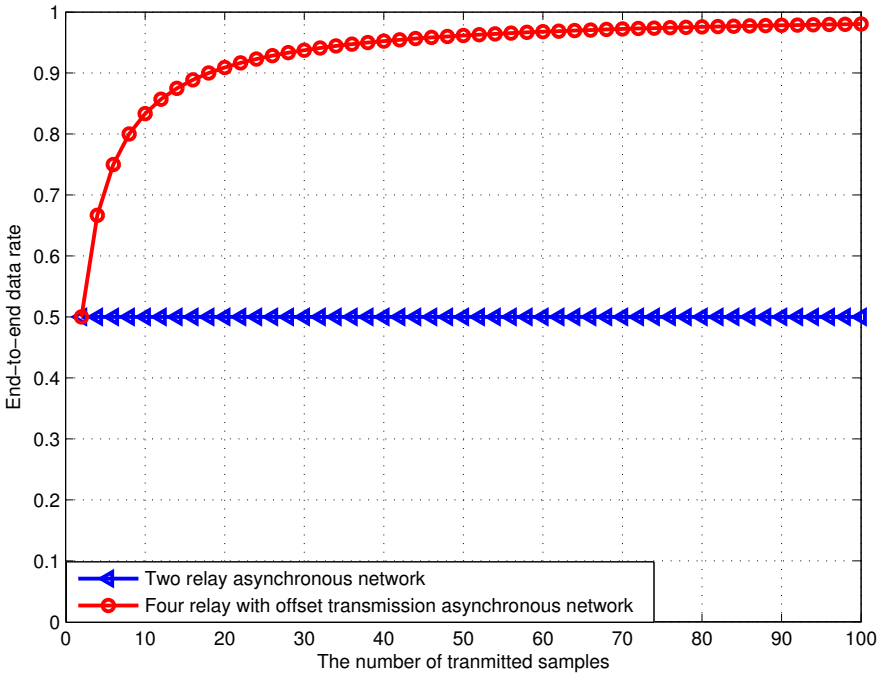

Figure 3.4. End-to-end transmission rate

beamforming, noise vectors are added to yield

$$\begin{aligned}
\mathbf{z}_{n-1,1,1} &= \beta\zeta(\mathbf{y}_{21})g_2(n-1) + \mathbf{n}_1' \\
\mathbf{z}_{n-1,1,2} &= \beta D((-\mathbf{y}_{42}^*)g_4(n-1)) + \mathbf{n}_2' \\
\mathbf{z}_{n-1,2,1} &= \beta\zeta(\mathbf{y}_{22})g_2(n-1) + \mathbf{n}_1' \\
\mathbf{z}_{n-1,2,2} &= \beta D(\mathbf{y}_{41}^* g_4(n-1)) + \mathbf{n}_2',
\end{aligned} \tag{3.2.27}$$

where all the elements of $\mathbf{n}_1'$ and $\mathbf{n}_2'$ are chosen to have noise powers at the relative levels of either -6 dB or -3 dB or 0 dB, and these three cases are denoted Assumption 2, Assumption 3 and Assumption 4. The degradation in BER is shown in Fig. 3.5, for example, at BER $= 10^{-3}$ the required transmit power increases from 21.5 dB to 22.5 dB and to 25 dB for the three cases.

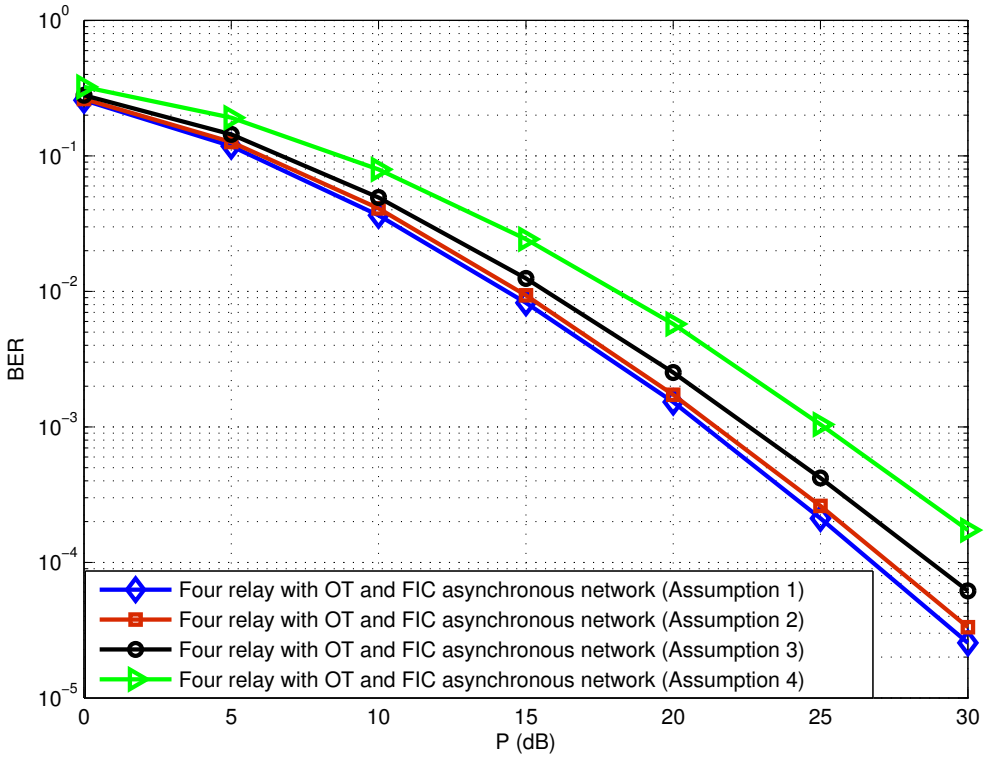

Figure 3.5. BER performance of the four relay with offset transmission and FIC and varying uncertainty in Assumption 1.

3.3 Two-way Distributed Relay Transmission Using the Golden Code

3.3.1 Overview of the Golden Code

The Golden Code is a full rate and full diversity 2×2 linear dispersion algebraic space-time code for a two transmit antennas and two or more receive antennas MIMO system [23]. The essence of the code is the Golden number $\frac{1+\sqrt{5}}{2}$ which is used to generate the best performance [23]. The Golden Code codeword is of the form as (3.3.1).

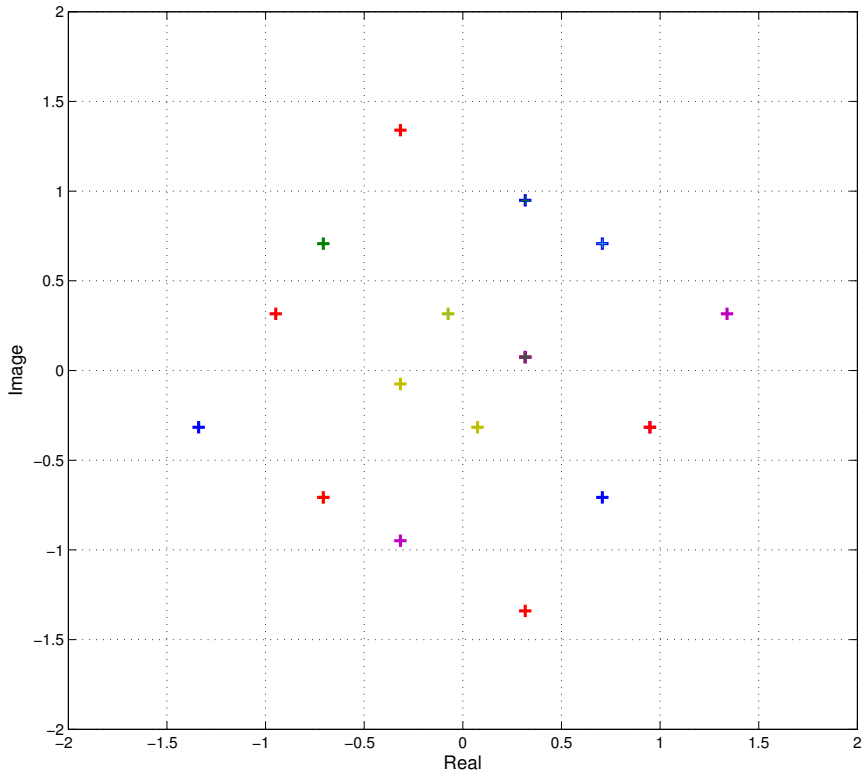

Figure 3.6. The transmitted rotated constellation of the Golden Code (4QAM)

.

$$\begin{aligned}\mathbf{C} &= \frac{1}{\sqrt{5}}\begin{bmatrix} \varphi(s_1+s_2\theta) & \varphi(s_3+s_4\theta) \\ \gamma\overline{\varphi}(s_3+s_4\overline{\theta}) & \overline{\varphi}(s_1+s_2\overline{\theta}) \end{bmatrix} \\ &= \frac{1}{\sqrt{5}}\begin{bmatrix} x_1 & x_2 \\ x_3 & x_4 \end{bmatrix},\end{aligned} \tag{3.3.1}$$

where s_1, s_2, s_3, s_4 describe the information symbol constellation; $\theta = \frac{1+\sqrt{5}}{2}$, $\overline{\theta} = \frac{1-\sqrt{5}}{2}$, $\varphi = 1 + i(1-\theta)$ and $\overline{\varphi} = 1 + i(1-\overline{\theta})$, and i is set as $\sqrt{-1}$. The $|\gamma|$ is set to unity to satisfy the non-vanishing determinant and ensures the same average power is transmitted [23]. To avoid vanishing determinants,

the factor $|\gamma|$ is set as unity, which guarantees that the same average power is transmitted from each antenna at each channel use [23]. For the Golden Code, the elements of the codeword matrix are from the information symbol constellation. The symbols per transmit antenna (i.e., the elements of the matrix codewords) are drawn from a "coded" constellation plotted in Fig. 3.6 which is a rotated regular QAM constellation. The Golden Code integer lattice structure provides efficient constellation shaping, so it may have the information lossless property [54]. The diversity multiplexing tradeoff is an essential tradeoff between the error probability and the data rate of a system. The Golden Code can achieve optimal diversity-multiplexing tradeoff for a 2 $\times$ 2 MIMO system [23]. Due to obtaining simultaneously both diversity and multiplexing gain, the Golden Code scheme is "Perfect". It will not only improve the link performance, but also increase the transmission rate when used in two-way transmission. Several decoding strategies for Golden Codes have been studied, such as full ML and sphere decoding (SD) [25]. In the next chapter, these two methods are adopted to decode the Golden Code at the destination assuming 4-QAM transmission.

3.3.2 Two-way Fixed Relay Scheme for the Golden Code

A cooperative two-way network is adopted as a basic transmission scenario for the Golden Code, as shown Fig. 3.7. The wireless network is equipped with two terminals namely the base station (BS) and user equipment (UE) respectively denoted by T_m, $m = 1, 2$, and R_j relays $j = 1, 2$, where each of the two terminal nodes has two antennas A_i and A_i', where i denotes i-th antenna, and only one antenna is available for each relay. Every node is half-duplex, so cannot transmit and receive simultaneously. The channels are set from T_1 to T_2 as the downlink, and channel coefficients are f_j from T_1 to relays and g_j from relays to T_2, and the uplink is from T_2 to T_1, because of the symmetrical system model, the channel coefficients are the same as

in the downlink. The signals are simultaneously encoded at the BS and UE with the Golden Code matrix. The channels are quasi-static Rayleigh flat fading, which are i.i.d. complex Gaussian random variables with zero-mean and unit-variance, i.e. $f_j \sim \mathcal{CN}(0,1)$ and $g_j \sim \mathcal{CN}(0,1)$.

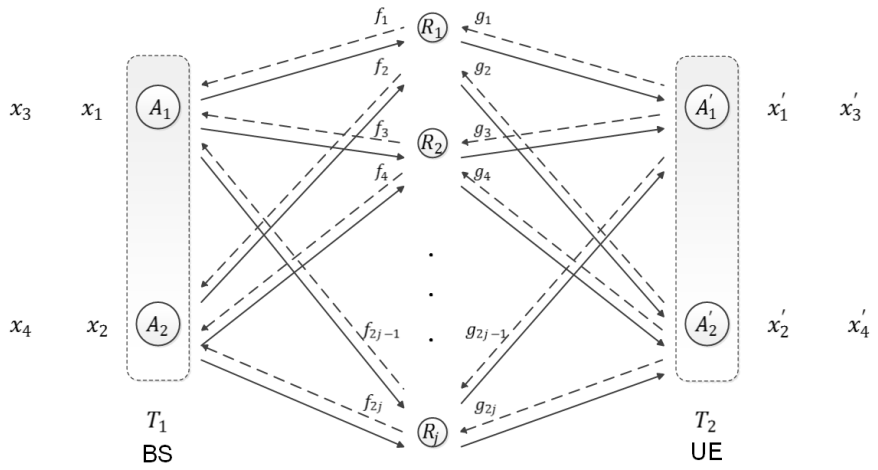

Figure 3.7. The system model for the use of the Golden Code over a two-way distributed wireless network. (The solid line is the downlink from BS to UE and the dashed line is the uplink from UE to BS.)

The information bits are modulated as s_k at the BS and s_k' at the UE, and then respectively encoded with the Golden Code matrix (3.3.1). The encoded symbols at the BS and UE are denoted as x_k and x_k' respectively, where $k = 1, 2, 3, 4$. Sending a Golden Codeword needs two slots. For a one-way relay scheme, a total of eight time slots are required to complete a bi-direction transmission of two codewords. For a two-way relay scheme, however, the number of symbols using the same time slot is doubled as compared to the one-way case, thereby doubling the rate. A two-way relay process for bi-direction transmission can be described as follows: the first phase (the $T_m - R$ phase), where two terminals simultaneously send their symbols to the relays and the second phase (the $R - T_m$ phase), where relays send the symbols without decoding to the terminals. In the $R - T_m$ phase,

due to the half-duplex antennas, the relays will use the last two time slots to amplify the power of the signal and directly resend to the corresponding terminals. The average power of the terminal T_m is P_{Tm}, $m = 1, 2$. Each relay can use the average power P_{Rj}, $j = 1, 2$, so the total power of the relays $P_R = 2P_{Rj}$.

The signal received by the j-th relay for the first two time slots can mathematically be expressed as

$$\begin{aligned} r_{t,j} &= \sqrt{4P_{T1}}(f_{2j-1}x_{2t-1} + f_{2j}x_{2t}) + n_{2j-1} \\ &+ \sqrt{4P_{T2}}(g_{2j-1}x^{'}_{2t-1} + g_{2j}x^{'}_{2t}) + n_{2j}, \end{aligned} \tag{3.3.2}$$

where $t = 1, 2$ denotes the time slot. The terms n_{2j-1} and n_{2j} are the AWGN at the j-th relay. Then, the relays implement the AF protocol by using a scale factor

$$\beta_j = \sqrt{\frac{2P_R}{N(4P_{T1} + 1)}}. \tag{3.3.3}$$

In this chapter, due to the symmetry in transmission, the transmission is from the BS to UE through the downlink channels. The redundant information is removed which occurred after exchanging the information at every relay. The signal received at the third time slot by the UE can be expressed as

$$\begin{aligned} z_{11} &= \beta_j(r_{11}g_1 + r_{12}g_3) + w_{2j-1} \\ z_{21} &= \beta_j(r_{11}g_2 + r_{12}g_4) + w_{2j}, \end{aligned} \tag{3.3.4}$$

at the fourth time slot, the UE receives

$$\begin{aligned} z_{12} &= \beta_j(r_{21}g_1 + r_{22}g_3) + w_{2j-1} \\ z_{22} &= \beta_j(r_{21}g_2 + r_{22}g_4) + w_{2j}, \end{aligned} \tag{3.3.5}$$

where w_{2j-1} and w_{2j} are the AWGN terms at the terminals. The antennas at the terminals perfectly know the signals they first transmitted. For example, in Fig. 3.7, at the BS, A_1 knows s_1 and s_2, and antenna A_2 knows s_3 and s_4

from the first time slot transmission. Due to the construction of the Golden Code, at the next time slot, A_1 sends x_3 which includes s_3 and s_4. At the terminal UE, the antennas $A_1^{'}$ and $A_2^{'}$ know their transmitted information as well. Therefore, the self-interference terms at the UE are shown as follow

$$\begin{aligned} t_{11} &= \beta_j\sqrt{4P_{T_2}}\big(g_1(g_1x_1^{'}+g_2x_2^{'})+g_3(g_3x_1^{'}+g_4x_2^{'})\big)\\ t_{21} &= \beta_j\sqrt{4P_{T_2}}\big(g_2(g_1x_1^{'}+g_2x_2^{'})+g_4(g_3x_1^{'}+g_4x_2^{'})\big)\\ t_{12} &= \beta_j\sqrt{4P_{T_2}}\big(g_1(g_1x_3^{'}+g_2x_4^{'})+g_3(g_3x_3^{'}+g_4x_4^{'})\big)\\ t_{22} &= \beta_j\sqrt{4P_{T_2}}\big(g_2(g_1x_3^{'}+g_2x_4^{'})+g_4(g_3x_3^{'}+g_4x_4^{'})\big) \end{aligned} \tag{3.3.6}$$

Finally, (3.3.6) is cancellated from (3.3.4) and (3.3.5), the UE obtain the signals as

$$\begin{aligned} z_{11} &= \sqrt{4P_1}\beta_j((f_1g_1+f_3g_3)x_1+(f_2g_1+f_4g_3)x_2)+u_1\\ z_{21} &= \sqrt{4P_1}\beta_j((f_1g_2+f_3g_4)x_1+(f_2g_2+f_4g_4)x_2)+u_2\\ z_{12} &= \sqrt{4P_1}\beta_j((f_1g_1+f_3g_3)x_3+(f_2g_1+f_4g_3)x_4)+u_3\\ z_{21} &= \sqrt{4P_1}\beta_j((f_1g_2+f_3g_4)x_3+(f_2g_2+f_4g_4)x_4)+u_4 \end{aligned}, \tag{3.3.7}$$

where u_1, u_2, u_3 and u_4 are

$$\begin{aligned} u_1 &= \beta_j((n_1+n_2)g_1+(n_3+n_4)g_3)+w_1^{'}\\ u_2 &= \beta_j((n_1+n_2)g_2+(n_3+n_4)g_4)+w_2^{'}\\ u_3 &= \beta_j((n_1+n_2)g_1+(n_3+n_4)g_3)+w_3^{'}\\ u_4 &= \beta_j((n_1+n_2)g_2+(n_3+n_4)g_4)+w_4^{'} \end{aligned}. \tag{3.3.8}$$

The terms $w_1^{'}, w_2^{'}, w_3^{'}$ and $w_4^{'}$ are the Gaussian noises at the relays and UE. The vector of symbols received at the UE is denoted as $\mathbf{y}$. Thus, the received signal can be written as

$$\mathbf{y} = \mathbf{H}\mathbf{x} + \mathbf{u}, \tag{3.3.9}$$

where $\mathbf{y}$ is the vector $[y_{11}, y_{21}, y_{12}, y_{22}]^T$ and $\mathbf{x}$ is the vector $[x_1, x_2, x_3, x_4]^T$.

$\mathbf{H}$ is a 4×4 block diagonal matrix of effective transmission channels which is given by $\mathbf{H} = \begin{bmatrix} \mathbf{M} & \mathbf{0} \\ \mathbf{0} & \mathbf{M} \end{bmatrix}$, where

$$\mathbf{M} = \begin{bmatrix} f_1 g_1 + f_3 g_3 & f_2 g_1 + f_4 g_3 \\ f_1 g_2 + f_3 g_4 & f_2 g_2 + f_4 g_4 \end{bmatrix} \tag{3.3.10}$$

and $\mathbf{0}$ represents a 2×2 full zero matrix. Note that the elements of $\mathbf{M}$ are not statistically independent as would be the case for the codes in [42]. Full ML is adopted for decoding the Golden Code:

$$\arg \min_{\mathbf{y} \in \mathbf{S}_c} \{\|\mathbf{y} - \mathbf{H}\mathbf{x}\|^2\}, \tag{3.3.11}$$

where $\mathbf{S}_c$ denotes the collection of possible symbol constellation points.

3.3.3 Discussion of Relay Selection for Two-Way Transmission of the Golden Code

Multi-relay selection for the Golden Code with the maximum-minimum strategy and the maximum-mean strategy were proposed in the one-way transmission environment [55]. In this section, the multi-relay selection with the Golden Code is used in wireless networks for the two-way case. Due to the special limitation of the Golden Code, the aim is to select the best two relays from the j relays for transmission in cooperative networks. The channels of candidate relays are used for transmitting information from BS to UE and vice versa. All of the assumptions are the same as the system model of the fixed case.

Firstly, the maximum-minimum selection method is implemented in the model.

$$R_{\min}^{(j)} = \min\{|f_{2j-1}|^2, |f_{2j}|^2, |g_{2j-1}|^2, |g_{2j}|^2\}. \tag{3.3.12}$$

These values are then calculated for all of the relays and stored in $\mathbf{R}_{\min}$. Choosing the relay node with the maximum value from all the minima

$$R_{\max}^{(j)} \in \mathbf{R}_{\min} \tag{3.3.13}$$

to be the best transmitted relay. The second best relay is decided by the relay node with the maximum of the remaining minima. The simulation of this selection strategy is provided in Section 3.3.4.

On the other hand, for maximum-means selection, the mean of these remaining four channels for the j-th relay is obtained as

$$R_{\text{mean}}^{(j)} = \frac{|f_{2j-1}|^2 + |f_{2j}|^2 + |g_{2j-1}|^2 + |g_{2j}|^2}{4}. \tag{3.3.14}$$

The mean value measures the average quality of each relay. Then, the maximum one is extracted from $R_{\text{mean}}^{(j)}$ as the best available relay

$$R_{\max}^{(j)} \in \mathbf{R}_{\text{mean}}, \tag{3.3.15}$$

where $\mathbf{R}_{\text{mean}}$ is the collection of all mean values for the relays. Consequently, for the remaining relays, choosing the relay node with the second maximum average quality is the second best relay to use.

As in the one-way case, this method can better balance the level among the remaining channels. One shortcoming of the maximum-minimum selection is that the quality of one link just depends on the minimum value of the channels. It means that an available relay may lose the chance to transmit. Therefore, the maximum-mean selection can be better for relay selection.

3.3.4 Discussion of the DMT of the Golden Code

In determining the PEP with the Chernoff Bound type analysis, the diversity gain is found to be $d = \min_{\text{rank}}[(\mathbf{C}-\hat{\mathbf{C}})(\mathbf{C}-\hat{\mathbf{C}})^H]$, where $\hat{\mathbf{C}}$ is the estimated

codeword matrix [42]. The rank of the difference matrix of $\mathbf{C} - \hat{\mathbf{C}}$ for the uncoded point-to-point Golden Code is more than zero. Therefore, it can achieve full diversity. Due to the code construction, it also obtains the full rate in a 2×2 MIMO system. With two transmit antennas and two receive antennas, the Golden Code is DMT-optimal and exhibits very good performance in terms of codeword error probability [15]. When the Golden Code is applied in distributed transmission, due to the non independent elements of the channel matrix as in (3.3.10), the diversity gain will generally be decreased, and the data rate is degraded as well by the multihop transmission. Therefore, using relay selection and two-way transmission can address these weaknesses.

3.3.5 Simulation Results

In this section, all of the simulated performances with and without relay selection based on the Golden Code for uncoded and coded two-way wireless networks will be shown. The performances are shown by end-to-end BER using QPSK symbols. The powers $P_{T1} = P_{T2} = 2P_{Rj} = 1$. The number of participating relays for selection with the two selection strategies is set to 4, 8 and 16, as described in Section 3.3.3.

In Fig. 3.8, the BER performances are compared for the no relay case selection in coded one-way and two-way transmission scenarios, and the coded to uncoded cases. Before encoding with the Golden Code, the convolutional code is used as the outer coding in the systems under study. The constraint length is equal to 3 at the coder and the code generator for the convolutional code is represented as [7 5] in octal. Obviously, the convolutional code means that the performance of the coded system is better than uncoded one by 2 dB at the BER of 10^{-3}. As the two Gaussian noises introduced in transmitting the data from the UE terminal to the relays cannot be removed, the simulation results confirm that the bit error rate performance of systems us-

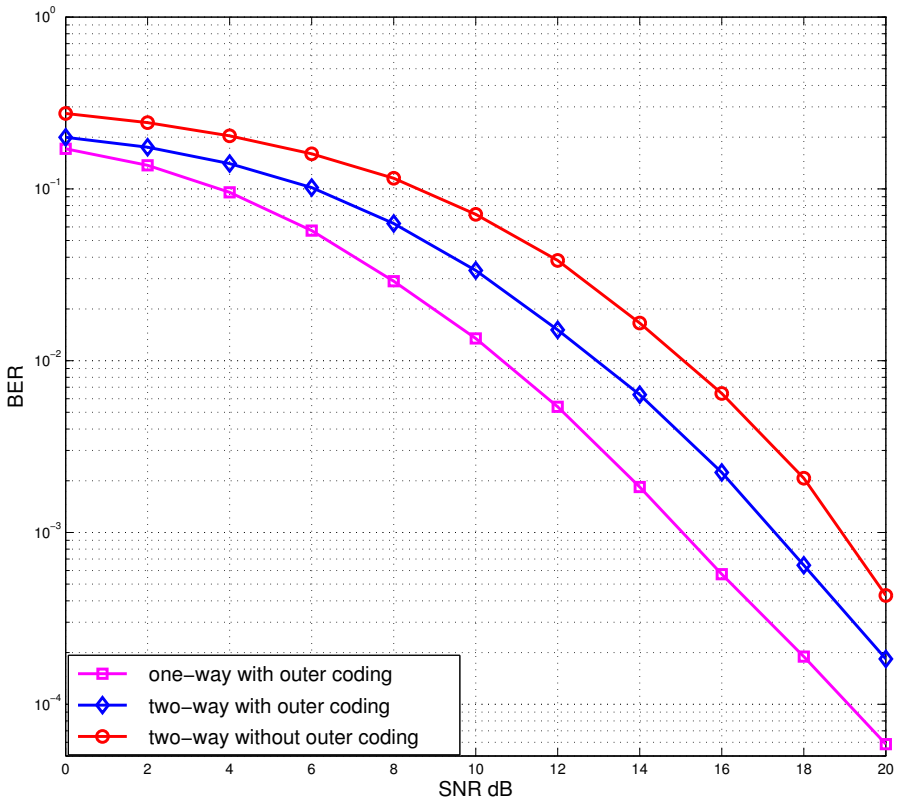

Figure 3.8. Comparison of BER performances of uncoded and coded distributed Golden Code for one-way and two-way cases without relay selection.

ing one-way transmission slightly outperform the two-way scenario, however at lower rate.

Fig. 3.9 presents the simulation results with maximum-min relay selection and no selection. Clearly, the BER performance of the maximum-min relay selection outperforms the fixed relay scheme at least by 2 dB. For example, the selection case can achieve 10^{-3} bit error rate at approximately 16 dB of SNR. If the no selection case wants to achieve the same performance, the system must have about 18 dB SNR. Moreover, with the increasing number of relays, the BER performances can be improved, i.e., when BER = 10^{-3}, the SNR of 4, 8 and 16 relay cases respectively attain approximately 15.5 dB, 14.5 dB and 14 dB.

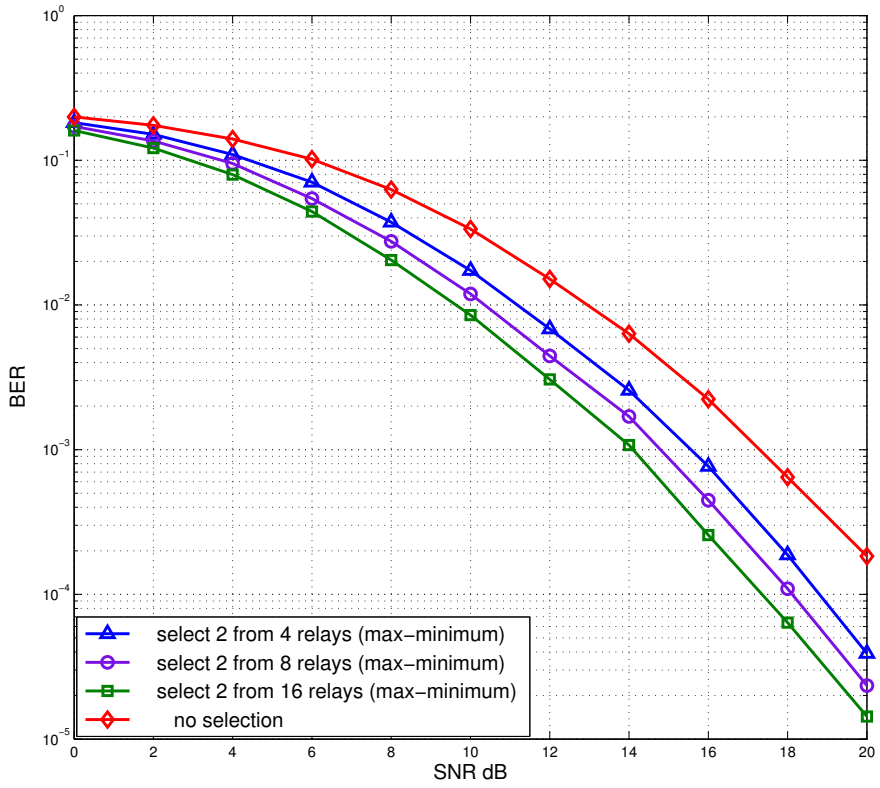

Figure 3.9. Comparison of BER performances of coded distributed Golden Code for two-way transmission with max-minimum relay selection.

Fig. 3.10 shows the comparison of performances of maximum-mean relay selection and no selection. The same case as for the maximum-minimum selection. The performance of selection has advantage over without selection. The superiority is larger than using maximum-minimum selection. Selection is better than without selection by approximately average 2 dB SNR; therefore, the result that the performances of maximum-mean selection outperforms the maximum-minimum selection. That is because the maximum-mean selection can better balance the channel qualities. Generally, when the number of selected relays equal to 4, 8, and 16, the maximum of means selection always has approximately one dB superiority.

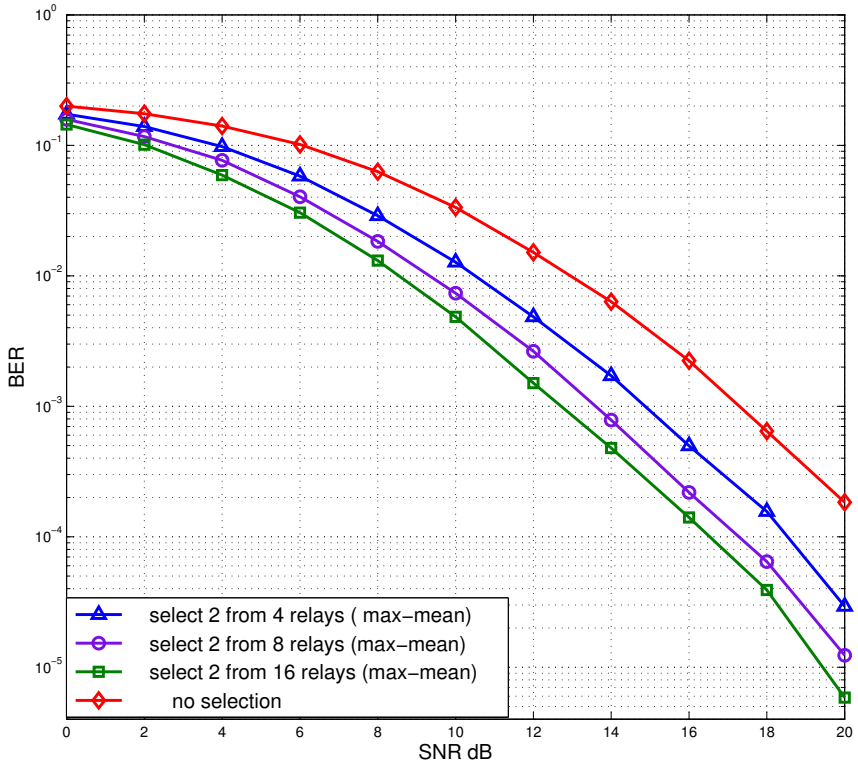

Figure 3.10. Comparison of BER performances of coded distributed Golden Code for two-way transmission with max-mean relay selection.

3.4 Summary

In this chapter, a simple offset transmission with FIC and OFDM scheme for a four path asynchronous cooperative relay system was proposed. In order to achieve asymptotically full data rate the source and one group of relays transmits on even transmission steps whilst on odd transmission steps a different group of relays transmits and the first group receiver. The approach achieves the same diversity of 2 as a previously proposed half rate scheme. OFDM and CP were used at the source to combat timing errors from the source to the destination node. Moreover, through the use of time reversal in the destination node, CP removal is avoided at the relays in order to decrease the complexity of relay decoding. In order to mitigate

the potential reduction in diversity gain due to dependent channel matrix elements in distributed Golden Code transmission, and the rate penalty of multihop transmission, relay selection based on two-way transmission is proposed. Simulation studies were used to evaluate the relative end-to-end BER performance of uncoded, coded, one-way and two-way networks with fixed and selected relays. The maximum-mean relay selection policy was shown to outperform the maximum-minimum approach. In the next chapter, relay selection in distributed relay network using the Golden Code will be introduced.

Chapter 4

RELAY SELECTION IN A DISTRIBUTED RELAY NETWORK USING THE GOLDEN CODE

The implementation of cooperative diversity with relays has advantages over point-to-point MIMO systems in particular overcoming correlated paths due to small inter-element spacing. A simple transmitter with one antenna may moreover exploit cooperative diversity or space time coding gain through distributed relays. In this chapter, similar distributed transmission is considered with a linear dispersion algebraic space-time code, namely the Golden Code, and a strategy for relay selection, called the maximum-mean selection policy, is introduced. This new strategy performs a channel strength tradeoff at every relay node to select the best two relays for transmission. It improves upon the established one-sided selection strategy of maximum-minimum policy. In addition, an effective scheme is proposed to achieve asynchronous distributed transmission with the Golden Code over a two-hop MIMO relay channel. Full ML decoding and sphere decoding (SD) are used as the detection approaches for distributed transmission in the synchronous and asynchronous wireless relay networks. Simulation results comparing the

BER based on different detectors and a scheme without relay selection, with the maximum-minimum and maximum-mean selection schemes confirm the performance advantage of relay selection and that the proposed strategy yields the best performance of the three methods.

4.1 Introduction

In a wireless network, independent paths between the source and destination exist when the multiple users act as relays for each other [42]. Cooperative diversity has been shown to be an effective technique to enable single-antenna users to share their antennas to create a virtual MIMO system [48]. Cooperative diversity has potential application in mobile wireless ad hoc networks. Better system performance gains can be achieved by exploiting relays due to path loss gains as well as diversity and multiplexing gains. In traditional direct link communication systems, it is difficult to achieve high QoS for users, but with the exploitation of relays higher quality and cost effective transmission can be achieved [10].

In recent years there has been considerable effort in the development of cooperative diversity schemes. Various cooperative schemes have been proposed. Among these strategies, perhaps the most important are amplify-and-forward (AF) and decode-and-forward (DF) approaches. For AF schemes, every relay cooperates and just retransmits its received signal scaled by its own transmitted power. For most DF schemes, every relay decodes the transmitted information before retransmitting it using its transmit power [20]. However, using all the relays may not obtain the optimal performance of the relay network, and present practical problems such as asynchronism [36] between the relays. Improved performance can be achieved by selecting the cooperating relays to employ. In particular, selection can aim to find the best relay for solving the problem of multiple relay transmissions by re-

questing only a single relay to forward the information from the source [21]. Such relay selection must be repeated as the channel conditions can change. In [56], a scheme was proposed for opportunistic relaying to exploit cooperative diversity. The scheme relies on distributed path selection considering the instantaneous end-to-end wireless channel conditions, and employs the maximum-minimum selection strategy. Relay selection in cooperative wireless networks with flat fading and frequency selective fading channels is considered in this chapter, with focus on an AF system. However, a maximum-minimum selection strategy cannot best balance the levels among the frequency flat channels for the Golden Code. Therefore, a new relay selection approach called maximum-mean strategy is proposed, and it is used in flat and frequency selective quasi-static fading channel environments.

On the other hand, space-time coding is also used to exploit spatial diversity in traditional point-to-point MIMO systems and in recent years such encoding has been adopted in distributed cooperative networks [57]. While space-time codes for MIMO systems can achieve full spatial diversity, a new full-rate and full-diversity linear dispersion algebraic space-time code based on the Golden number was proposed in [23]. Due to the performance of the algebraic construction, the Golden Code outperforms the Alamouti code in the flat fading channels. However, in frequency selective channels environment, the Golden Code lose its properties because of the inter-symbol interference (ISI) [24]. For overcoming this weakness, the orthogonal frequency division multiplexing (OFDM) modulation can be used. The channel coding is adopted to improve the performance of the Golden Code in MIMO system. The Golden Code also provides full-rank, cubic shaping, non-vanishing minimum determinant and optimal diversity-multiplexing gain tradeoff [15]. It is best matched to a 2×2 coherent MIMO system. The minimum determinant of the Golden Code matrix does not depend on the size of the signal constellation and it achieves the diversity-multiplexing tradeoff (DMT) [15]

and [43], which for the single-antenna non-orthogonal amplify-and-forward (NAF) channel can be characterised by [16],

$$d_{NAF}(r) = (1 - r) + N(1 - 2r)^{+} \tag{4.1.1}$$

where $(x)^{+}$ means the $\max\{x, 0\}$, r is the multiplexing gain and d_{NAF} is the diversity gain, which are given by

$$\lim_{SNR\to\infty} \frac{R(SNR)}{\log SNR} = r \quad \text{and} \quad \lim_{SNR\to\infty} \frac{\log P_e(SNR)}{\log SNR} = -d_{NAF} \tag{4.1.2}$$

where $R(SNR)$ is the data rate measured by bits per channel usage and $P_e(SNR)$ is the average error probability using the ML decoder. The construction of the Golden Code allows application of spatial multiplexing so that it has higher bit rates. Meanwhile, the spatial diversity can improve the bit error performance [1]. These features of the Golden Code should therefore be exploited in distributed transmission in order to improve link performance. A MIMO system using space-time coding techniques can potentially achieve a huge capacity increase over a single wireless link. In such processing, the received signal is given by a linear combination of the data symbols with additive noise. As the best detection method, ML, depends on searching all of the transmitted signal possibilities in the constellation and chooses the closest to the received signals as the estimated transmitted signal [58], but it has high complexity. On the other hand, due to redundant information which can make the space-time system orthogonal, the linear decoder can approach approximate ML performance with lower complexity [59]. For overcoming the weaknesses of ML detection, the sphere decoder was proposed by Pohst in [60].

As mentioned above, practical problems such as asynchronism exist in distributed transmission, while most previous research assumes synchronous transmission. Synchronisation of transmission is a critical issue in exploiting

cooperative diversity in wireless ad hoc networks so that the signals arrive effectively at the destination simultaneously. In a wireless network, the nodes are geographically dispersed and hence the inter-node channels will have varying strengths and delays [61]. In the presence of such time delays, a simple Alamouti space-time transmission scheme for asynchronous cooperative systems is proposed in [36] based on an OFDM scheme. In [62] and [63], the authors respectively proposed a new 2×2 delay tolerant code based on the Golden Code and a bounded delay-tolerant STBC for asynchronous cooperative networks. However, in this chapter, the original Golden Code is still used to transmit over a two-hop MIMO relay channel with asynchronism.

This chapter focuses on multiple relay selection in synchronous and asynchronous distributed transmission based on the Golden Code. Section 4.2.1 and Section 4.2.2 build and analyse the basic fixed relay selection scheme using full ML and SD for detection. Section 4.2.3 elaborates further upon the two different relay selection strategies. In this section, based on previous relay selection strategies of optimal-SNR and maximum-minimum selection, a maximum-mean selection approach for distributed Golden Code transmission is proposed. The SNR-maximising multiple relay selection can be achieved over all relays [20]. However, its complexity is exponential in the numbers of relays in the networks. Computer simulation results are presented in Section 4.2.4 which show the new strategy proposed in this chapter has advantage for a distributed Golden Code in wireless networks. The asynchronous cooperative transmission schemes with the Golden Code over flat fading and frequency selective channels are shown in Section 4.3.1 and Section 4.4.1. Two strategies for relay selection in the asynchronous cooperative transmission are also elaborated in Section 4.4.2. Finally, the simulation results and summary are drawn in Section 4.4.3 and Section 4.5, respectively.

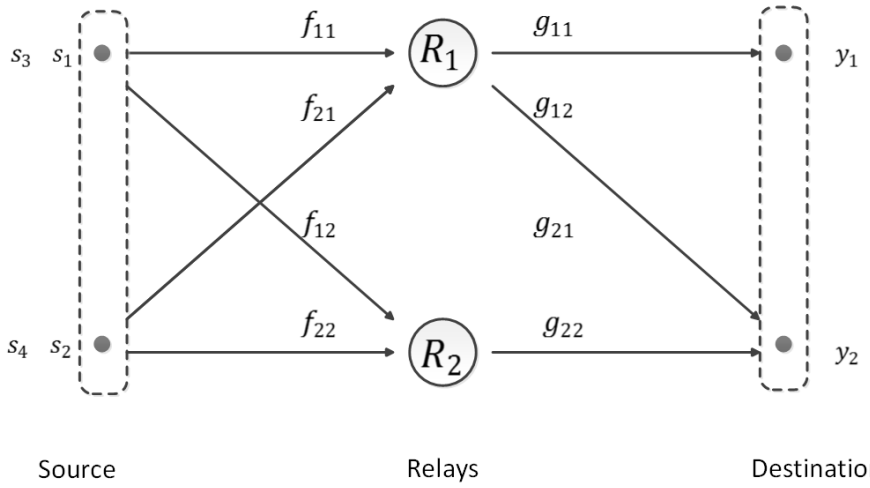

Figure 4.1. The two-input two-output relay network transmission structure for the Golden Code.

4.2 Relay Selection Based on the Golden Code in Synchronous Wireless Networks

4.2.1 Fixed Relay Scheme with the Golden Code

For satisfying the basic environment of a 2×2 MIMO channel when transmitting a Golden Code, the fixed relay scheme adopts the model shown in Fig. 4.1. It is composed of one source, two relays and one destination. There are respectively two antennas at the source and the destination, but only one antenna at each relay. Each node is half-duplex. The information symbols are coded with the Golden Code in the source rather than in the relays. The channels are quasi-static Rayleigh flat fading with coefficients f_{ij} and g_{ji}, which are i.i.d. complex Gaussian random variables with zero-mean and unit-variance, subscript i represents the ith antenna at the source and the destination, and j denotes the jth relay. There are two transmission phases in the model. In step one, from (3.3.1), s_1 and s_2 are broadcast respectively by the source to the destination through relays R_1 and R_2, and then the

source broadcasts s_3 and s_4 in the second symbol period. Mathematically, the signal received by the jth relay can be expressed as

$$r_j^k = \sqrt{P_t}(s_{2k-1}h_{1j} + s_{2k}h_{2j}) + n_{rj}^k, \tag{4.2.1}$$

where P_t denotes the average transmit power of the source, and $k \in (1, 2)$ is the symbol index; n_{rj}^k is the AWGN at the jth relay. The signal received by the ith antenna of the destination, during the relaying phase, can be expressed as

$$y_i^k = \sum_{j=1}^{2} \sqrt{P_r} r_j^k g_{ji} + n_{di}^k, \tag{4.2.2}$$

where P_r represents the average transmit power of the relay node, n_{di}^k is the AWGN at the ith antenna of the destination. The power of every transmitting antenna in the source and relays is given by

$$P_t = P_r = \frac{P}{2A}, \tag{4.2.3}$$

where P is the total transmit power of the system [5], and A denotes the number of relays used. The vector of symbols received at the destination across the two antennas is denoted as $\mathbf{y}$. Thus, the received signal can be written as

$$\mathbf{y} = \mathbf{H}\mathbf{s} + \mathbf{n}, \tag{4.2.4}$$

where $\mathbf{y}$ is the vector $\begin{bmatrix} y_1^1 & y_2^1 & y_1^2 & y_2^2 \end{bmatrix}^T$ and $\mathbf{s}$ is the source vector $\begin{bmatrix} s_1 & s_2 & s_3 & s_4 \end{bmatrix}^T$. $\mathbf{H}$ is a 4×4 block diagonal matrix of effective transmission channels which is given by

$$\mathbf{H} = \begin{bmatrix} \mathbf{M} & \mathbf{0} \\ \mathbf{0} & \mathbf{M} \end{bmatrix} \tag{4.2.5}$$

where,

$$\mathbf{M} = \begin{bmatrix} f_{11}g_{11} + f_{12}g_{21} & f_{21}g_{11} + f_{22}g_{21} \\ f_{11}g_{12} + f_{12}g_{22} & f_{21}g_{12} + f_{22}g_{22} \end{bmatrix}, \tag{4.2.6}$$

and $\mathbf{0}$ represents a 2×2 full zero matrix. The total noise $\mathbf{n}$ is the vector $\begin{bmatrix} n_1^1 & n_2^1 & n_1^2 & n_2^2 \end{bmatrix}^T$. The elements of $\mathbf{n}$ can be written as

$$n_i^k = \sum_{j=1}^{2} \sqrt{P_r} n_{rj}^k g_{ji} + n_{di}^k. \tag{4.2.7}$$

As known the received signals above, next section will focus on the comparison of decoding approaches such as Maximum-likelihood decoding and Sphere decoding.

4.2.2 Maximum-likelihood Decoding and Sphere Decoding

Maximum-likelihood Decoding

First, the full ML approach is used for decoding the Golden Code:

$$\hat{\mathbf{s}} = arg \min_{\mathbf{s} \in \mathbf{S}_c} \{\|\mathbf{y} - \mathbf{H}\mathbf{s}\|_2\}, \tag{4.2.8}$$

where $\mathbf{S}_c$ denotes the collection of all member of the symbol constellation. The principle of ML detection is to compare all possible values of the received signals and transmitted one-by-one, and then to take the closest one to be the estimated signal [2]. In the AWGN channel environment, in the sense of obtaining the minimum BER for every antenna, this decoding approach has the best performance. From (4.2.8), when calculating one $\hat{\mathbf{s}}$, it has to compare one-by-one all the possible signals transmitted to determine the estimated signals. Therefore, with the increasing number of transmitted antennas and modulation levels, the complexity of maximum-likelihood detection increases exponentially. It causes so large a calculation that it would be very difficult to realize. For overcoming this computational complexing

weakness of ML, lower complexity sphere decoding is applied.

Sphere Decoding

All possible received signals can be represented in a lattice structure, therefore, the SD algorithm is easily used for decoding the MIMO system [64]. The principle of the SD algorithm is to search the closest lattice points to the received signal within a radius c of a sphere centred at the particular received signal value [65]. The choice of c is crucial to the speed of the algorithm. Decreasing the radius r, the number of signal points to be searched can be reduced and the speed of calculation will rise [66], however the performance of the decoding may be affected.

A. Initial Radius

As for the basic ML algorithm (4.2.8), the sphere decoder of the Golden Code searches over only a radius c centred around the received signal vector, i.e. $\|\mathbf{y} - \mathbf{Hs}\|^2 \leq c^2$ [67]. From (3.3.1), the new channel matrix $\widetilde{\mathbf{H}}$ can be obtained

$$\widetilde{\mathbf{H}} = \frac{1}{\sqrt{5}} \begin{bmatrix} \varphi & \varphi\theta \\ \bar{\varphi} & \bar{\varphi}\bar{\theta} \end{bmatrix}. \tag{4.2.9}$$

Therefore, the initial radius can defined as [1]

$$c^2 = \left\| \mathbf{y} - \tilde{\mathbf{H}}\mathbf{s}_{zf} \right\|_2, \tag{4.2.10}$$

where $\mathbf{s}_{zf}$ denotes the initial estimate, which is the Zero-Forcing (ZF) detection solution. Therefore,

$$\mathbf{s}_{zf} = \tilde{\mathbf{H}}^{+}\mathbf{y}, \tag{4.2.11}$$

where $\tilde{\mathbf{H}}^{+}$ denotes the pseudo-inverse of $\tilde{\mathbf{H}}$

$$\tilde{\mathbf{H}}^{+} = (\tilde{\mathbf{H}}^{T}\tilde{\mathbf{H}})^{-1}\tilde{\mathbf{H}}^{T}. \tag{4.2.12}$$

B. Derivation

Assuming the channel is known at the receiver and taking the QR factorisation of the channel matrix $\tilde{\mathbf{H}}$ (4.2.9)

$$\tilde{\mathbf{H}} = \mathbf{Q} \begin{bmatrix} \mathbf{R} \\ \mathbf{0} \end{bmatrix}, \tag{4.2.13}$$

where $\mathbf{R}$ is an upper triangular matrix with positive diagonal elements, $\mathbf{0}$ is a null matrix, and $\mathbf{Q} = \begin{bmatrix} \mathbf{Q}_1 & \mathbf{Q}_2 \end{bmatrix}$ is unitary matrix. Therefore,

$$\begin{aligned} c^2 &\geq \left\| \mathbf{y} - \begin{bmatrix} \mathbf{Q}_1 & \mathbf{Q}_2 \end{bmatrix} \begin{bmatrix} \mathbf{R} \\ \mathbf{0} \end{bmatrix} \mathbf{s} \right\|_2 = \left\| \begin{bmatrix} \mathbf{Q}_1^* \\ \mathbf{Q}_2^* \end{bmatrix} \mathbf{y} - \begin{bmatrix} \mathbf{R} \\ \mathbf{0} \end{bmatrix} \mathbf{s} \right\|_2 \\ &= \|\mathbf{Q}_1^* \mathbf{y} - \mathbf{R}\mathbf{s}\|_2 + \|\mathbf{Q}_2^* \mathbf{y}\|_2. \end{aligned} \tag{4.2.14}$$

where $(\cdot)^*$ here denotes Hermitian matrix transposition, and

$$c^2 - \|\mathbf{Q}_2^* \mathbf{y}\|_2 \geq \|\mathbf{Q}_1^* \mathbf{y} - \mathbf{R}\mathbf{s}\|_2 \tag{4.2.15}$$

are easily obtained. Setting $y^{'} = \mathbf{Q}_1^* \mathbf{y}$ and $c^{'2} = c^2 - |\mathbf{Q}_2^*|\mathbf{y}$, (4.2.15) can be rewritten as

$$c^{'2} \geq \sum_{i=1}^{m} (y_i^{'} - \sum_{j=i}^{m} r_{i,j} s_j)^2, \tag{4.2.16}$$

where $r_{i,j}$ denotes the (i, j) entry of $\mathbf{R}$. Expanding (4.2.16) yields

$$c^{'2} \geq (y_m^{'} - r_{m,m} s_m)^2 + (y_{m-1}^{'} - r_{m-1,m} s_m - r_{m-1,m-1} s_{m-1})^2 + \cdots. \tag{4.2.17}$$

From (4.2.17), the first term depends only on s_m, the second term depends on $\{s_m, s_{m-1}\}$ and so on. Therefore, a necessary condition $c^{'2} \geq (y_m^{'} - r_{m,m} s_m)^2$ leads to

$$\left\lceil \frac{-c^{'} + y_m^{'}}{r_{m,m}} \right\rceil \leq s_m \leq \left\lfloor \frac{c^{'} + y_m^{'}}{r_{m,m}} \right\rfloor, \tag{4.2.18}$$

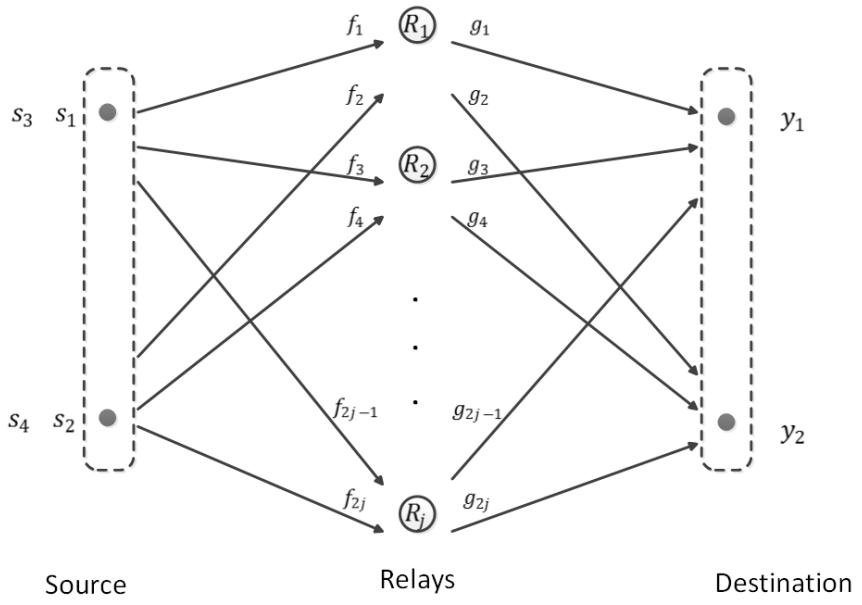

Figure 4.2. Relay selection scheme with the Golden Code in distributed wireless networks.

where $\lceil \cdot \rceil$ and $\lfloor \cdot \rfloor$ denote rounded up and rounded down. For every s_m satisfying (4.2.18), s_{m-1} in (4.2.17) can be obtained. According to the iteration, s_{m-2} can be easily found. Three results can be obtained: if $c^{'} < c$, the initial radius is changed to $c^{'}$; if not, the process has to return to the last step to continue to calculate until the entire set $\{s_m, s_{m-1}, \cdots, s_2, s_1\}$ is found; if the entire collection cannot be found, the value of the initial radius needs to be increased. In the simulation section of this chapter, the simulation results of the Golden Code with ML detection and SD will be given.

4.2.3 Relay Selection with the Golden Code

A multi-relay selection strategy approach is represented in Fig. 4.2 for distributed Golden Code transmission in wireless networks. In the figure, the channels from the source to the jth relay are denoted as f_j and from jth relay to the destination as g_i. All of assumptions are the same as the sys-

tem model of Fig. 4.1. Firstly, the maximum-minimum selection method is adopted, then, a selection scheme which finds the mean of maximum value among the channels is used. The aim is to select the best two relays from j relays for transmission in the cooperative network as in Section 3.3.3.

A. Maximum-minimum selection

The conventional strategy of relay selection was first considered in [56] for distributed two-hop implementation. It required no explicit communication among the relays and is based on local measurements of the instantaneous channel conditions from the source to relays and relays to the destination in slow fading wireless environments, however, the approach that is considered in this work is somewhat different. To achieve basic 2×2 MIMO transmission channels, each relay node has four channel connections. Two channels from the source to the relay denoted by f_{2j-1} and f_{2j}, and two other channels from the relay to the destination denoted g_{2j-1} and g_{2j}. Then, the best and the second best relays from the j available relays are chosen as the most effective for transmission. For example, in Fig. 4.2, comparing these four channels for the jth relay, the worst channel is found as

$$R_{min}^{(j)} = \min\{|f_{2j-1}|^2, |f_{2j}|^2, |g_{2j-1}|^2, |g_{2j}|^2\}. \tag{4.2.19}$$

These values are then calculated for all of the relays and stored in the vector $\mathbf{R}_{min}$. The relay corresponding to the maximum of these minima is selected, together with the relay which has the maximum of the remaining minima.

B. Maximum-mean selection

The second selection approach is based on calculating the mean of the strengths of the channels connected to each relay. The mean of these four

channels for the jth relay is obtained as

$$R_{mean}^{(j)} = \frac{|f_{2j-1}|^2 + |f_{2j}|^2 + |g_{2i-1}|^2 + |g_{2i}|^2}{4}. \tag{4.2.20}$$

This mean value is then calculated for all relays and stored in the vector $\mathbf{R}_{mean}$. The relay with the maximum value of these minima is selected as the relay with the maximum of the remaining means. Comparing with the maximum-minimum selection, this method can better balance the level among the channels, since the maximum-minimum selection just depends on the minimum value of one channel, rather than an overall performance measure. Therefore, the maximum-mean selection can be better for relay selection. In the next section, the performance of these schemes is evaluated.

4.2.4 Simulation Results

In this simulation section, first the full diversity and full rate Golden Code with 4-QAM is used in the point-to-point MIMO system and the distributed MIMO system. The number of transmit antennas and receive antennas is two, and the number of available relays is two. The assumptions are that the channels are quasi-static flat fading and perfectly known at the receiver. Fig. 4.3 and Fig. 4.4 show the BER performances with increased SNR.

Fig. 4.3 is the comparison of the performances of the Golden Code in the point-to-point MIMO system with the maximum-likelihood detection, the sphere detection with the radius 2 and zero-forcing detection. Clearly, from 0 dB to 8 dB SNR, the performance of SD is worse than the ML approach. When the SNR is approximately 0 dB, almost every symbol is decoded in error when using SD. However, the slope of the SD curve decreases rapidly. Therefore, when the SNR equals to approximately 8 dB, the meeting point with these two curves occurs, and after that, the performance of SD can reach the performance of ML. On the other hand, due to using zero-

forcing detection, the noise is increasing by $\mathbf{H}^{\dagger}\mathbf{n}$, where $\mathbf{H}^{\dagger}$ is the Moore pseudo-inverse of the channel matrix. Therefore, the performance curve of zero-forcing detection is much worse than ML detection and SD.

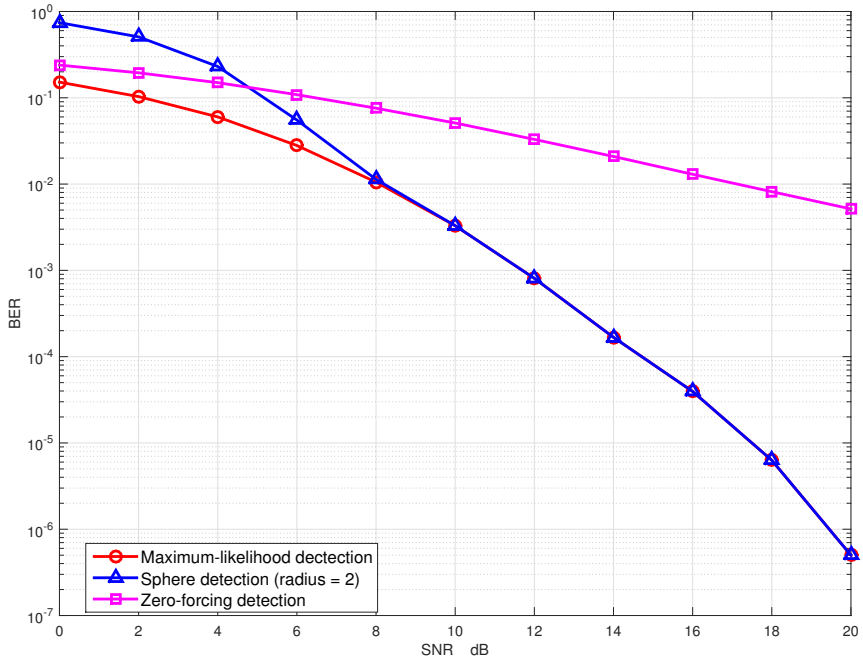

Figure 4.3. Bit error rate performances of the Golden Code in the MIMO system with the maximum-likelihood detection, the sphere detection and zero-forcing detection.

Fig. 4.4 shows the comparison of the performances of the Golden Code in the distributed MIMO system with different radii in the sphere decoding. The simulation is based on radius values of 2, 5 and 8. Therefore, it is easy to show that the BER of the system decreased with increasing the value of SNR. When the radius is equal to 5 and 8, the performances of the system are nearly the same at 8 dB of SNR, after that these two are always the same. When the radius is 2, the system performance approaches to the performance of the system with radii 5 and 8 at 10 dB SNR. Therefore, for high SNR, based on the different radii of sphere detection the performance of the system is nearly the same.

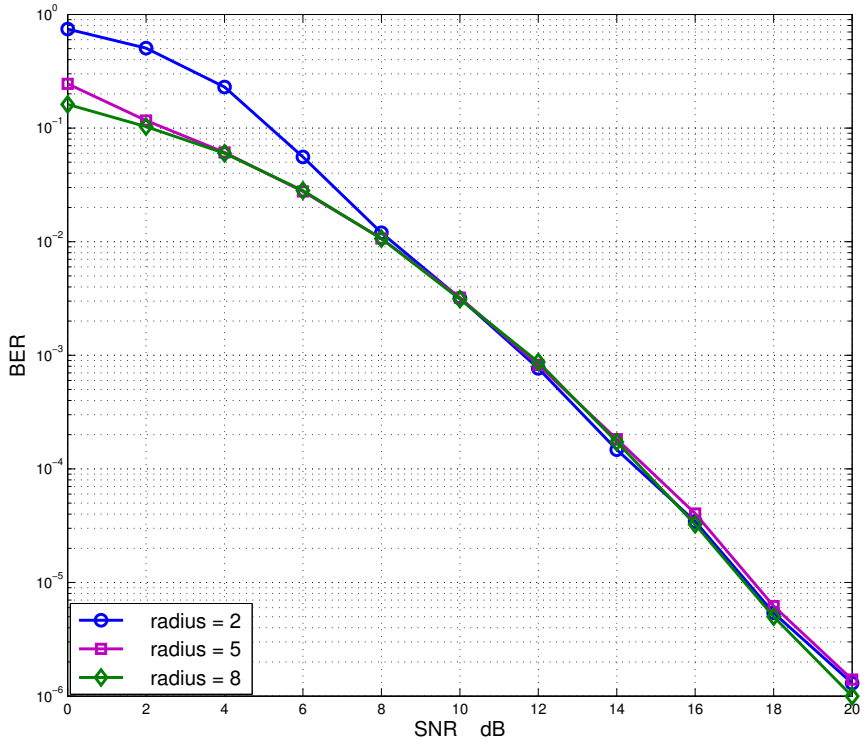

Figure 4.4. Bit error rate performances of the Golden Code in the distributed MIMO system with the different radii of the sphere decoding.

Secondly, the simulated performance of the relay selection with distributed transmission based on the Golden Code in wireless networks is studied. The performance is shown by BER using QPSK symbols. The total transmission power of the system is fixed as P and the additive noise variance at each receiving node is unity. The selection of two relays from a total of 4, 6 and 8 relays is for the above two different selection strategies.

In Fig. 4.5, the BER performances of fixed relay and maximum-minimum relay selection schemes are compared. The BER performance with fixed relays is clearly worse than with the maximum-minimum relay selection. For example, to obtain BER performance of 10^{-3} with four participated relays, the maximum-minimum relay selection scheme needs essentially 13 dB total power, P, but the fixed relay system requires almost 14 dB. The

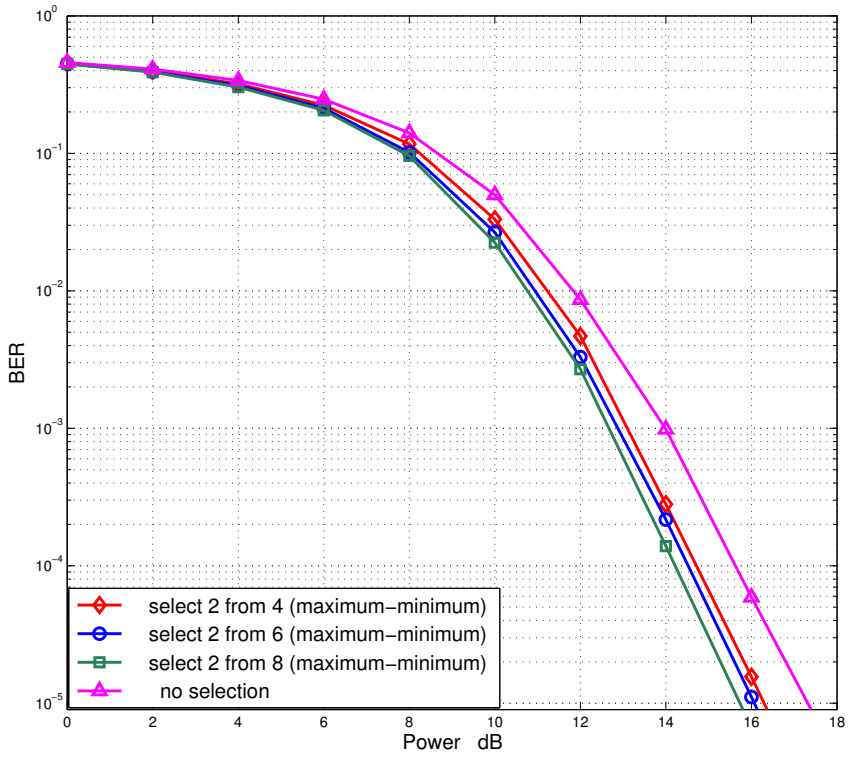

Figure 4.5. Bit error rate performances of maximum-minimum relay selection with Golden Code based transmission.

figure also shows a small improvement in performance as the total number of relays is increased.

Fig. 4.6 includes the simulation results of BER performance of the maximum-mean relay selection and the fixed relay scheme. Obviously, the BER performance of the maximum-mean relay selection outperforms the fixed relay scheme. For example, the selection case requires approximately 12 dB of total power, P, and the power of the no selection case is 14 dB at BER 10^{-3}. Moreover, with increasing the total number of relays, the BER performances can be improved, i.e., when BER $= 10^{-3}$, the total transmission powers of the 4, 6 and 8 relay cases respectively need approximately 13.5 dB, 12.5 dB and 12 dB.

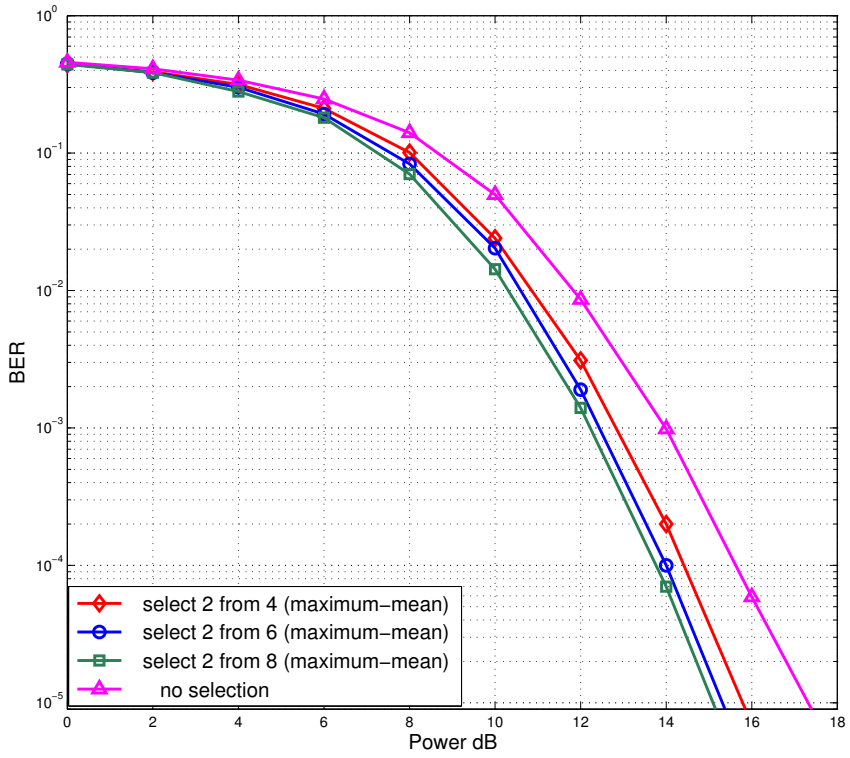

Figure 4.6. Bit error rate performances of maximum-mean relay selection with Golden Code based transmission.

Fig. 4.7 shows a direct comparison of performances of maximum-minimum strategy and maximum-mean strategy. The dashed curves represent the performances of maximum-minimum selection, and the solid curves show the performances of maximum-minimum selection. Clearly, the maximum-mean scheme shows a small advantage. Generally, when the number of selected relays equals to 4, 6, and 8, the maximum of means selection always has approximately 1 dB superiority. That is because the maximum-mean selection can better balance the channel qualities.

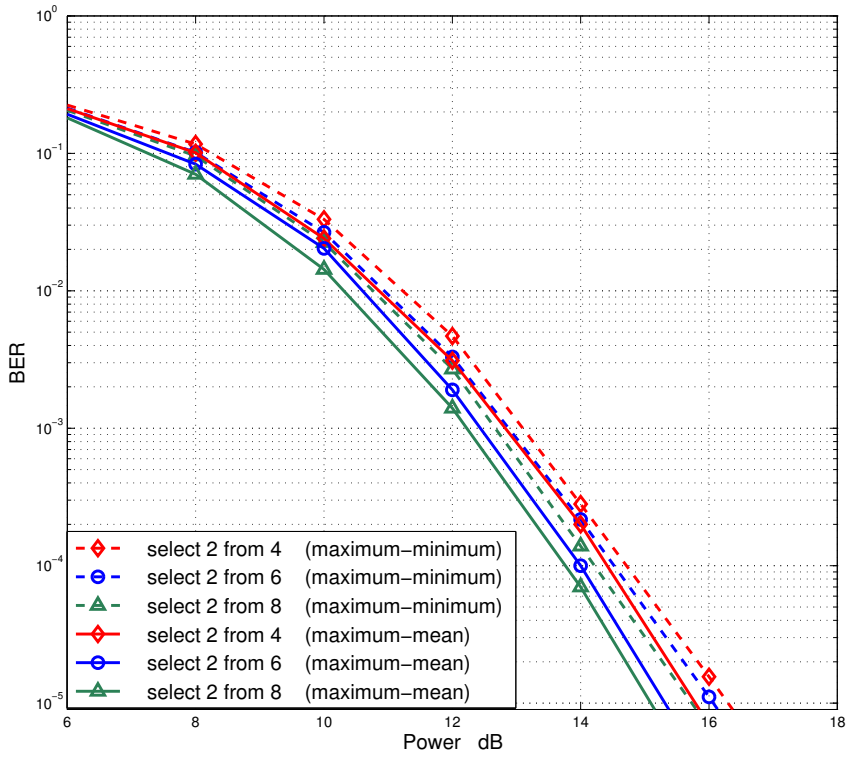

Figure 4.7. Bit error rate performances of maximum-minimum strategy and maximum-mean strategy with Golden Code based transmission.

4.3 Transmission strategy of the Golden Code in coded MIMO-OFDM System

4.3.1 Channel Models

The coherence bandwidth measures the separation in frequency after which two signals will experience uncorrelated fading [43]. In flat fading, the coherence bandwidth of the channel is larger than the bandwidth of the signal. Therefore, all frequency components of the signal will experience the same magnitude of fading. In frequency-selective fading, the coherence bandwidth of the channel is smaller than the bandwidth of the signal. Different frequency components of the signal therefore experience varying levels of fading.

A. Flat Fading MIMO Channel

The delays associated with different signal paths in a multipath fading channel change in an unpredictable manner and can only be characterised statistically. When there is a large number of paths, the central limit theorem can be applied to model the time-variant impulse response of the channel as a complex-valued Gaussian random process [43]. When the impulse response is modelled as a zero mean complex-valued Gaussian process, the channel is said to be a Rayleigh fading channel. If the coherence bandwidth of the channel is much greater than the bandwidth of the signal, the channel is frequency-flat since it affects all signal frequencies in essentially the same manner [43]. A frequency-flat $N_t \times N_r$ MIMO link can be modelled by

$$\mathbf{r} = \mathbf{H}\mathbf{x} + \mathbf{n}, \tag{4.3.1}$$

where $\mathbf{r} \in C^{N_r \times 1}$ is the received vector, $\mathbf{x} \in C^{N_t \times 1}$ is the transmitted vector and $\mathbf{n} \in C^{N_r \times 1} \sim \mathcal{CN}(\mathbf{0}_{N_r \times 1}, \mathbf{N}_0\mathbf{I}_{N_r})$ is the noise vector, and $\mathbf{H}$ is the MIMO channel matrix.

B. Frequency Selective MIMO Channel

Frequency selective channels are characterised by a constant gain and linear phase response over a bandwidth which is smaller than the bandwidth of the signal to be transmitted [24]. Equivalently, in the time domain, the length of the impulse response of the channel is equal to or longer than the width of the modulation signal in high data rate wireless systems. For frequency-selective MIMO channels, the channel impulse response between the q^{th} transmitted antenna and p^{th} received antenna is modelled by

$$h^{p,q}(t) = \sum_{l=0}^{L-1} h^{q,p}(l)\delta(t-l), \tag{4.3.2}$$

where $q = 1, \ldots, N_t$ and $p = 1, \ldots, N_r$. The parameter $h^{q,p}(l)$ is the strength of the l^{th} path from the q^{th} transmitting antenna to the p^{th} receiving antenna and L is the length of all impulse responses. Thus, the received signal $r^p(t)$ at the p^{th} received antenna is

$$r^p(t) = \sum_{q=1}^{N_t} \sum_{l=0}^{L-1} h^{q,p}(l) x^q(t-l) + n^p(t) \tag{4.3.3}$$

where $x^q(t)$ is the symbol scalar transmitted by the q^{th} antenna and $n^p(t)$ is an AWGN scalar. For the received signal vector, it also can be written as

$$\mathbf{r}(t) = \sum_{l=0}^{L-1} \mathbf{H}(l)\mathbf{x}(t-l) + \mathbf{n}(t), \tag{4.3.4}$$

where $\mathbf{r}(t)$ is the received vector of dimension $N_r \times 1$. Assuming $N_r < N_t$, $\mathbf{H}(l)$ is defined as

$$\begin{bmatrix} h^{1,1}(l) & 0 & 0 & \ldots & 0 \\ 0 & h^{2,2}(l) & 0 & \ldots & 0 \\ \vdots & \ddots & \ddots & \ddots & \vdots \\ 0 & 0 & \ldots & h^{N_r,N_t}(l) & 0 \end{bmatrix}, \tag{4.3.5}$$

and $\mathbf{x}(t)$ is the transmitted vector of dimension $N_t \times 1$ and $\mathbf{n}(t)$ is the AWGN noise vector of dimension $N_r \times 1$. Next, a distributed asynchronous MIMO channel is considered.

4.3.2 System Model

In this section, the Golden Code is used in the MIMO-OFDM system model as Fig. 4.8. The transmitted binary source sequence s_i is 4-QAM modulated. The 4-QAM symbols s_k go through Series-Parallel (S/P) and form as v_k signals. v_k are then encoded using convolutional channel coding and encoded using the Golden Code matrix (3.3.1).

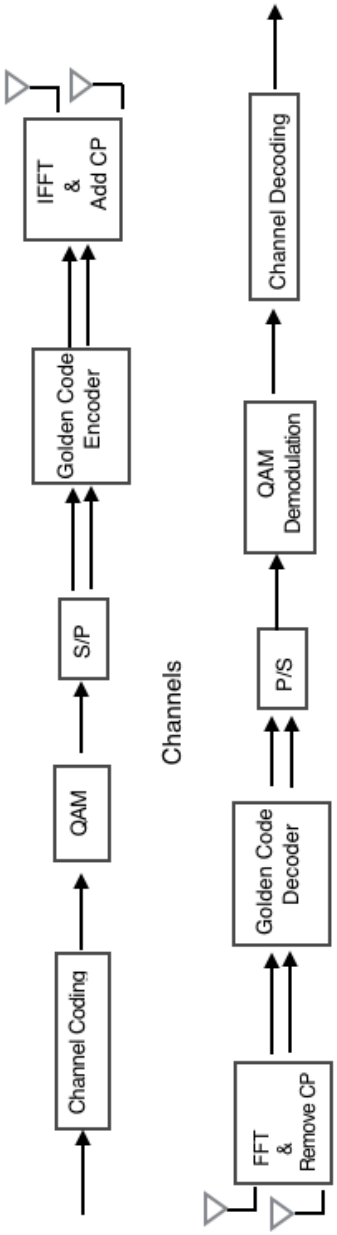

Figure 4.8. The coded MIMO-OFDM transceiver structure within the Golden Code.

x_k is then fed to OFDM modulators with n_c subcarriers and a cycle prefix (CP) of length n_g. The two columns of (3.3.1) is transmitted by two antennas. The sequence x_k^q is at the q^{th} OFDM modulator, where $q^{th}(q = 1, 2)$ column of (3.3.1). The OFDM modulator uses an inverse fast Fourier transform (IFFT) module and a CP is added. The overall vectors of length $n_c + n_g$ are transmitted over a frequency and time selective MIMO channels. The CP length n_g is assumed to be longer than the largest multipath delay spread in order to avoid OFDM inter-symbol interference. $\mathbf{x}_{n,k}$ is the $n_t \times 1$ MIMO vector to be transmitted on the n^{th} subcarrier at time k. The k^{th} MIMO-OFDM symbol is then given by

$$\mathbf{u}_k = \xi_1 \sqrt{n_c}(\mathbf{F}^{-1} \otimes \mathbf{I}_n t)\mathbf{x}_k \tag{4.3.6}$$

where $\mathbf{F}^{-1}$ is the $n_c \times n_c$ Fourier matrix, of which the element is $\exp(-j2\pi nk/n_c)$, $\otimes$ is the Kronecker product, $\mathbf{I}_n t$ represents the n_t identity matrix, and $\mathbf{x}_k$ is an vector $n_c n_t \times 1$ vector given by

$$\mathbf{x}_k = \begin{pmatrix} \mathbf{x}_{1,k} \\ . \\ . \\ . \\ \mathbf{x}_{n,k} \end{pmatrix} \tag{4.3.7}$$

and ξ_1 is the CP adding matrix given by

$$\xi_1 = \left[\begin{pmatrix} 0 & \mathbf{I}_n g \\ & \mathbf{I}_n c \end{pmatrix} \otimes \mathbf{I}_n t \right] \tag{4.3.8}$$

The $n_t(n_c + n_g)$ length MIMO-OFDM symbol is transmitted over a frequency selective channel. As mentioned above, the channel impulse response between q^{th} transmitting antenna and p^{th} receiving antenna is given by a

tapped delay line (4.3.2) as [24]. The channel taps sequence $h_k^{p,q}(l)$ is a correlated complex Gaussian process with zero mean, the same variance σ_h^2. Therefore, the received signal during the k^{th} MIMO-OFDM symbol is

$$\mathbf{y}_k^p = \sum_{q=1}^{n_t} \sum_{l=0}^{L-1} h_k^{p,q}(l)\mathbf{u}_k^q(k-l) + \mathbf{w}_k^p \tag{4.3.9}$$

where $\mathbf{u}_k^q$ is the symbol vector transmitted by the q^{th} antenna and $\mathbf{w}_k^p$ is a zero mean white Gaussian complex noise.

In order to decode the Golden Code by sphere decoding, the code matrix has to be vectorized, furthermore real and imaginary part are separated. Thereby, an 8×8 real part matrix $\mathbf{R}$ can be obtained as

$$\mathbf{R} = \sqrt{\frac{1}{5}} \begin{bmatrix} 1 & -\sigma(\theta) & \theta & 1 & 0 & 0 & 0 & 0 \\ \sigma(\theta) & 1 & -1 & \theta & 0 & 0 & 0 & 0 \\ 0 & 0 & 0 & 0 & -\theta & -1 & 1 & -\sigma(\theta) \\ 0 & 0 & 0 & 0 & 1 & -\theta & \sigma(\theta) & 1 \\ 0 & 0 & 0 & 0 & 1 & -\sigma(\theta) & \theta & 1 \\ 0 & 0 & 0 & 0 & \sigma(\theta) & 1 & -1 & \theta \\ 1 & -\theta & \sigma(\theta) & 1 & 0 & 0 & 0 & 0 \\ \theta & 1 & -1 & \sigma(\theta) & 0 & 0 & 0 & 0 \end{bmatrix} \tag{4.3.10}$$

and signal sent over a channel also described by 8×8 matrix $\mathbf{H}_O$

$$\mathbf{H}_O = \begin{bmatrix} Re(h_{11}) & -Im(h_{11}) & Re(h_{12}) & -Im(h_{12}) & 0 & 0 & 0 & 0 \\ Im(h_{11}) & Re(h_{11}) & Im(h_{12}) & Re(h_{12}) & 0 & 0 & 0 & 0 \\ Re(h_{21}) & -Im(h_{21}) & Re(h_{22}) & -Im(h_{22}) & 0 & 0 & 0 & 0 \\ Im(h_{21}) & Re(h_{21}) & Im(h_{22}) & Re(h_{22}) & 0 & 0 & 0 & 0 \\ 0 & 0 & 0 & 0 & Re(h_{11}) & -Im(h_{11}) & Re(h_{12}) & -Im(h_{12}) \\ 0 & 0 & 0 & 0 & Im(h_{11}) & Re(h_{11}) & Im(h_{12}) & Re(h_{12}) \\ 0 & 0 & 0 & 0 & Re(h_{21}) & -Im(h_{21}) & Re(h_{22}) & -Im(h_{22}) \\ 0 & 0 & 0 & 0 & Im(h_{21}) & Re(h_{21}) & Im(h_{22}) & Re(h_{22}) \end{bmatrix} \tag{4.3.11}$$

Finally, the decoding of the 8-dimensional lattice with generator matrix $\mathbf{HR}$ can be performed using the sphere decoding.

4.3.3 Channel Coding - Convolutional Code

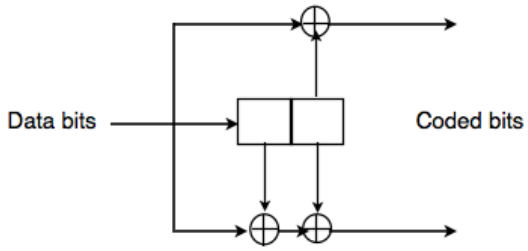

Figure 4.9. Block diagram for a simple convolutional encoder.

Convolutional codes was invented in 1954 by P.Elias, constitute a family of error correcting codes whose decoding simplicity and good performances [68]. However, the convolutional codes do not device a defined block structure. A continuous flowing data stream will be encoded into a continuously flowing code word. The length of a code word is given by other requirements than the structure of the code. Convolutional encoder is a linear and time-invariant system given by the convolution of a binary data stream with generator sequences. Fig.4.9 shows a simple example of such an encoder with rate $R_c = 1/2$ and memory $m = 2$.

Given an input bit stream b_i, a convolutional encoder of code rate $R_c = 1/n$ produces n parallel data streams $c_{v,i}$, $v = 1, \cdots, n$ that may be multiplexed to one serial code word before transmission. Therefore, it can be written as

$$c_{v,i} = \sum_{k=0}^{m} g_{v,k} b_{i-k}, \tag{4.3.12}$$

where setting $b_i = 0$ and $g_{v,k}(v = 1, \cdots, n); (k = 0, \cdots, m)$ are the generators that can also be written as generator polynomials

$$g_v(D) = \sum_{k=0}^{m} g_{v,k} D^k, \tag{4.3.13}$$

where D is a formal variable that can be interpreted as delay [68]. Using example Fig. 4.9 can obtain

$$g_1(D) = 1 + D^2 \equiv (101) \equiv 5_o ct$$
$$g_2(D) = 1 + D + D^2 \equiv (111) \equiv 7_o ct.$$

Above formula are the binary vector notation and the octal notation for the generators. While, adopting the above coded word in coded MIMO-OFDM system simulated the performance of the Golden Code transmission.

4.3.4 Simulation Results

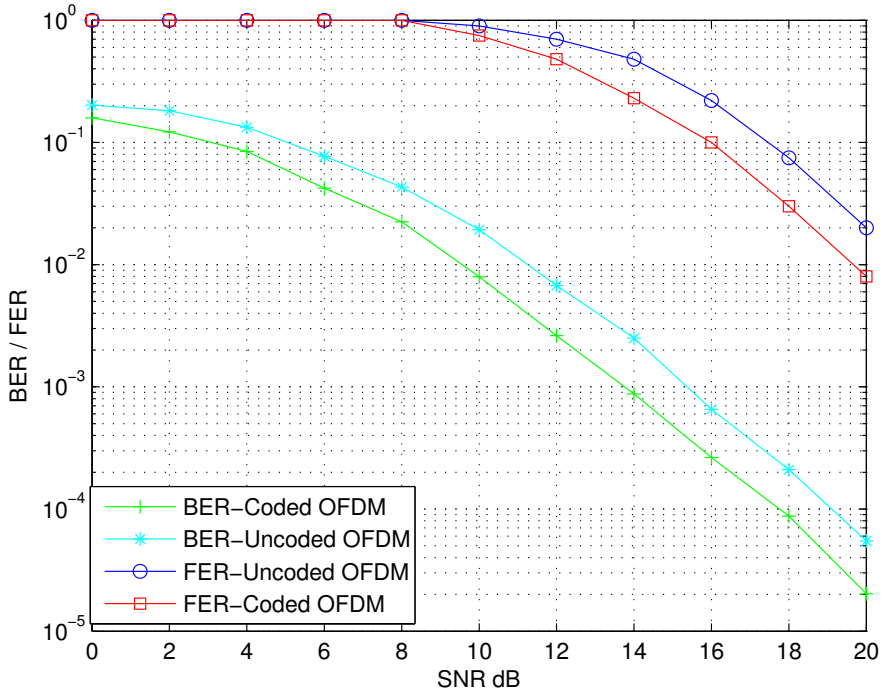

Figure 4.10. The BER and FER performances of the Golden Code in uncoded and coded MIMO-OFDM.

Fig.4.10 shows the simulated results on the performances of the Golden Code in uncode and coded MIMO-OFDM system. QPSK symbols are trans-

mitted at the source. The length of symbol is 128, CP sets the length of 32 and the channel length is 3. The decoding approach is full maximum-likelihood. It is clear that the bit error rate of MIMO-OFDM system with channel coding outperforms the no channel coding approximately 2 dB generally in the same error bits case. i.e. when SNR is from 4 dB to 20 dB. Moreover, increasing with the values of SNR, this gap is increasing as well. The other performance frame error rate (FER) of the Golden Code in uncoded and coded MIMO-OFDM is also shown in Fig.4.10. The curve with circle mark is the Golden Code in uncoded system and with square mark is the Golden Code in coded system. From 0 dB to 8 dB SNR, every frame is uncorrect, therefore the FER values always equal to 1 for these two curves. After 10 dB of SNR, the curves decreased. However, the SNR value of coded system outperforms uncoded system approximate 2 dB when the FER is fixed.

4.4 Relay Selection over Asynchronous Two-hop MIMO Relay Channels

4.4.1 System Model

Due to the basic transmission environment of the Golden Code, a 2×2 MIMO channel scheme is adopted. The cooperative scheme in general contains two phases of transmission, a broadcast phase and a cooperation phase as represented in Fig. 4.11. The network is composed of one source, j relays and one destination. There are respectively two antennas at the source and the destination, but only one antenna at each relay. Each node is half-duplex. The information symbols are coded with the Golden Code in the source rather than in the relays. As mentioned, these j relay nodes are geographically dispersed, with a random time delay τ in the cooperation phase. For instance, there is a τ time difference between the signals from

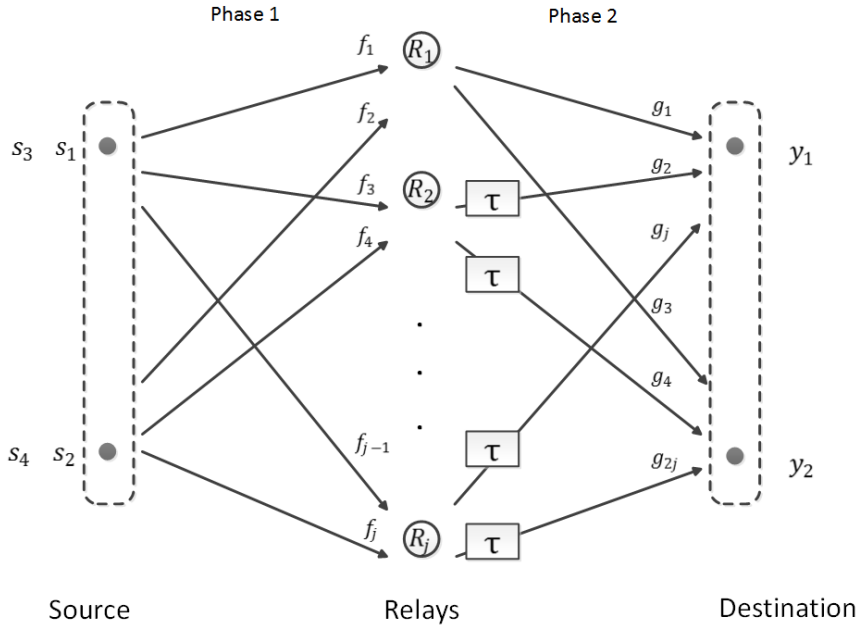

Figure 4.11. Relay selection with the Golden Code in an asynchronous two-hop MIMO wireless network.

the R_1 relay and the signals from R_2 to the destination node. Moreover, the length of the cyclic prefix $l_{cp} \geqslant \tau + L$ and the subcarriers are orthogonal to each other. The other assumption is that the channels are either quasi-static Rayleigh flat fading or frequency selective fading with coefficients f_j and g_j, or sets of L coefficients which are i.i.d. complex Gaussian random variables with zero-mean and unit-variance, subscript j denotes the jth relay.

A. Implementation at the source

The block diagram Fig. 4.12 illustrates the whole transmission scheme. Combining with Fig. 4.11, the information symbols are modulated as QPSK and stored as vectors $\mathbf{s}_1$, $\mathbf{s}_2$, $\mathbf{s}_3$ and $\mathbf{s}_4$, and then encoded with the Golden Code matrix (3.3.1). The encoded symbol vectors are $\mathbf{x}_1$, $\mathbf{x}_2$, $\mathbf{x}_3$ and $\mathbf{x}_4$. Each block of N modulated symbols is fed to an OFDM modulator of N subcarriers. Four OFDM blocks which are modulated by an N-Point IDFT

can be obtained : $\mathbf{tx}_v = [tx_{0,v}, tx_{1,v}, tx_{2,v} \cdot \cdot, tx_{N-1,v}]^T$, $v = 1, 2, 3$ and 4. Then each block is preceded by a CP with the length l_{cp}. The CP length l_{cp} is set to be not less than or equal to the time delay τ, and $l_{cp} \geq (L - 1) + (L - 1) + \tau_{\max}$ where L is the number of multipaths. $\mathbf{tx}_1$ and $\mathbf{tx}_2$ are broadcasted respectively by the source to the destination through two relay nodes, and then the source broadcasts $\mathbf{tx}_3$ and $\mathbf{tx}_4$ in the second period.

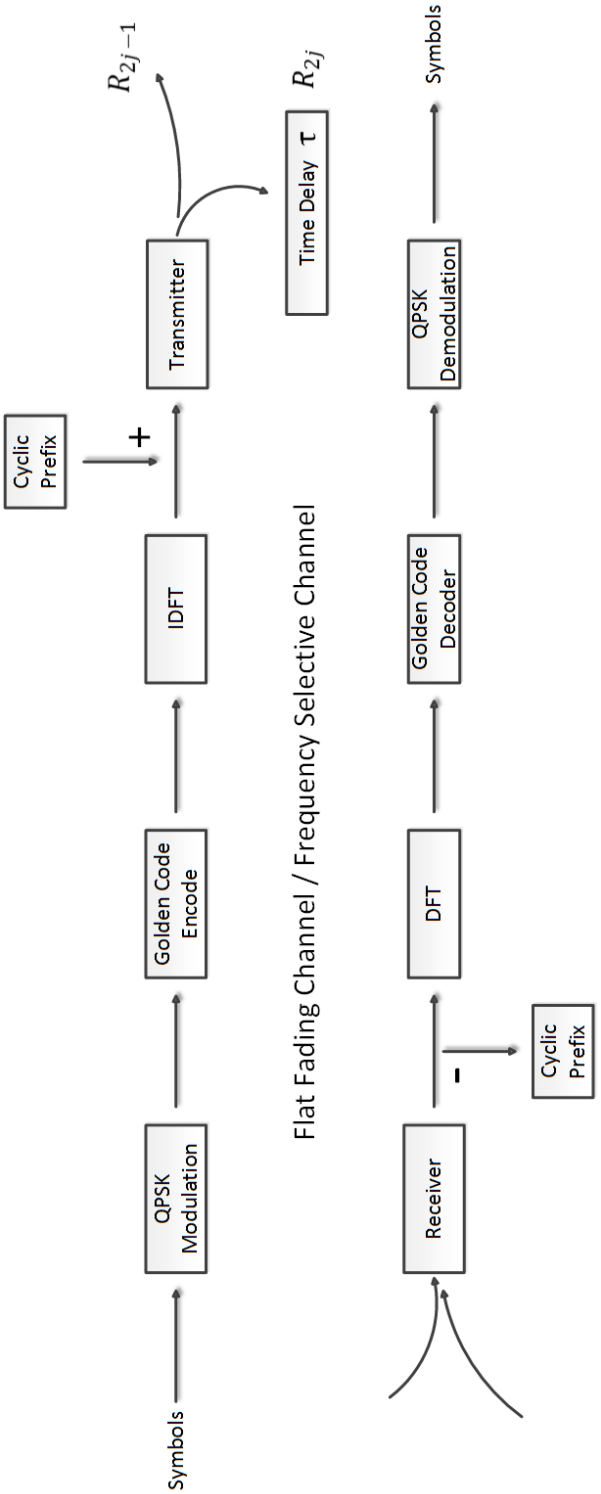

Figure 4.12. Block diagram of the transmission of the Golden Code in an asynchronous wireless network.

In the fixed relay case, only two relays R_1 and R_2 are used. The signal received by the jth relay can be expressed in the time domain as

$$\mathbf{tr}_j^k = \sqrt{P_t}(\mathbf{tx}_{2k-1} \circledast \mathbf{f}_{j-1} + \mathbf{tx}_{2k} \circledast \mathbf{f}_j) + \mathbf{tn}_{rj}^k, \tag{4.4.1}$$

where $\circledast$ denotes discrete time convolution operation and $\mathbf{f}_{2j-1}$ and $\mathbf{f}_{2j}$ are channel vectors from the source to the relays. P_t denotes average transmit power of the source, and $k \in (1, 2)$ is the symbol index; $\mathbf{tn}_{rj}^k$ is the vector of the AWGN at the jth relay in the time domain.

B. Implementation at the destination

As mentioned, due to the timing errors, there is a τ sample delay between the signals from the R_1 relay and the signals from R_2 to the destination node. The signal received by the ith antenna of the destination, during the relaying phase in the time domain, can be expressed as

$$\mathbf{ty}_i^k = \sqrt{P_r}(\mathbf{tr}_1^k \circledast \mathbf{g}_{2i-1} + (\mathbf{tr}_2^k \circledast \mathbf{g}_{2i})_\tau) + \mathbf{tn}_{di}^k, \tag{4.4.2}$$

where P_r represents the average transmit power of the relay node, $\mathbf{tn}_{di}^k$ is the AWGN at the ith antenna of the destination, and $(\cdot)_\tau$ denotes the timing offset due to asynchronism.

The power allocation is the same as (4.2.3). After the removal of the CP and the DFT operation at the receiver, the time domain operation in (4.4.2) can be equivalently written in the frequency domain as

$$\mathbf{y}_i^k = \sqrt{P_r}(\mathbf{r}_1^k \circ \mathbf{g}_{2i-1}^{'} + \mathbf{r}_2^k \circ \mathbf{g}_{2i}^{'} \circ \mathbf{m}^\tau) + \mathbf{n}_{di}^k, \tag{4.4.3}$$

where $\mathbf{g}_{2i-1}^{'}$ and $\mathbf{g}_{2i}^{'}$ represent the DFTs of $\mathbf{g}_{2i-1}$ and $\mathbf{g}_{2i}$, and the time delay in the time domain corresponds to a phase change in the frequency

domain [36] which in vector form becomes

$$\mathbf{m}^{\tau} = [1, e^{-j2\pi\tau/N}, \cdots, e^{-j2\pi\tau(N-1)/N}]^T. \tag{4.4.4}$$

Thus, the total received signal vector in the frequency domain for the asynchronous network $\mathbf{y}_\alpha$ can be written as

$$\mathbf{y}_\alpha = \mathbf{H}_\alpha \mathbf{x}_\alpha + \mathbf{n}_\alpha, \tag{4.4.5}$$

where $\mathbf{y}_\alpha$ is the vector $[\mathbf{y}_1^{1T}, \mathbf{y}_2^{1T}, \mathbf{y}_1^{2T}, \mathbf{y}_2^{2T}]^T$ and $\mathbf{x}_\alpha$ is the source vector $[\mathbf{x}_1^T, \mathbf{x}_2^T, \mathbf{x}_3^T, \mathbf{x}_4^T]^T$. $\mathbf{H}_\alpha$ is a 4×4 block diagonal matrix of effective transmission channels which is given by

$$\mathbf{H}_\alpha = \begin{bmatrix} \mathbf{M} & \mathbf{0} \\ \mathbf{0} & \mathbf{M} \end{bmatrix}, \tag{4.4.6}$$

where,

$$\mathbf{M} = \begin{bmatrix} diag\{\mathbf{f}_1^{'} \circ \mathbf{g}_1^{'} + \mathbf{f}_3^{'} \circ \mathbf{g}_2^{'} \circ \mathbf{m}^{\tau}\} & diag\{\mathbf{f}_2^{'} \circ \mathbf{g}_1^{'} + \mathbf{f}_4^{'} \circ \mathbf{g}_2^{'} \circ \mathbf{m}^{\tau}\} \\ diag\{\mathbf{f}_1^{'} \circ \mathbf{g}_3^{'} + \mathbf{f}_3^{'} \circ \mathbf{g}_4^{'} \circ \mathbf{m}^{\tau}\} & diag\{\mathbf{f}_2^{'} \circ \mathbf{g}_3^{'} + \mathbf{f}_4^{'} \circ \mathbf{g}_4^{'} \circ \mathbf{m}^{\tau}\} \end{bmatrix}, \tag{4.4.7}$$

$\mathbf{0}$ represents a 2×2 full zero matrix, and $\mathbf{f}_j^{'}$ represents the DFT of $\mathbf{f}_j$ and $\mathbf{g}_i$. The total noise $\mathbf{n}_\alpha$ is the vector $[\mathbf{n}_1^{1T}, \mathbf{n}_2^{1T}, \mathbf{n}_1^{2T}, \mathbf{n}_2^{2T}]^T$. The elements of $\mathbf{n}_\alpha$ can be written as

$$\mathbf{n}_i^k = \sqrt{P_r}(\mathbf{n}_{r1}^k \circ \mathbf{g}_{2i-1}^{'} + \mathbf{n}_{r2}^k \circ \mathbf{g}_{2i}^{'}) + \mathbf{n}_{di}^k. \tag{4.4.8}$$

The decoding method of $\mathbf{y}_\alpha$ in (4.4.5) is considered next.

First, using a full ML for decoding the Golden Code

$$\widehat{\mathbf{x}} = \underset{\mathbf{x}_\alpha \in \mathbf{S}_c}{\arg\min}\{\|\mathbf{y}_\alpha - \mathbf{H}_\alpha \mathbf{x}_\alpha\|^2\}, \tag{4.4.9}$$

where $\mathbf{S}_c$ denotes the collection of all members of the symbol constellation and $\widehat{\mathbf{x}}$ represents the estimated signal vectors. Due to the orthogo-

nality in the OFDM channels, however, this decoding can be performed on a frequency-by-frequency basis as in the frequency flat case. For example, without noise,

$$\begin{bmatrix} \mathbf{y}_1^1(\omega_u) \\ \mathbf{y}_2^1(\omega_u) \\ \mathbf{y}_1^2(\omega_u) \\ \mathbf{y}_2^2(\omega_u) \end{bmatrix} = \begin{bmatrix} (\mathbf{f}_1^{'}(\omega_u)\mathbf{g}_1^{'}(\omega_u) + \mathbf{f}_3^{'}(\omega_u)\mathbf{g}_2^{'}(\omega_u)\mathbf{m}^{\tau}(\omega_u))\mathbf{x}_1(\omega_u) \\ (\mathbf{f}_2^{'}(\omega_u)\mathbf{f}_1^{'}(\omega_u) + \mathbf{f}_4^{'}(\omega_u)\mathbf{f}_2^{'}(\omega_u)\mathbf{m}^{\tau}(\omega_u))\mathbf{x}_2(\omega_u) \\ (\mathbf{f}_1^{'}(\omega_u)\mathbf{g}_3^{'}(\omega_u) + \mathbf{f}_3^{'}(\omega_u)\mathbf{g}_4^{'}(\omega_u)\mathbf{m}^{\tau}(\omega_u))\mathbf{x}_3(\omega_u) \\ (\mathbf{f}_2^{'}(\omega_u)\mathbf{g}_3^{'}(\omega_u) + \mathbf{f}_4^{'}(\omega_u)\mathbf{g}_4^{'}(\omega_u)\mathbf{m}^{\tau}(\omega_u))\mathbf{x}_4(\omega_u) \end{bmatrix}, \quad (4.4.10)$$

where ω_u denotes the uth frequency and $u = 1, 2, \cdots, N$. In the AWGN channel environment, due to obtaining the minimum BER for every antenna, this decoding approach has the best performance. However, with the increasing number of transmitted antennas and modulation levels, the complexity of maximum-likelihood detection increases and becomes difficult to realize. For overcoming this computational complexty weakness of full ML, the low complexity SD is applied.

The sphere decoding algorithm is easily used for decoding the MIMO system. When received signals can be represented in a lattice structure, SD detection will search the closest lattice points to the received signal within a radius c (4.2.17). Selection of c corresponds crucially to the speed of this algorithm. Once the radius c is decreased, the number of signal points which are searched can be reduced in order to increase the calculation speed, although the performance of the decoding will generally be decreased at lower SNRs.

4.4.2 A Relay Selection Scheme in Asynchronous Distribution System

The aim is to select the best two relays for the Golden Code transmission in a cooperative asynchronous network as in Fig. 4.11. Firstly, the maximum-

minimum selection strategy is used as in [56]. Then, the other selection scheme which finds the mean of the maximum values among the channels is considered.

A. Maximum-minimum selection

To build the basic 2×2 relay MIMO transmission channel, every relay node has four channels linked to it. Therefore choosing the best relay and the second best from j relays yield the most effective transmission.

$$L_{min}^{(j)} = \min\{|f_{j-1}|^2, |f_j|^2, |g_j|^2, |g_{2j}|^2\}, \tag{4.4.11}$$

and in a frequency selective channel environment, the optimal relay selection can be expressed as

$$L_{min}^{(j)} = \min\{\sum_{l=1}^{L} |f_{j-1,l}|^2, \sum_{l=1}^{L} |f_{j,l}|^2, \sum_{l=1}^{L} |g_{j,l}|^2 \sum_{l=1}^{L} |g_{2j,l}|^2\}. \tag{4.4.12}$$

These values are then calculated for all of the relays and stored in $\mathbf{L}_{min}$. The relay corresponding to the maximum of these minima is selected, together with the relay which has the maximum of the remaining minima.

B. Maximum-mean selection

The second selection approach is based on calculating the mean of the strengths of the channels connected to each relay. The mean of these four flat fading channels for the jth relay is obtained as

$$L_{mean}^{(j)} = \frac{|f_{j-1}|^2 + |f_j|^2 + |g_j|^2 + |g_{2j}|^2}{4}, \tag{4.4.13}$$

and the mean of four frequency selective channels for the jth relay is obtained as

$$L_{mean}^{(j)} = \frac{\sum_{l=1}^{L} |f_{j-1,l}|^2 + \sum_{l=1}^{L} |f_{j,l}|^2 + \sum_{l=1}^{L} |g_{j,l}|^2 + \sum_{l=1}^{L} |g_{2j,l}|^2}{4}. \tag{4.4.14}$$

This mean value is then calculated for all relays and stored in $\mathbf{L}_{mean}$. In contrast to maximum-minimum selection, this method can best balance the levels among the channels, while the maximum-minimum selection just depends on the minimum value of one channel. Next, these schemes are evaluated in simulations.

4.4.3 Simulation Results

This section shows the simulated performances of the relay selection with the distributed transmission using maximum-likelihood and sphere detection based on the Golden Code in asynchronous wireless networks. The performance is shown by BER using QPSK symbols. The total transmission power of the system is fixed as P. The transmitted symbol block size is 64. The assumptions are that the channel is quasi-static flat fading and perfectly known at the receiver.

Fig. 4.13 presents the comparison of performances of the Golden Code in the asynchronous distributed system with ML and the SD. Clearly, from 0 dB to 12 dB of power, the performance of SD is slightly worse than the ML. However, the slope of the SD curve decreases rapidly. Therefore, when the power equals to approximately 12 dB, the meeting point with these two curves occurs, and after that, the performance of SD can reach the performance of ML. The speed of calculation of SD is considerably faster than the ML decoding. In simulation on a dual-core PC under Windows 7 and MATLAB 7.1, the simulations presented in Fig. 4.13 would take more than 6 hours with full ML whereas this time is halved with SD.

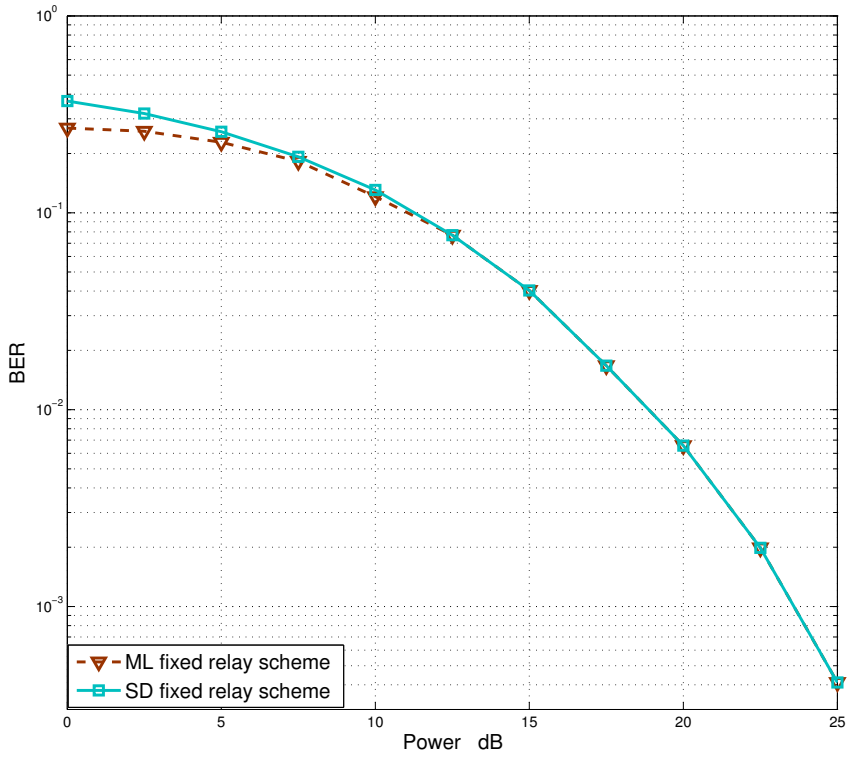

Figure 4.13. End-to-end BER performances of the Golden Code in the asynchronous distributed system with the maximum-likelihood detection and the sphere detection.

In Fig. 4.14, the BER performances are compared for the fixed relay, maximum-minimum relay selection and maximum-mean relay selection with the Golden Code in the asynchronous distributed system over SD. Obviously, the BER performance of the fixed relay scheme is worse than those based on relay selections. For example, the BER reaches 10^{-2} and the power must reach 19 dB in the fixed relay scheme. While in the relay selection scheme, two relays are selected out of four relays using maximum-minimum selection strategy and the same BER is achieved with only 15dB power. For the relay selection cases, the dashed curve shows the performance of maximum-minimum strategy and the solid curves present the maximum-mean strategy. The performance of maximum-minimum selection is worse

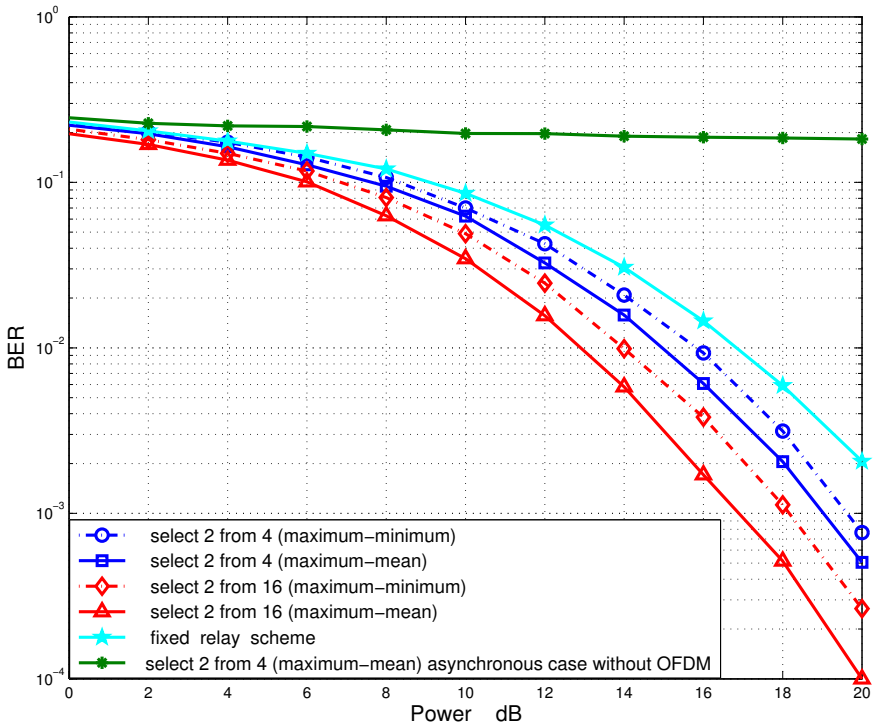

Figure 4.14. End-to-end bit error rate performances of no selection, maximum-minimum,maximum-mean relay selections and to deal with time delay without OFDM in asynchronous distributed system with the sphere detection.

than the maximum-mean selection 1 dB to 2 dB power generally with the same BER, such as BER equals to 10^{-3}. Moreover, when the number of participating relays is increased, the performance is further improved.

On the other hand, the BER performances of the relay selection transmission with the Golden Code in an asynchronous wireless relay network over frequency selective channel is shown in Fig. 4.15. In the frequency selective channel environment, the relay selection based on the maximum-minimum relay selection strategy outperforms the maximum-mean strategy. Generally, based on the same BER performance, the selection case needs power less than the fixed relay scheme 0.5 dB to 1 dB. By contrast, there is approximately 0.2-0.5 dB power superiority using the maximum-minimum strategy.

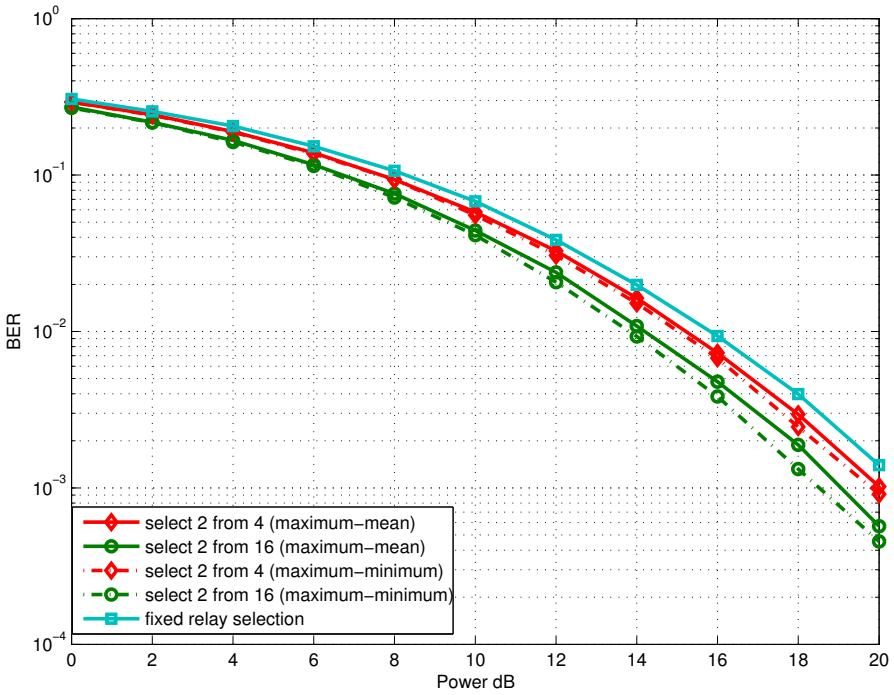

Figure 4.15. End-to-end bit error rate performances of no selection, maximum-minimum and maximum-mean relay selections in asynchronous distributed system over frequency selective fading channel with the sphere detection.

Finally, the simulated performance of relay selection over a sparse frequency selective channel is compared with that for flat fading and general frequency selective channels in Fig. 4.16. In the range of low power, the performance of maximum-minimum selection is almost the same as the maximum-mean selection over frequency selective channels. From 16 dB to 20 dB power, this property of performance is reversed. The BER performance of maximum-minimum restore the case which is worse than maximum-mean selection. Thus, there is 0.5-1 dB power general superiority for the maximum-mean selection over frequency selective channels. Generally, bit error rate performance of wireless transmission over flat fading channel is better than over frequency selective channel. OFDM was adopted in this case, which overcomes the weak of frequency selective channel. The signals from multi-

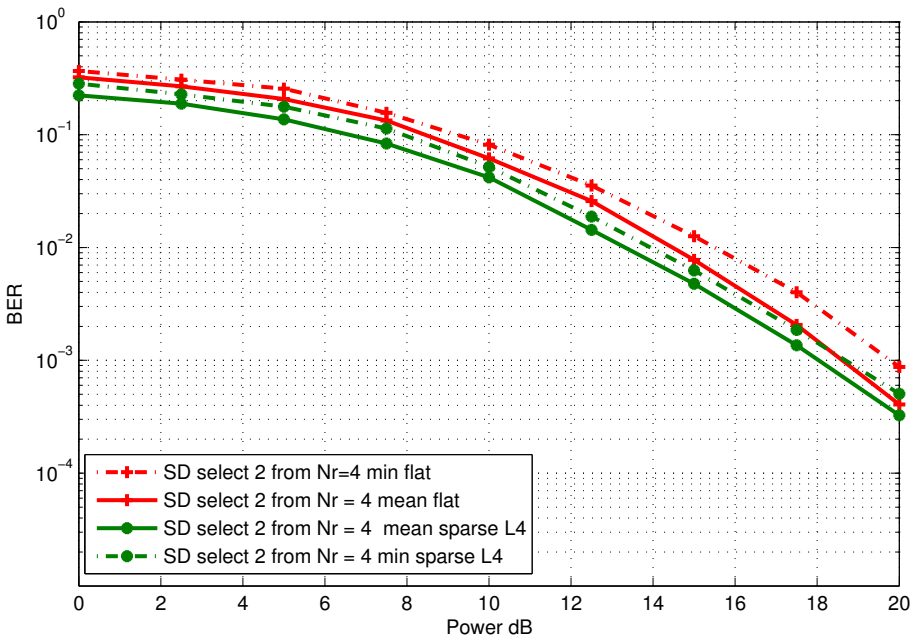

Figure 4.16. Bit error rate performances of relay selections in asynchronous distributed system over flat fading channel and sparse frequency selective channel with the sphere detection.

path can be combined to form stronger signals. Therefore, the performance over frequency selective channel has better performance in this case.

4.5 Summary

Distributed transmission using the Golden Code in wireless relay networks, and a new multiple relay selection strategy, were proposed in this chapter. Through end-to-end BER simulations, the maximum of the channel parameter means selection was shown to achieve the best performance. The improvement was because this approach performs an overall channel strength tradeoff at every relay node to select the best two relays. Therefore, this new maximum-mean policy appears valuable for cooperative diversity systems based on the Golden Code.

The Golden Code was also implemented in an asynchronous wireless relay network over frequency flat and selective channels, and a simple approach

to overcome asynchronism was proposed in this chapter. As in synchronous wireless relay networks, the maximum of the channel parameter means selection was shown to still achieve the best performance for the relay selection through BER simulations with computationally efficient SD in a flat fading channel environment. The improvement was because this approach performs an overall channel strength tradeoff at every relay node to select the best two relays. In the frequency selective channel case, however, the advantage of the maximum-mean selection was lost. Performance analysis of Golden Code based transmission with antenna selection in MIMO systems will be provided in the next chapter. This analysis also provides guidance for distributed MIMO systems operating in DF mode of transmission, which also applies to Chapter 6.

Chapter 5

MULTI-ANTENNA SELECTION POLICIES USING THE GOLDEN CODE IN MIMO SYSTEMS

In MIMO systems, multiple-antenna selection has been proposed as a practical scheme for improving signal transmission quality as well as reducing realisation cost due to minimising the number of radio frequency chains. In this chapter, transmit antenna selection for MIMO systems with the Golden Code is investigated. Two antenna selection schemes are considered: maximum-minimum and maximum-sum approaches. The outage and pairwise error probability performance of the proposed approaches are analysed. Simulations are also given to verify the analysis. The results show the proposed methods provide useful schemes for antenna selection.

5.1 Introduction

MIMO wireless communications increases spectrum efficiency by spatial multiplexing and improves link reliability by antenna diversity [2] and [6]. Although many benefits of multi-antenna systems have been verified, the de-

ployment of multiple antennas requires multiple radio-frequency (RF) chains associated with each antenna. A conventional MIMO system, with N_t transmit and N_r receive antennas, requires N_t and N_r RF chains respectively. These RF chains include multiple analog-digital converters, low noise amplifiers, and downconverters. This leads to a considerable increase in the cost and complexity of implementing such systems and represents a major practical drawback. To reduce the number of RF chains and keep the system simple and inexpensive, antenna selection (AS) algorithms are proposed to feed the most favourable subsets of transmit and/or receive antennas to RF chains.

Antenna selection selects a subset of antennas to feed to the RF chains. The selection algorithm is based on the SNR of the received signals. This benefits diversity but not spatial multiplexing. A reduced-complexity MIMO scheme that selects the L_r best available from N_r receive antennas was proposed in [6], wherein an upper bound on the capacity was also derived that can be expressed as the sum of the logarithms of ordered chi-square distributed variables. In [69], a MIMO scheme combining transmit antenna selection and receiver maximal-ratio combining was investigated. The impact of antenna selection on the PEP for space-time code systems was approximately analysed in [70]. In [71], theoretical performance analysis including PEP for multi-antenna systems with antenna selection was presented. A practical algorithm for antenna selection in MIMO wireless communication systems employing STBC was described in [72], where the outage probability was analyzed. The outage probability of multiuser diversity in a transmit antenna selection system was derived for Nakagami-m channels in [73]. Both single transmit and single receive antenna selection were examined for flat Nakagami-m fading channels in [18]. Based on two-way relay networks, [74] proposed two strategies for transmit and receive antenna selection, where outage probability results revealed that the joint relay and antenna selection

strategies achieve significant diversity and array gains over their single relay counterparts. The authors of [75] presented a unified asymptotic framework for transmit antenna selection in MIMO multirelay networks with Rician, Nakagami-m, Weibull, and generalized-K fading channels and derived new closed-form expressions for the outage probability and symbol error rate of the AF relaying in MIMO multirelay networks with two distinct protocols: transmit antenna selection with receiver maximal-ratio combining and transmit antenna selection with receiver selection combining.

This chapter describes the analysis of outage probability and PEP of transmit antenna selection schemes for a Golden Code network. Selecting the best two transmit antennas from N participating antenna by using maximum-minimum and maximum-sum selection schemes is proposed. Comparison of the outage probability of these two approaches, and derivation of an upper bound for the PEP and the diversity order are also shown in this chapter. Simulations are finally used to verify the theoretical analysis.

5.2 System Model

A point-to-point MIMO network as a basic transmission scenario for the Golden Code is shown in Fig. 5.1. One BS as the transmitter and one UE as a receiver; moreover, the wireless network has N transmit antennas at the BS, and two receive antennas at the UE. Every antenna is half-duplex, so that it cannot transmit and receive simultaneously. Channel coefficients are denoted from BS to UE as $g_{A_n D_k}$, where n represents the nth antenna at the BS and k represents the kth antenna at the UE, $n \in \{1, \cdots, N\}$ and $k \in \{1, 2\}$. The signals are encoded at the BS with the Golden Code (3.3.1). The two transmit antennas which achieve the highest SNR are selected to transmit the signal encoded with the Golden Code. The channels are quasi-static Rayleigh flat fading, which are i.i.d. complex Gaussian random variables

with zero-mean and unit-variance, i.e. $g_{A_nD_k} \sim \mathcal{CN}(0,1)$. The instantaneous SNR for channel $g_{A_nD_k}$ is $\gamma_{A_nD_k} = |g_{A_nD_k}|^2 E_s/N_0$, where E_s is the average power per symbol and N_0 is the noise variance. E_s is assumed unity and the noise variances are the same in all antennas at the destination in this chapter. Perfect CSI is assumed known at the destination node. The information bits

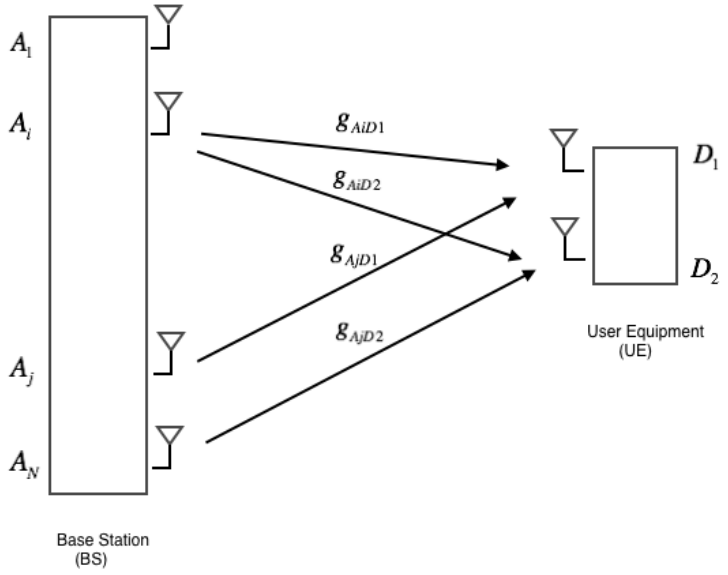

Figure 5.1. The system model of antenna selection at the transmitter, i.e. the ith and jth Antenna are selected.

are respectively encoded with the Golden Code matrix (3.3.1). Sending a Golden codeword needs two time slots. The transmission process is listed as below if the best two transmit antennas are selected. The signal received at the UE kth antenna at the first time slot, $t = 1$,

$$y_k^1 = \sqrt{\frac{P}{2}}(g_{A_iD_k}x_1 + g_{A_jD_k}x_2) + n_k^1 \tag{5.2.1}$$

and at the second time slot, $t = 2$

$$y_k^2 = \sqrt{\frac{P}{2}}(g_{A_iD_k}x_3 + g_{A_jD_k}x_4) + n_k^2 \tag{5.2.2}$$

where $\frac{P}{2}$ is the transmitted energy at every antenna, n_k is AWGN with variance σ_k^2. At the receiver, maximum-likelihood decoding is used to estimate the original signal

$$\arg\min_{\mathbf{x}\in\mathbf{S}_c}\{\|\mathbf{y} - \mathbf{H}_c\mathbf{x}\|_2\}, \tag{5.2.3}$$

where $\mathbf{S}_c$ denotes the collection of possible symbol constellation points and $\|\cdot\|$ denotes the Euclidean norm. $\mathbf{H}_c$ is the selected channel matrix which contains $g_{A_iD_k}$ and $g_{A_jD_k}$, for example

$$\mathbf{H}_c = \begin{bmatrix} g_{A_1D_1} & g_{A_2D_1} & 0 & 0 \\ g_{A_1D_2} & g_{A_2D_2} & 0 & 0 \\ 0 & 0 & g_{A_1D_1} & g_{A_2D_1} \\ 0 & 0 & g_{A_1D_2} & g_{A_2D_2} \end{bmatrix} \tag{5.2.4}$$

$\mathbf{y}$ is the received signal vector which takes the form

$$\mathbf{y} = \begin{bmatrix} y_1^1 & y_2^1 & y_1^2 & y_2^2 \end{bmatrix}^T. \tag{5.2.5}$$

Next, the outage probability of the antenna selection scheme is analysed.

5.3 Multi-antenna Selection with Outage Probability Analysis

The outage probability is defined as $P(C_d < R)$, where C_d denotes the channel capacity and R is the target rate. Therefore, the SNR at D_1 is $\gamma_{D_1} = \frac{|g_{A_iD1}|^2+|g_{A_jD1}|^2}{\sigma_k^2}$ and at D_2 is $\gamma_{D_2} = \frac{|g_{A_iD2}|^2+|g_{A_jD2}|^2}{\sigma_k^2}$. An outage standard

$$\gamma_d = \frac{|g_{A_iD_1}|^2 + |g_{A_iD_2}|^2 + |g_{A_jD_1}|^2 + |g_{A_jD_2}|^2}{\sigma_k^2}. \tag{5.3.1}$$

is defined as total end-to-end SNR which is similar to the real SNR. Then the capacity between source and destination is given by

$$C_d = \log_2(1 + \gamma_d). \tag{5.3.2}$$

The multiple transmit antenna selection chooses the most suitable two from N transmit antennas. The transmit signals must be such that their superposition at the receiver results in maximal receive SNR. Two antenna selection schemes are considered in this section: the maximum-minimum and maximum-sum antenna selection, respectively.

5.3.1 Maximum-Minimum Selection

Because the Golden Code requires two antennas at the transmitter, the aim is to select the best two transmit antennas from N available antennas. In the maximum-minimum selection scheme, the best two links can be selected as:

$$\begin{aligned} i &= arg\max\{\min_{i\in\{1,\cdots,N\}}(\gamma_{A_iD_1}, \gamma_{A_iD_2})\} \\ j &= arg\max\{\min_{j\in\{1,\cdots,N-1\},j\neq i}(\gamma_{A_jD_1}, \gamma_{A_jD_2})\}, \end{aligned} \tag{5.3.3}$$

where i indexes the best antenna, and j is the second best. To be specific, the maximum-minimum selection as is shown in (5.3.3) contains two steps:

1) For every transmission antenna $A_{i(j)}$, choosing the channel with the minimum gain represents as $\gamma_{A_{i(j)}D} = \min(\gamma_{A_{i(j)}D_1}, \gamma_{A_{i(j)}D_2})$, where $\gamma_{A_{i(j)}D_1}$ and $\gamma_{A_{i(j)}D_2}$ are the channel SNRs from $A_{i(j)}$ to the two receiving antennas D_1 and D_2 respectively;

2) Then the transmission antennas are selected with the two largest $\gamma_{A_{i(j)}D}$ among all transmission antennas.

In order to obtain the outage probability for the maximum-minimum

selection scheme, the probability density function (PDF) of the four channel SNRs for the two selected antennas need to be obtained. However, from "step 1" in the maximum-minimum selection rule, for each selected antenna, only the distribution of the smaller channel SNR can be obtained. For the larger channel SNR, as only known that it is larger than the other but do not know by how much. Thus the PDF of the larger channel SNR for the selected antenna is very hard (if not impossible) to obtain. This leads to the bound in (5.3.4), which again leads to the outage upper bound. Because the "larger channel SNR-s" themselves are random numbers and can not be controlled by the specific values, there exist sizeable gaps between the derived outage upper bounds and the numerical results. With this observation, the final SNR with the selected i and j is given by (5.3.1) which is lower-bounded as

$$\gamma_d \geq \ 2 \max_{i\in\{1,\cdots,N\}} \{\min(\gamma_{A_iD_1}, \gamma_{A_iD_2})\} + 2 \max_{j\in\{1,\cdots,N-1\}, j\neq i} \{\min(\gamma_{A_jD_1}, \gamma_{A_jD_2})\}. \tag{5.3.4}$$

For all Rayleigh flat-fading channels, the PDF and the cumulative distribution function (CDF) of the SNR are given by

$$\begin{aligned} f_{\gamma_v}(\gamma) &= \frac{1}{\overline{\gamma}_v} e^{-\frac{\gamma}{\overline{\gamma}_v}} \\ F_{\gamma_v}(\gamma) &= 1 - e^{-\frac{\gamma}{\overline{\gamma}_v}} \end{aligned}, \tag{5.3.5}$$

respectively, where $\gamma_v \in (\gamma_{A_nD_1}, \gamma_{A_nD_2})$, $\gamma > 0$ and $\overline{\gamma}_v$ is the average mean SNR of all links. The channels are i.i.d. and $\overline{\gamma}_{A_nD_1} = \overline{\gamma}_{A_nD_2} = \overline{\gamma}_v$. Thus,

the CDF of $\min(\gamma_{A_nD_1}, \gamma_{A_nD_2})$ can be expressed as

$$\begin{aligned} F(\gamma) &= 1 - (P_r(\gamma_{A_nD_1} > \gamma))(P_r(\gamma_{A_nD_2} > \gamma)) \\ &= 1 - (1 - P_r(\gamma_{A_nD_1} \leq \gamma))(1 - P_r(\gamma_{A_nD_2} \leq \gamma)) \\ &= 1 - (1 - F_{\gamma_{A_nD_1}}(\gamma))(1 - F_{\gamma_{A_nD_2}}(\gamma)) \\ &= 1 - e^{-\frac{2\gamma}{\overline{\gamma}_v}}. \end{aligned} \tag{5.3.6}$$

Then, the PDF of γ_v can be obtained as

$$f(\gamma_v) = \frac{dF(\gamma)}{d(\gamma)} = \frac{2}{\gamma_v} e^{-\frac{\gamma_v}{\overline{\gamma}_v}}. \tag{5.3.7}$$

In this approach, the best two antennas are selected with the largest two SNRs among all N available transmitted antennas. According to [41], the joint distribution of the L largest values from N candidates can be obtained as

$$f(x_1, x_2, \cdots, x_L) = L! \binom{N}{L} [F(x_L)]^{N-L} \prod_{i=1}^{L} f(x_i), \tag{5.3.8}$$

where $x_1 \geq x_2 \cdots \geq x_T \cdots \geq x_N$. Substituting $L = 2$ into (5.3.8) yields the joint PDF of the two largest SNRs as

$$f(\gamma_i, \gamma_j) = N(N-1)F(\gamma_j)^{N-2} f(\gamma_i) f(\gamma_j), \tag{5.3.9}$$

Substituting (5.3.6) into (5.3.9), and using binomial expansion $(1-x)^n =$

$\sum_{k=0}^{n} \binom{n}{k} (-x)^k$ gives

$$\begin{aligned} f(\gamma_i, \gamma_j) &= N(N-1)(1 - e^{-\frac{2\gamma_j}{\overline{\gamma}_v}})^{N-2} \frac{2}{\overline{\gamma}_v} e^{-\frac{\gamma_i}{\overline{\gamma}_v}} \frac{2}{\overline{\gamma}_v} e^{-\frac{\gamma_j}{\overline{\gamma}_v}} \\ &= N(N-1) \underbrace{\sum_{u=0}^{N-2} \binom{N-2}{u} (-e^{-\frac{2\gamma_j}{\overline{\gamma}_v}})^u}_{Binomial \quad expansion} \frac{2}{\overline{\gamma}_v} e^{-\frac{\gamma_i}{\overline{\gamma}_v}} \frac{2}{\overline{\gamma}_v} e^{-\frac{\gamma_j}{\overline{\gamma}_v}}. \end{aligned} \tag{5.3.10}$$

Let $\gamma_{low} = \gamma_i + \gamma_j$, the CDF $F_{\gamma_{low}}(\gamma)$ is obtained as

$$\begin{aligned} F_{\gamma_{low}}(\gamma) &= Pr\{\gamma_i + \gamma_j \leq \gamma\} \\ &= \int_0^{\frac{\gamma}{2}} \int_y^{\gamma - y} f(x, y) dx dy \\ &= 2N(N-1) \int_0^{\frac{\gamma}{2}} \frac{\left(- e^{\frac{2y}{\overline{\gamma}_v^2}} + 1 \right)^{N-2} \left(\frac{1}{e^{-\frac{4y}{\overline{\gamma}_v^2}}} - e^{-\frac{2\gamma}{\overline{\gamma}_v^2}} \right)}{\overline{\gamma}_v^2} dy. \end{aligned} \tag{5.3.11}$$

According to the definition of outage probability, an outage occurs when the average end-to-end SNR falls below a certain threshold value γ_{th}, namely, according to (5.3.4), target SNR $\gamma_{th} = (2^R - 1)/2$. For any N and γ_v, (5.3.11) can be obtained numerically with, for example Matlab or Maple [76]. The outage probability can be expressed as

$$P_{out} = F_{\gamma_{low}}(\gamma_{th}). \tag{5.3.12}$$

5.3.2 Maximum-Sum Selection

In this section, the maximum-sum selection scheme is proposed. The sum SNRs is first obtained from the transmit antenna to the two receive antennas, and then two antennas are chosen which achieve the two largest sum SNRs

as:

$$\begin{aligned} i &= arg \max_{i\in\{1,\cdots,N\}} \{\gamma_{A_iD_1} + \gamma_{A_iD_2}\} \\ j &= arg \max_{j\in\{1,\cdots,N-1\},j\neq i} \{\gamma_{A_jD_1} + \gamma_{A_jD_2}\}. \end{aligned} \tag{5.3.13}$$

The PDF of the sum $\gamma_\mu = \gamma_{A_{i(j)}D_1} + \gamma_{A_{i(j)}D_2}$ can be expressed as

$$f_{\gamma_\mu}(\gamma) = \frac{\gamma}{\overline{\gamma}_\mu^2} e^{-\frac{\gamma}{\overline{\gamma}_\mu}}, \tag{5.3.14}$$

where $\overline{\gamma}_\mu$ is the average mean SNR of γ_μ. Then the CDF of γ_μ is

$$F(\gamma) = 1 - \frac{\gamma}{\overline{\gamma}_\mu} e^{-\frac{\gamma}{\overline{\gamma}_\mu}} - e^{-\frac{\gamma}{\overline{\gamma}_\mu}} = 1 - e^{-\frac{\gamma}{\overline{\gamma}_\mu}}(1 + \frac{\gamma}{\overline{\gamma}_\mu}). \tag{5.3.15}$$

And substituting (5.3.14) and (5.3.15) to (5.3.9) gives the PDF of the final SNR. Then the CDF of the final SNR can be obtained as

$$\begin{aligned} F_{\gamma_e}(\gamma) &= \int_0^{\frac{\gamma}{2}} \int_y^{\gamma-y} N(N-1) \\ &\cdot \sum_{u=0}^{N-2} \binom{N-2}{u} (-1)^u e^{-\frac{yu}{\overline{\gamma}_\mu}} \sum_m^u \binom{u}{m} \cdot (\frac{y}{\overline{\gamma}_\mu})^m \frac{xy}{\overline{\gamma}_\mu^4} e^{-\frac{x+y}{\overline{\gamma}_\mu}} dxdy \\ &= \int_0^{\frac{\gamma}{2}} \frac{\xi \cdot \eta \cdot \varphi}{\omega} dy, \end{aligned} \tag{5.3.16}$$

where

$$\begin{aligned} \xi &= N(N-1)y, \\ \eta &= \sum_{a=0}^{N} \binom{N}{a} (-1)^a e^{-\frac{ya}{\overline{\gamma}_\mu}} \sum_{b=0}^{a} \binom{a}{b} (\frac{y}{\overline{\gamma}_\mu})^b, \\ \varphi &= -y - \overline{\gamma}_\mu + e^{\frac{2y-\gamma}{\overline{\gamma}_\mu}} (\overline{\gamma}_\mu + \gamma - y), \end{aligned}$$

and

$$\omega = -\overline{\gamma}_\mu y^2 - 2y\overline{\gamma}_\mu^2 + 2y\overline{\gamma}_\mu^2 e^{\frac{y}{\overline{\gamma}_\mu}} - \overline{\gamma}_\mu^3 + 2\overline{\gamma}_\mu^3 e^{\frac{y}{\overline{\gamma}_\mu}} - e^{\frac{2y}{\overline{\gamma}_\mu}} \overline{\gamma}_\mu^3.$$

Finally, using the target SNR $\gamma_{th} = 2^R - 1$, the exact outage probability of the maximum-sum selection scheme can be obtained. Similarly, for any N and γ_μ, the outage can be obtained by using a numerical method [76].

5.4 PEP Analysis of the Maximum-Sum Multi-Antenna Selection with the Golden Code

In this section, the PEP over flat fading channels is analysed and the diversity order of the point-to-point Golden Code is investigated. For convenience, the $2 \times N$ channel is written in the form of the following matrix

$$\mathbf{H}_c = \begin{bmatrix} g_{A_1D_1} & g_{A_2D_1} & \cdots & g_{A_ND_1} \\ g_{A_1D_2} & g_{A_2D_2} & \cdots & g_{A_ND_2} \end{bmatrix}. \tag{5.4.1}$$

The antenna selection can be described as choosing the two columns with the highest norm as the best transmitted antennas. Finding the joint PDF of the largest two norms is the first step. In [71] the joint PDF of the selected $\widetilde{\mathbf{H}}_c$ which represents $\widetilde{\mathbf{H}}_c = [\mathbf{g}_i \ \mathbf{g}_j]$ can be written as

$$f(\mathbf{g}_i, \mathbf{g}_j) = \frac{N!}{(N-2)!2} \cdot \sum_{l=1}^{2} (1 - e^{-\|\mathbf{g}_l\|_2} - e^{-\|\mathbf{g}_l\|_2} \|\mathbf{g}_l\|_2)^{N-2} I_{R_l}(\mathbf{g}_i, \mathbf{g}_j)) \frac{e^{-(\|\mathbf{g}_i\|_2 + \|\mathbf{g}_j\|_2)}}{\pi^4}, \tag{5.4.2}$$

where, $\|\mathbf{g}_i\|_2$ and $\|\mathbf{g}_j\|_2$ are the largest and the second largest squared Euclidean norms, let $I(\mathbf{g}_i, \mathbf{g}_j)$ be the indicator function. If $(\mathbf{g}_i, \mathbf{g}_j) \in R_l$, $I_{R_l}(\mathbf{g}_i, \mathbf{g}_j)$ is 1 and else equals zero; l denotes the column in $\mathbf{g}_l$, where R_l is a region defined by$\{\mathbf{g}_1, \cdots, \mathbf{g}_L : \|\mathbf{g}_l\| < \|\mathbf{g}_c\|$,
$c = 1, \cdots, l-1, l+1, \cdots, L\}$. The PEP can be upper bounded by using the

Chernoff bound [45],

$$P(\mathbf{X} \to \widehat{\mathbf{X}}) \leq e^{-\frac{\rho}{4\mathrm{M}}\|\mathbf{H}_c\mathbf{E}\|_F^2}, \tag{5.4.3}$$

where $\mathbf{E} = \mathbf{X} - \widehat{\mathbf{X}}$ is the code error matrix and the number of transmit antennas is M, which sets 2. $\mathbf{X}$ is the transmitted code matrix in (3.3.1) and $\widehat{\mathbf{X}}$ is the expected received code matrix, $\|\cdot\|_F^2$ represents the sum of magnitude squares of all entries of a matrix, i.e. the squared Frobenius norm, ρ is the expected SNR at the receive antenna. Using the new selected channel matrix $\widetilde{\mathbf{H}}_c$ of matrix $\mathbf{H}_c$ with all channels, it follows that the averaged upper bound from (5.4.2) is

$$P(\mathbf{X} \to \widehat{\mathbf{X}}) \leq \sum_{l=1}^{2} \int\int_{R_l} e^{-\frac{\rho}{8}\|\widetilde{\mathbf{H}}_c\mathbf{E}\|_2} \frac{N!}{(N-2)!2}(1 - e^{-\|\mathbf{g}_l\|_2} - e^{-\|\mathbf{g}_l\|_2}\|\mathbf{g}_l\|_2)^{N-2} \cdot \frac{e^{-\sum_{c=1}^{L=2}\|\mathbf{g}_c\|_2}}{\pi^4} d\mathbf{g}_i d\mathbf{g}_j. \tag{5.4.4}$$

One property of the Golden Code is a full rank space-time code, so the eigenvalues of the matrix $\mathbf{E}\mathbf{E}^H$ are nonzero, where $(\cdot)^H$ is the Hermitian of matrix $\mathbf{E}$. The PEP bound can be simplified by using

$$\|\widetilde{\mathbf{H}}\mathbf{E}\|_F^2 = trace((\widetilde{\mathbf{H}}\mathbf{U})\mathbf{\Lambda}(\widetilde{\mathbf{H}}\mathbf{U})^*) = \sum_{z=1}^{2} \lambda_z \|\mathbf{g}_z\|_2, \tag{5.4.5}$$

where $\mathbf{U}$ is a unitary matrix and $\mathbf{\Lambda}$ is a diagonal matrix with eigenvalues of $\mathbf{E}\mathbf{E}^H$. The minimum of λ_z is denoted by $\widetilde{\lambda}$, where $z = 1, \cdots, L$. The upper bound PEP can thus be rewritten as

$$P(\mathbf{X} \to \widehat{\mathbf{X}}) \leq \sum_{l=1}^{2} \int\int_{R_l} e^{-\frac{\rho}{8}\sum_{i=1}^{2}\widetilde{\lambda}\|\mathbf{g}_z\|_2} \cdot \frac{N!}{(N-2)!2}(1 - e^{-\|\mathbf{g}_l\|_2} - e^{-\|\mathbf{g}_l\|_2}\|\mathbf{g}_l\|_2)^{N-2} \frac{e^{-\sum_{c=1}^{L=2}\|\mathbf{g}_c\|_2}}{\pi^4} d\mathbf{g}_i d\mathbf{g}_j. \tag{5.4.6}$$

As in [71], (5.4.6) can be simplified by using

$$g(v) = 1 - e^{-v} \sum_{n=0}^{N-1} \frac{v^n}{n!} \leq \frac{v^N}{N!} \tag{5.4.7}$$

where $v > 0$. Therefore, (5.4.6) becomes

$$P(\mathbf{X} \to \widehat{\mathbf{X}}) \leq \frac{N!}{(N-2)!2} \int_{R_l} e^{-\frac{\rho}{8} \sum_{i=1}^{2} \widehat{\lambda} \|\mathbf{g}_z\|_2} \Big(\frac{\|\mathbf{g}_l\|_2^4}{2} \Big)^{N-2} \frac{e^{-(\|\mathbf{g}_i\|_2 + \|\mathbf{g}_j\|_2)}}{\pi^4} d\mathbf{g}_i d\mathbf{g}_j. \tag{5.4.8}$$

Exponentials are used to represent g_{nl}, $g_{nl} = a_{nl} e^{b_{nl}}$, and set $c_{nl} = a_{nl}^2$, where $\|\mathbf{g}_l\|^2 = \sum_{n=1}^{2} c_{nl}$, while $dh_{nl} = a_{nl} da_{nl} db_{nl}$ and evaluating the integral with respect to db over $[0, 2\pi]$, yields,

$$\begin{aligned} P(\mathbf{X} \to \widehat{\mathbf{X}}) \leq \frac{N!}{(N-2)!2} \int_0^\infty \cdots \int_0^\infty e^{-\frac{\rho}{8} \widetilde{\lambda} (c_{11} + c_{21} + c_{12} + c_{22})} \\ \cdot \Big[\frac{(c_{1l} + c_{2l})^2}{2} \Big]^{N-2} \cdot e^{-(c_{11} + c_{21} + c_{12} + c_{22})} dc_{11} dc_{21} dc_{12} dc_{22} \end{aligned} \tag{5.4.9}$$

A looser upper bound occurs by evaluating the integral throughout the whole space. For mathematical derivation, using Q represents $P(\mathbf{X} \to \widehat{\mathbf{X}})$. The upper bound of Q in (5.4.9) can be rewritten as $Q \leq Q_{1^{(l)}} Q_{2^{(l)}}$, where

$$\begin{aligned} Q_{1^{(l)}} = \frac{N!}{(N-2)!2} \int_0^\infty \int_0^\infty e^{-\frac{\rho}{8} \widetilde{\lambda} \sum_{i=1, i \neq l}^{L} \sum_{n=1}^{N} c_{ni}} \cdot e^{-(\sum_{i=1, i \neq l}^{L} \sum_{n=1}^{N} c_{ni})} \\ \cdot \prod_{i=1, i \neq l}^{L} \prod_{n=1}^{N} dc_{ni} \end{aligned}$$

and

$$Q_{2^{(l)}} = \int_0^\infty \int_0^\infty e^{-(\frac{\rho}{8} \widetilde{\lambda} + 1)(c_{1l} + c_{2l})} \Big[\frac{(c_{1l} + c_{2l})^2}{2} \Big]^{N-2} \cdot dc_{1l} dc_{2l}. \tag{5.4.10}$$

Since $\int_0^\infty e^{-\varepsilon x} dx = \frac{1}{\varepsilon}$,

$$Q_{1^{(l)}} = \frac{N!}{(N-2)!2} \Big[\frac{1}{(1 + \frac{\rho \widetilde{\lambda}}{4})(1 + \frac{\rho \widetilde{\lambda}}{8})} \Big]^2. \tag{5.4.11}$$

On the other hand, c_{nl} is denoted by p_n and then it follows that

$$\Big(\sum_{n=1}^{2} p_n\Big)^{2(N-2)} = \sum_{n_1=1}^{2} \cdots \sum_{n_{2(N-2)}=1}^{2} p_{n_1} \cdots p_{n_{2(n-2)}}, \tag{5.4.12}$$

where $p_{n_1} \cdots p_{n_{2(N-2)}} = \prod_{n=1}^{2} (p_n)^{l_n}$. Hence, $\sum_{n=1}^{2} l_n = 2(N-2)$, and then

$$Q_{2^{(l)}} = \Big(\frac{1}{2}\Big)^{N-2} \int_0^{\infty} \int_0^{\infty} e^{-\sum_{n=1}^{2}(\frac{\rho\widetilde{\lambda}}{8}+1)p_n} \sum_{n_1=1}^{2} \cdots \sum_{n_{2(N-2)}=1}^{2} (p_1)^{l_1}(p_2)^{l_2} dp_1 dp_2. \tag{5.4.13}$$

Using $\int_0^{\infty} x^m e^{-ax} dx = \frac{m!}{a^{m+1}}$ yields

$$Q_{2^{(l)}} = \Big(\frac{1}{2}\Big)^{N-2} \sum_{n_1=1}^{2} \cdots \sum_{n_{2(N-2)}=1}^{2} \frac{l_1! l_2!}{(\frac{\rho\widetilde{\lambda}}{8}+1)^{l_1+1}(\frac{\rho\widetilde{\lambda}}{8}+1)^{l_2+1}}. \tag{5.4.14}$$

At the high SNRs, therefore,

$$P(\mathbf{X} \to \widehat{\mathbf{X}}) \leq \frac{N!}{(N-2)!2^{N-1}} \Big(\frac{1}{\widetilde{\lambda}^{2N}}\Big) \Big(\sum_{n_1=1}^{2} \cdots \sum_{n_{2(N-2)}=1}^{2} l_1! l_2!\Big) \Big(\frac{\rho}{8}\Big)^{-2N}. \tag{5.4.15}$$

In general, the diversity order is $N \times M$, which M is the number of receive antennas. From (5.4.15), the diversity order is $2N$ for the full diversity system, and $\widetilde{\lambda}$ is nonzero since the Golden Code is a full rank code. Maximizing $\widetilde{\lambda}$ can thereby design a code useful for transmit antenna selection.

5.5 Simulation Results

In this section, in order to verify the above mathematical expressions, the simulation of the outage performance of the antenna selection scheme with the maximum-minimum and maximum-sum selection scenarios using the Golden Code is shown. In addition, the PEP performance for the maximum-sum selection scheme is also simulated. Assuming 4, 6 and 8 participating

transmitted antennas are exploited in this scheme. Four different symbols would be transmitted in two time slots by the Golden Code. The target rate is set as 2.

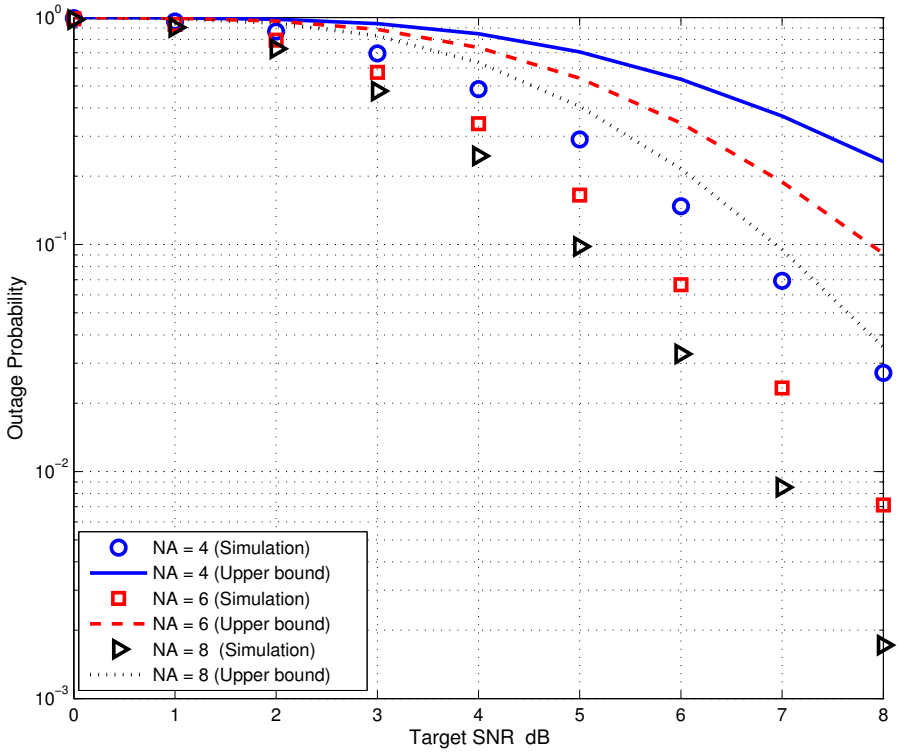

Figure 5.2. The outage probability for the maximum-minimum antenna selection in the Golden Code system.

Fig. 5.2 compares the simulated and theoretical upper bounds of the outage probability for the maximum-minimum selection scheme. The gap between the simulation results and the theoretical upper bounds comes from the lower bounds for the end-to-end SNR as is shown in (5.3.4). It can be seen that with more participating transmit antennas, the outage probability becomes smaller. For example, with the total number of available antennas increased from 6 to 8, the target SNR of the best two antenna selection is decreased from approximately 7.6 dB to 6.8 dB when the probability is 0.1. When choosing the best two from 6 antennas, the outage probability

upper bound is 0.189 at 7 dB target SNR, while the outage is 0.023 in the simulation.

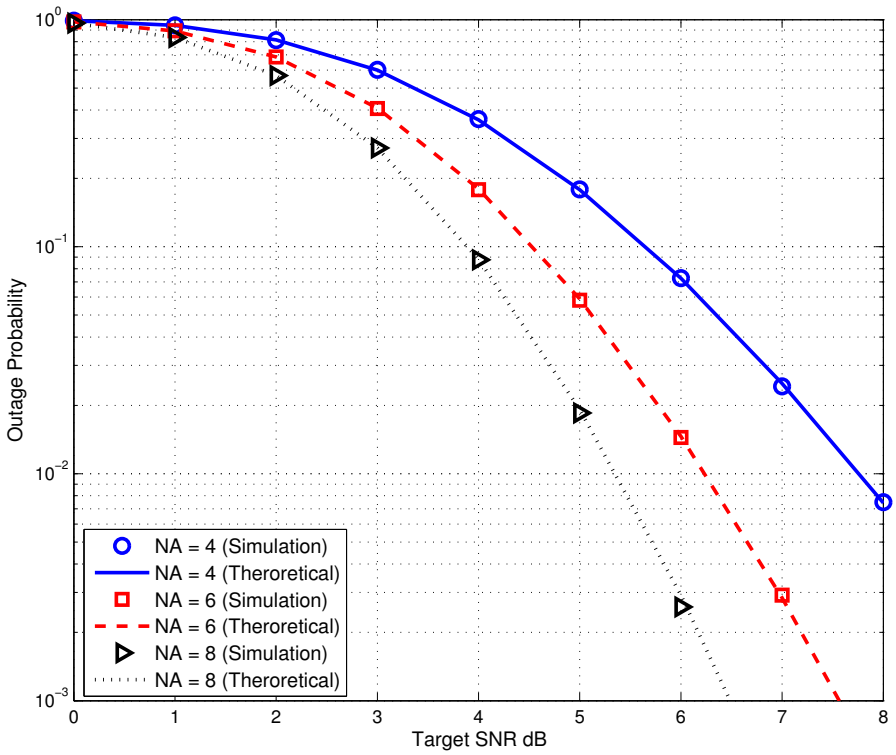

Figure 5.3. The outage probability for the maximum-sum antenna selection in the Golden Code system.

Fig. 5.3 shows the outage probability for the maximum-sum antenna scenario scheme. It is shown that, when the number of participating transmit antennas is increased from 6 to 8, the outage probability still decreases. The mathematical analysis results well match the simulation results. Comparing Fig. 5.2 and Fig. 5.3 clearly shows that the maximum-sum selection significantly outperforms maximum-minimum selection in the outage performance.

Fig. 5.4 shows the PEP performance for the maximum-sum antenna selection scheme. It is clearly shown that the derived Chernoff bound provides a fairly tight upper bound for the PEP performance at the high SNR

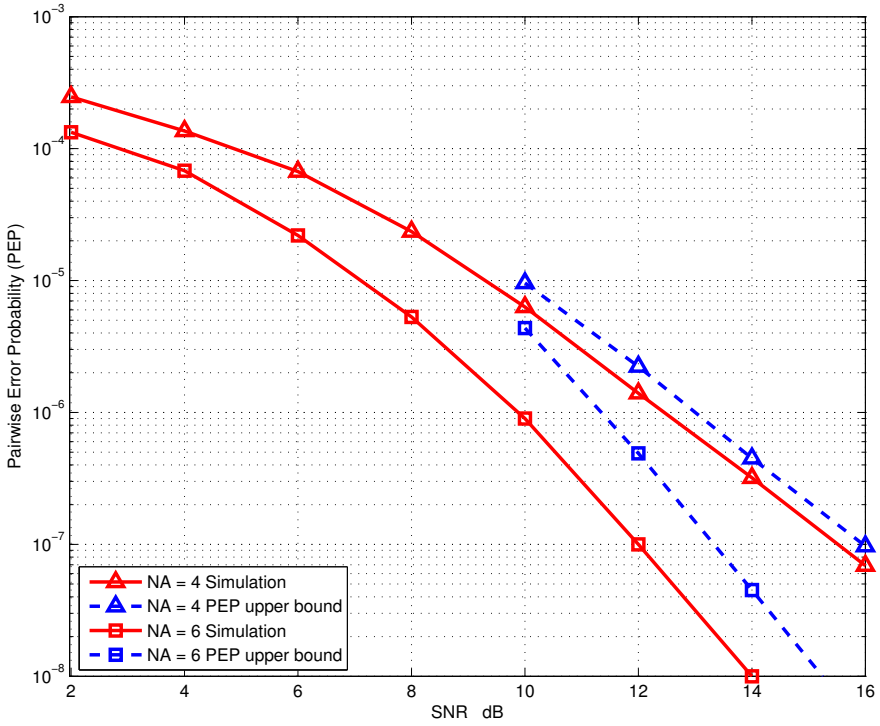

Figure 5.4. The PEP for the maximum-sum antenna selection in the Golden Code system.

ranges. Note, that as in [71], the bound is not shown for SNRs less than 10 dB, where the high SNR assumption does not hold. As is expected, with more available transmit antennas, the PEP performance becomes better and the diversity order is clearly increased.

5.6 Summary

The chapter examined the best two transmit antenna selection for the Golden Code in a MIMO system with instantaneous channel conditions by using maximum-minimum and maximum-sum selection. Mathematical derivation and analysis of the PDF and CDF of end-to-end SNR were performed for Rayleigh fading channels. The numerical results presented the outage probability, based on the different participating transmit antennas, and the outage

events of antenna selection for a MIMO system using maximum-sum selection which was shown to outperform the maximum-minimum selection. The PEP analysis was performed for maximum-sum transmit antenna selection within the Golden Code and the diversity order was obtained. The results confirmed that full diversity can be achieved by the full rank Golden Code. The next chapter analyses buffer-aided distributed multi-antenna selection for cooperative diversity system.

Chapter 6

BUFFER-AIDED DISTRIBUTED MULTI-ANTENNA SELECTION FOR COOPERATIVE NETWORKS

In MIMO systems, multiple-antenna selection has been proposed as a practical scheme for improving signal transmission quality as well as reducing realisation cost due to minimising the number of radio frequency chains. In this chapter, a relay station with fiber-connected distributed multi-antenna (DMA) selection is investigated for reception and transmission with buffers in cooperative decode-and-forward (DF) MIMO systems. The maximum-sum of signal-to-noise ratio (SNR) strategy is used to choose the best two antennas which respectively are receiving the signal from source to the relay station and transmitting from the relay station to the destination. This new scheme incorporates the instantaneous strength of the wireless links as well as the status of the finite buffer of a relay station and adapts the antenna selection decision on the strongest link. Based on the DMA selection, the

outage performance of the system is analysed by using a theoretical framework represented by a Markov Chain (MC). The construction of the state transition matrix and related steady state of the MC are studied. Simulations are also given to verify the analysis. The results show the proposed methods provide useful schemes for buffer-aided DMA selection in a cooperative diversity system.

6.1 Introduction

In Chapter 4, a major practical drawback of multiple-input and multiple-output (MIMO) wireless communication systems is considered, namely, the number of multiple radio frequency (RF) chains associated with multiple antennas which leads to increase in cost and hardware complexity. However, this can mitigated by antenna selection.

Antenna selection selects a subset of antennas to feed to the RF chains, the associated antenna selection rules are described in [3] and [77]. The selection algorithm is typically based on the largest SNR of the received signals. A fast reliable feedback link from the destination to relay station is assumed to exists. The bit error rate analysis for single transmit antenna selection and outage probability analysis for transmit antenna selection with a receiver maximal-ratio combining scheme over flat Rayleigh fading channels are given in [78]. In [79], the authors presented the diversity-multiplexing tradeoff for a multi-antenna relay network, but the multi-antennas appear in terminals for the construction of this system. In the system this chapter proposes, however, multi-antenna not only exist at terminals but also at relays. In [19], the authors proposed two joint relay-and-antenna selection schemes which combine opportunistic relaying and selection cooperation with a DF transmission policy. A new source transmit antenna selection (STAS) scheme which selects antennas among transmit antennas at the

source has been shown to achieve full diversity based on both channel state information and a transmission scheme for the MIMO DF relay networks in [80]. On the other hand, in 1987 in the context of indoor radio propagation measurements, a building was divided into one or more large cells, each served from a distributed antenna (DA) system which attains the dramatic reductions in multi-path delay spread and signal attenuation compared to a centralised system [81]. A novel distributed transmit antenna selection concept for dual-hop fixed-gain amplify-and-forward (AF) relaying systems was proposed and analysed in [82], where a multi-antenna source transmits information to a single-antenna destination by using a single-antenna half-duplex relay. In [83], cooperative network coding strategies for relay-aided two-source two-destination wireless networks with a backhaul connection between the source nodes was investigated. In practice the backhaul normally has much higher capacity and lower error rates than the forward wireless channels. Therefore, in the system in [83] the backhaul is assumed to be error free and of sufficiently high capacity (higher than the forward average capacity). Recently, the authors of [84] proposed a DA relay system in which DAs are connected to a central control unit (CCU) by radio-over-fibre (RoF) techniques. In this chapter, a DF policy is also adopted to implement transmission on two-hop DMA selection wireless networks which are fibre-connected.

Although antenna selection has various benefits, the performance is constrained by using the same selected antenna at the relay for receive and transmission. Instead by using buffers, the best channel always links the receive antenna and transmission antenna at the relays. In [85], the authors explored two buffering relay models: a fixed buffering relay model and a dynamic buffering relay model, and verified for arbitrary fading statistics, both models offered significant performance advantages. An opportunistic buffered DF protocol was proposed in [86] to exploit both relay buffering and

relay mobility to enhance the system throughput and the end-to-end packet delay under bursty arrivals. The authors of [87] employed max-max relay selection (MMRS) and best relay selection (BRS). They made the idealistic assumption that the buffer of the relay selected for reception (transmission) is not full (empty), which is only possible for buffers of infinite size. For a practical finite size of buffer, the relay selection has to depend on MMRS and BRS at the same time. In order to overcome this drawback, a max-link relay selection approach was proposed in [88] according to the instantaneous quality of the links and the status of the relays buffers. For analysis of outage probability in [88], the authors exploit a Markov Chain (MC) the theoretical framework incorporating a state transition matrix to model the buffer.

This chapter proposes a max-sum selection scheme for distributed multi-antenna selection for wireless relay networks with buffering. To avoid the limitation of the state of the buffer, the max-sum strategy is used twice independent for two-hop DF transmission policy. Selecting the multi-antenna from the DAs at the relay station while the multi-antenna at the terminals are fixed. A stationary distribution for the MC is adopted to obtain the theoretical framework for analysing the outage probability. Finally, the effect of buffer size is studied, and the outage probabilities under different buffer sizes, different target rates and different numbers of available participating antennas are analysed.

The remainder of this chapter is organised as follows. Section 6.2 introduces and proposes the system model and details the max-sum antenna selection method; Section 6.3 describes the outage probability analysis of the stationary distribution of the MC; Section 6.4 shows the simulation results which support the theoretical derivation, and Section 6.5 concludes this chapter.

6.2 System Model and Maximum-Sum DMA selection

6.2.1 System Model

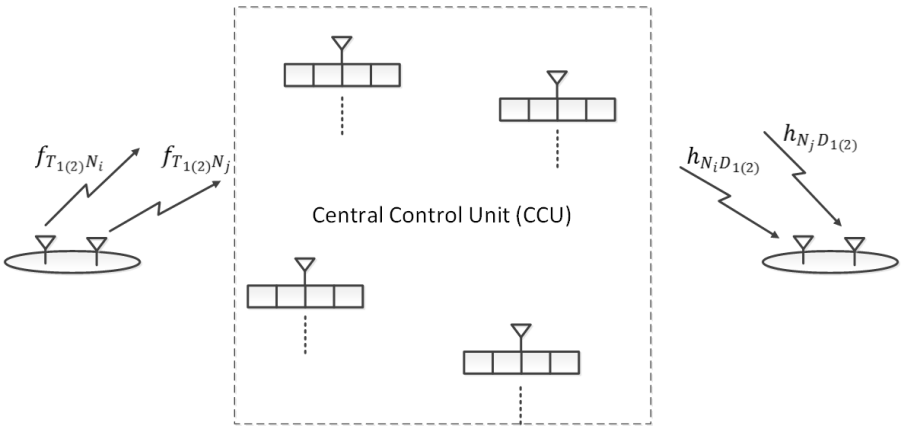

Figure 6.1. The system model of the distributed multi-antenna selection with buffers, i.e. the i-th and j-th antenna, are selected namely the best and the second best for reception and re-transmission. The fiber-connected DMAs use RoF to connect to the CCU.

The wireless relay network is composed of one source node with two antennas, one half-duplex DF relay station with N fixed distributed antennas and one destination node with two antennas. Each antenna in relay station is equipped with an independent buffer. N fixed distributed antennas form distributed multi-antennas, which connected to the CCU by the RoF technique. The transmission of the considered system model is organised in two time slots as shown in Fig. 6.1. In the first time slot, the best two antennas are selected from N by using the CCU for reception, which receives an Alamouti coded packet that is transmitted from the source node to DMAs. The selected received antennas decode them and then stored in their corresponding buffers. In the second time slot, the best two transmit antennas from the CCU are chosen to transmit a coded packet from the relay station to the destination. The distributed antennas are selected that provide the highest equivalent receive SNR. Assuming that a direct link between the source

and the destination does not exist or, if it does exist, it is not exploited for simplicity of implementation. Furthermore, the decoded Alamouti code in DMAs are reciprocal via the CCU, which offers a convenience method to encode at the CCU. The channel coefficients from source to relay are $f_{T_k N_{i(j)}}$ and from relay to destination are $h_{N_{i(j)} D_k}$, where $k = 1, 2$ represents the k-th antenna at the source and destination, $i, j = 1, 2, 3, \cdots, N$ represent the i-th antenna and j-th antenna at the relay. The channel coefficients $f_{T_k N_{i(j)}}$ and $h_{N_{i(j)} D_k}$ are mutually independent zero-mean complex Gaussian random variables (Rayleigh fading) with unit-variance, i.e. $f_{T_k N_{i(j)}} \sim \mathcal{CN}(0, 1)$ and $h_{N_{i(j)} D_k} \sim \mathcal{CN}(0, 1)$. The instantaneous SNR for channel $f_{T_k N_{i(j)}}$ is $\gamma_{T_k N_{i(j)}} = |f_{T_k N_{i(j)}}|^2 E_s / N_0$ and $\gamma_{N_{N_{i(j)} D_k}} = |h_{N_{i(j)} D_k}|^2 E_s / N_1$, where E_s is the average energy per symbol at the source and selected transmit antennas, respectively. N_0 and N_1 are respectively the noise variances of the additive white Gaussian noise (AWGN) at the selected receive antennas in the relay station and the destinations. For convenience, E_s is assumed unity and the noise variances are the same in all antennas of the relay and the destination.

Assuming that the CCU does not know the channel state information (CSI) but destination node has perfect CSI. The destination node informs the CCU to select antennas via an error-free feedback channel. It is worth noting that the antenna selected for reception is active during the first time slot and the DMA selected for transmission is active during the second time slot, whereas the remaining DAs are idle during both time slots.

6.2.2 Buffering Max-Sum Antenna Selection

One benefit of selecting two antennas with buffers is the signals can be stored and wait to be re-transmited until the corresponding channel links are sufficiently strong. For the DF transmission scheme, the sum of largest SNRs is obtained from two selected receive antennas at the CCU and the other largest SNRs is obtained from the received antenna at the destination.

Therefore, the best antenna selection for reception at the relay station, is selected based on

$$(r_i, r_j) = arg \max_{i\in 1,\cdots,N} \max_{j\in 1,\cdots,N, j\neq i} \{\gamma_{T_1 N_{i(j)}} + \gamma_{T_2 N_{i(j)}}\}, \tag{6.2.1}$$

where r_i and r_j are respectively the selected best two. The corresponding buffer stores the packet received from the source. The packet is decoded, and remains in the buffer until this antenna is selected again for transmission. If the buffer of the antenna, which is selected has no useful coded packet, no selected antenna send useful uncoded signal to the former, so that, the selected two antennas for re-transmission can cooperatively encode. Therefore, all packets in a queue wait for selection and re-transmission. The buffer operation status with a given signal sequence is shown as Table 6.1. For instance, the source node broadcasts an Alamouti code $\begin{bmatrix} -x_2^* x_1 \\ x_1^* \ x_2 \end{bmatrix}$ in first time slot T_1. The selected antennas receive, decode and store them in their own buffers. For preparing the second time transmission, the buffer status will behave as following: The buffers of A_1 and A_2 both store $00x_2x_1$,

Case1 and the re-transmit antennas nicely are the same A_1 and A_2. Therefore, the sequence x_2x_1 can successfully encode and forward to the destination.

Case2 and the antennas A_1 and A_3 are selected to re-transmit, while the Buffer3 of A_3 is empty. The central control unit picks up the sequence from the Buffer2 to Buffer3. Then, A_3 can cooperatively encode with A_1 and forward.

Case3 and the selected two re-transmit antennas A_3 and A_4 neither have sequences. The CCU will collect the corresponding information from A_1 and A_2 and give A_3 and A_4 so that the re-transmission can proceed successfully.

Time slots		T_1	T_2			
Selected antennas		r_i, r_j	t_i, t_j			
Buffer status		A_1A_2	A_1A_2	A_1A_3		A_3A_4
	Buffer1	$00x_2x_1$	$00x_2x_1$	$00x_2x_1$		0000
	Buffer2	$00x_2x_1$	$00x_2x_1$	0000	or	0000
	Buffer3	0000	0000	$00x_2x_1$		$00x_2x_1$
	Buffer4	0000	0000	0000		$00x_2x_1$

Table 6.1. Operation of the Max-Sum strategy for a given sequence with four distributed antennas $N = 4$.

If each buffer is half empty and half full, the above reciprocality still exist. This benefit can relax the limitation of buffer state that at least one buffer can be full and empty respectively for reception and empty. It is unlike the usage of buffers in [87] which not full and not empty all the time ensures that all buffers are available to use. For the re-transmission antenna at the relay,

$$(t_i, t_j) = arg \max_{i\in 1,\cdots,N} \max_{j\in 1,\cdots,N, j\neq i} \{\gamma_{N_{i(j)}D_1} + \gamma_{N_{i(j)}D_2}\}, \tag{6.2.2}$$

where t_i and t_j are the selected best two transmit antennas. During the second time slot, the selected antennas transmit the re-coded packet in the queue of its buffer, which received in a previous time slot.

On the other hand, sending a sufficient number of packets from the source to the CCU before the system starts can guarantee the operational status of all buffers. Given the buffer size in the system is finite the buffer state has two constraints

$$\begin{aligned} &\sum_{i(j)=1}^{N} b_{i(j)} = N_b \\ &0 \leq b_{i(j)} \leq L-1 \qquad (i, j \in \{1, \cdots, N\}, j \neq i), \end{aligned} \tag{6.2.3}$$

where N_b is the total number of full elements of all buffers. For example, this system uses three antennas $N = 3$ at the relay station and the buffer

size of each relay is $L = 4$. The best two antennas is $K = 2$. The state of the corresponding MC has to satisfy the constraints (6.2.3):

$$\begin{aligned} b_1 + b_2 + b_3 &= 6, \\ 0 \leq b_1 &\leq 4, \\ 0 \leq b_2 &\leq 4 \\ \text{and} & \\ 0 \leq b_3 &\leq 4. \end{aligned} \tag{6.2.4}$$

Moreover, when the available relays receive the latest signals, the temporary buffer state satisfies $b_1 + b_2 + b_3 = 8$.

6.3 Outage Performance Analysis Based Markov Chain Stationary Distribution

For the max-sum antenna selection of the DF scheme, the outage probability is defined as $P_{out}(C < R)$, where C denotes the channel capacity

$$C = \begin{cases} \frac{1}{2}\log_2(1+\gamma_{TN}) \\ \frac{1}{2}\log_2(1+\gamma_{ND}) \end{cases} \tag{6.3.1}$$

and R is the target rate. The end-to-end SNRs at the relays and destination are respectively γ_{TN} and γ_{ND}.

In order to show clearly the buffers operation process, for each time slot, the buffer status can be described as follows: the number of elements of one selected receive antenna buffer can be increased by one, when the source successfully transmits; the buffer status retrieves its current status or returns to its last status in the case of outage, either the outage event occurs in source or in the relay station; the number of elements of one selected transmit antenna buffer can be decreased by one, when the relays successfully

transmission. To analyze the max-sum antenna selection, the possible states of the buffers and the transitions between the states are modelled as an MC. The total number of buffer states of the MC is given by $S_t = 2\binom{N_b+2}{2} - 3(N_b - L) * (N_b - L + 1) - 4$. The optimal N_b is $\frac{N*L}{2}$. In the case of $N = 3$ and $L = 4$, the state MC topology is presented in Fig. 6.3. $S_u = \binom{N_b+2}{2} - \frac{3(N_b-L)*(N_b-L+1)}{2}$ is the buffer initial state and $T_v = S_u - 4$ is the buffer temporary transition state, $1 \leq u \leq S_u$ and $1 \leq v \leq T_v$.

The state transition matrix represents the MC of the states of the buffers and the connectivity between them. Setting matrix $\mathbf{S}$ is represented state transition. The size of $\mathbf{S}$ is $S_t \times S_t$. Each element in $\mathbf{S}$ is $\mathbf{S}_{m,n} = Pr(s_m \rightarrow s_n)$, which represents the transition probability to move from s_m at time t to state s_n at time $(t+1)$. The number of available participated receive and transmit antenna corresponding links is decided by the buffer status. Thereby, the transition probability has to change with different number of participating antennas which depend on buffer states.

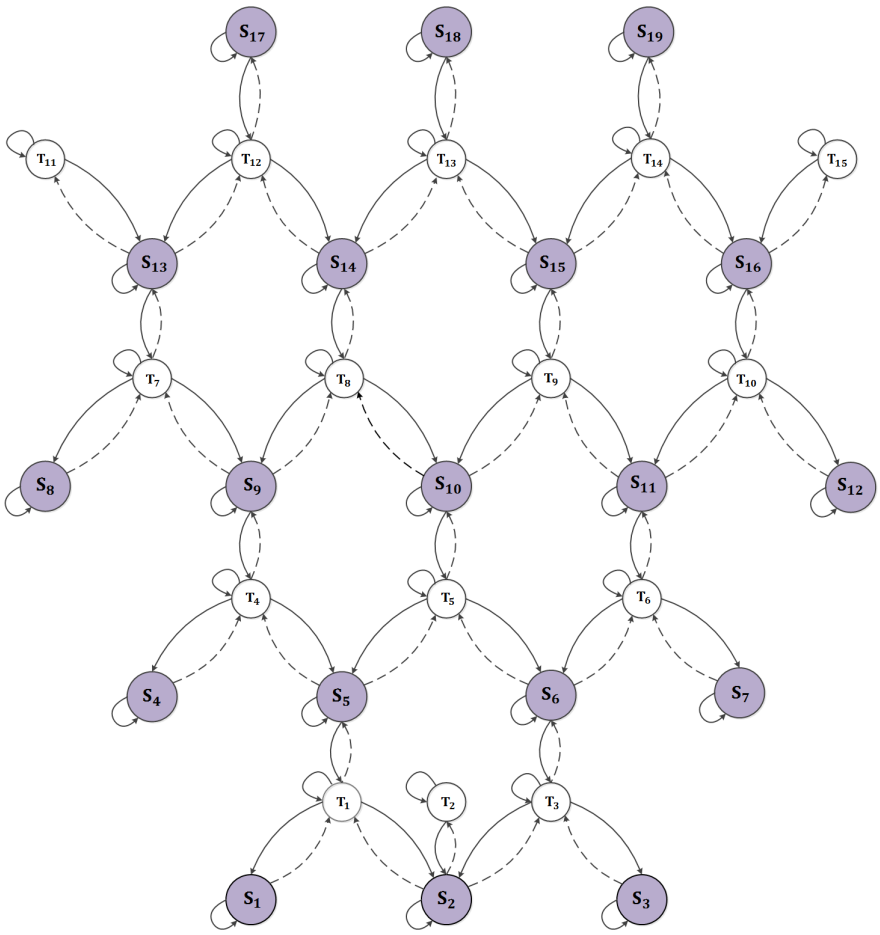

Figure 6.2. State diagram of MC representing the states of the buffers and the transitions between them for a case with L =4, N=3.

For symmetric links, firstly, from source to relay antennas the state m is considered. The PDF of the sums $\gamma_{TN} = \gamma_{T_1 N_{i(j)}} + \gamma_{T_2 N_{i(j)}}$ can be expressed as

$$f_{\gamma_\mu}(\gamma) = \frac{\gamma}{\overline{\gamma}_\mu^2} e^{-\frac{\gamma}{\overline{\gamma}_\mu}}, \tag{6.3.2}$$

where $\overline{\gamma}_\mu$ is the average mean SNR of $\gamma_{T_1 N_{i(j)}} + \gamma_{T_2 N_{i(j)}}$. Then the CDF of γ_μ is

$$F(\gamma) = 1 - \frac{\gamma}{\overline{\gamma}_\mu} e^{-\frac{\gamma}{\overline{\gamma}_\mu}} - e^{-\frac{\gamma}{\overline{\gamma}_\mu}} = 1 - e^{-\frac{\gamma}{\overline{\gamma}_\mu}} (1 + \frac{\gamma}{\overline{\gamma}_\mu}). \tag{6.3.3}$$

In this approach, the best two antennas are selected with the largest two SNRs among all K available transmitted antennas. According to [41], the joint distribution of the l largest values from K candidates can be obtained as

$$f(x_1, x_2, \cdots, x_l) = l! \begin{pmatrix} K \\ l \end{pmatrix} [F(x_l)]^{K-l} \prod_{i=1}^{l} f(x_i), \tag{6.3.4}$$

where $x_1 \geq x_2 \cdot \cdot \geq x_K$. Substituting $l = 2$ into (6.3.4) given the joint PDF of the two largest SNRs as

$$f((\gamma_i, \gamma_j) = K(K-1)F(\gamma_j)^{K-2} f(\gamma_i) f(\gamma_j), \tag{6.3.5}$$

Then the CDF of the final SNR can be obtained as (5.3.16).

Finally, using the same target SNR $\gamma_{th} = 2^{2R} - 1$, the exact outage probability of the max-sum selection scheme can be obtained and expressed as $P^m_{re_{out}} = F_{\gamma_e}(\gamma_{th})$. As shown the sample above, when the number of DMAs $N = 3$, the closed form of the exact outage probability can be obtained as

$$\begin{aligned} P^m_{re_{out}} &= \int_0^{\frac{r}{2}} \int_y^{r-y} \frac{N(N-1)xy}{\overline{\gamma}_\mu{}^4} \\ &\cdot \sum_{k=0}^{N-2} \left(\begin{pmatrix} N-2 \\ k \end{pmatrix} (-1)^k e^{-\frac{yk}{\overline{\gamma}_\mu}} \sum_{m=0}^{k} \begin{pmatrix} k \\ m \end{pmatrix} \left(\frac{y}{\overline{\gamma}_\mu} \right)^m \right) e^{-\frac{x+y}{\overline{\gamma}_\mu}} dxdy \\ &= -\frac{1}{2\overline{\gamma}_\mu{}^3} \left(e^{-1/2\frac{r}{\overline{\gamma}_\mu}} r^3 + 6r^2 \overline{\gamma}_\mu e^{-1/2\frac{r}{\overline{\gamma}_\mu}} - 64\overline{\gamma}_\mu{}^3 e^{-1/2\frac{r}{\overline{\gamma}_\mu}} - 2\overline{\gamma}_\mu{}^3 e^{\frac{r}{\overline{\gamma}_\mu}} \right. \\ &\left. + r^3 + 3r^2\overline{\gamma}_\mu - 30r\overline{\gamma}_\mu{}^2 + 66\overline{\gamma}_\mu{}^3 \right) e^{-\frac{r}{\overline{\gamma}_\mu}} \end{aligned} \tag{6.3.6}$$

Similarly, for any N and $\overline{\gamma}_\mu$, the outage can be obtained by using a numerical method [76]. Due to the symmetry of two-hop selection scheme, the outage probability $P^m_{tr_{out}}$ from relays to destinations also use the same expression as above. For i.i.d. symmetric channel links, the probability to select a specific

link is $\frac{1}{C_K^2}$. Therefore, the probability of changing buffer state (successfully receive and transmission) is equal to

$$P_{succ}^{m} = \frac{1}{C_{K_m}^2}(1 - P_{re(tr)out}^{m}). \tag{6.3.7}$$

A transition matrix contains

$$\mathbf{A} = \begin{cases} P_{re(tr)out}^{m} & \text{if } \ m = n; \\ P_{succ}^{m} & \text{if } \ m \neq n; \\ 0 & \text{no transition state.} \end{cases} \tag{6.3.8}$$

The state transition matrix **A** of the MC that describes the buffer states is a column stochastic matrix. Setting the stationary distribution $\pi_m, m > 0$, $\pi_n = \sum_{m=1}^{S_t} \mathbf{A}_{m,n}$. The sum of all possible state transition probabilities, for any column

$$\sum_{m=1}^{S_t} \mathbf{A}_{m,n} = 1. \tag{6.3.9}$$

The transition matrix **A** is not symmetric. The number of available participating receive and transmit antennas is not fixed and does not have a regular pattern. Therefore, the transition probability is column stochastic but not doubly stochastic. On the other hand, noting that **A** is also reversible [89], $\pi_m Pr(X_{(t+1)} = n \mid X_t = m) = \pi_n Pr(X_{(t+1)} = m \mid X_t = n)$ for all times t.

Since the MC considered is irreducible and aperiodic, then there exists a unique solution $\boldsymbol{\pi} = (\pi_1 \pi_2 \dots \pi_{(L+1)K})^T$ such that

$$\mathbf{A}\boldsymbol{\pi} = \boldsymbol{\pi}, \tag{6.3.10}$$

$$\sum_{i=1}^{(L+1)^k} \boldsymbol{\pi}_i = 1. \tag{6.3.11}$$

In this case, (6.3.11) is written as

$$\mathbf{B}\boldsymbol{\pi} = \mathbf{b}, \tag{6.3.12}$$

where $\mathbf{b} = (11\ldots1)^T$ and $\mathbf{B}_{i,j} = 1$. Then, through mathematical analysis, (6.3.10) and (6.3.12) become

$$\mathbf{A}\boldsymbol{\pi} - \boldsymbol{\pi} + \mathbf{B}\boldsymbol{\pi} = \mathbf{b}. \tag{6.3.13}$$

Meanwhile, letting $\mathbf{z}$ be a zero vector.

$$\mathbf{z}(\mathbf{A} - \mathbf{I} + \mathbf{B}) = \mathbf{0}. \tag{6.3.14}$$

It is sufficient to show that the inverse of $(\mathbf{A} - \mathbf{I} + \mathbf{B})$ exists. Equation (6.3.14) is multiplied by $\boldsymbol{\pi}$,

$$\mathbf{z}(\mathbf{A} - \mathbf{I} + \mathbf{B})\boldsymbol{\pi} = \mathbf{z}(\mathbf{A}\boldsymbol{\pi} - \mathbf{I}\boldsymbol{\pi} + \mathbf{B}\boldsymbol{\pi}) = \mathbf{z}\mathbf{b} = \mathbf{0}. \tag{6.3.15}$$

The stationary distribution $\boldsymbol{\pi}$ exists and has a unique solution

$$\boldsymbol{\pi} = (\mathbf{A} - \mathbf{I} + \mathbf{B})^{-1}b, \tag{6.3.16}$$

As known above, $\boldsymbol{\pi}$ is positive. $\mathbf{A}$ is a nonnegative and irreducible matrix. Due to no changes in the buffer status, outage occurs. Therefore, the outage probability of the system can be expressed as

$$P_{out} = \sum_{m=1}^{S_t} \boldsymbol{\pi}_m P^m_{re(tr)out} = diag(\mathbf{A})\boldsymbol{\pi} \tag{6.3.17}$$

The above expression shows that the construction of the state matrix A and the computation of the related steady state $\boldsymbol{\pi}$ consists of a simple theoretical framework for the computation of the outage probability for the max-sum antenna selection with finite buffers.

6.4 Simulation Results

In this section, in order to verify the proposed system model and the above mathematical expressions, the outage performance of the aided-buffer antenna selection scheme is simulated over a DF transmission scenario. The antenna selection is max-sum for both sides from source to relays and from relays to the destination. Different target rates, and the number of available antennas and different buffer size of the system are simulated and discussed.

Fig. 6.3 shows the outage probability with different target rate R = 1, 2, and 3 bits/sec/Hz for a simulation with and without buffers, and theoretical mathematical analysis by using available antenna N=3 and buffer size L=4. Obviously and generally, if without buffers, the outage performance is worse than using buffers independent of the target rate. The system can achieve the diversity order 4. The target rate R is increased from 1 to 3 bits/sec/Hz and the system capacity is unchanged, the outage probability significantly increases from 10^{-6} to 1 at 15 dB channel SNR. If to achieve the outage probability 10^{-4} is kept, the system SNR of the target rate 3 is in the high region while low target rate 1 in the low region.

Fig. 6.4 indicates the variation of the outage probability by different buffer size L=4, 10, 30 and 50, participating antenna N=3 and system target rate R=3. Setting half of elements of buffers are in initial state, e.g. $\frac{N*L}{2} = N_b$. Comparing clearly shows that the outage probability curve decreased to a limitation about L=50 with increasing the buffer size.

Fig. 6.5 shows the investigate the effect of different the number of participating antennas at relay N=3, 4 and 5 on the buffer size L=4 and target rate R=3. The same as the previous research simulation results without buffer aided, with increasing the number of available antennas, the outage probability of the aided-buffer antenna selection is also decreased. In Fig. 6.5, the total number of available antennas increased from 3 to 4, the channel

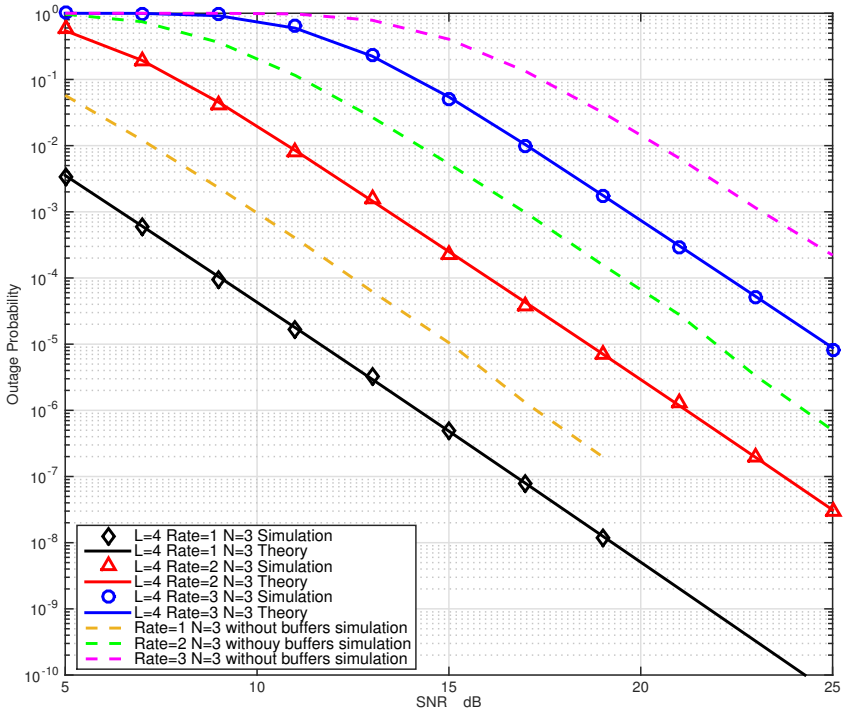

Figure 6.3. The outage probability for a simulation with and without buffers, and theory of target rate R=1, 2 and 3bits/sec/Hz.

SNR of the best two antenna selection is decreased from approximately 20 dB to 22.5 dB when the probability is 10^{-4}.

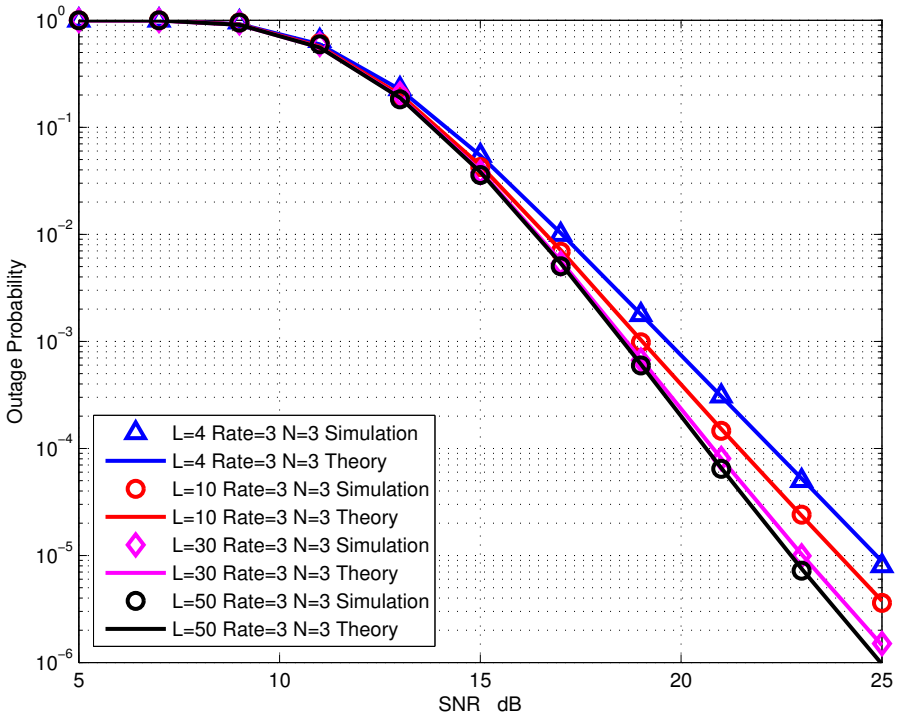

Figure 6.4. The outage probability for a simulation and theory of buffer size L=4, 10, 30 and 50.

6.5 Summary

In this chapter, fibre-connected distributed multi-antenna selection with finite buffers for cooperative wireless networks was realised. Max-sum antenna selection as the selection scenario was used for DF scheme over Rayleigh fading channels. The buffer states transition was described by the formed MC. The state stationary property of MC was used to analyse the outage probability performance of the system. Given participated number of antennas N, the performance can be derived in closed form. Numerical results were presented and verified the outage probability, based on different target rates, variation of buffer size and increasing the participating available antennas.

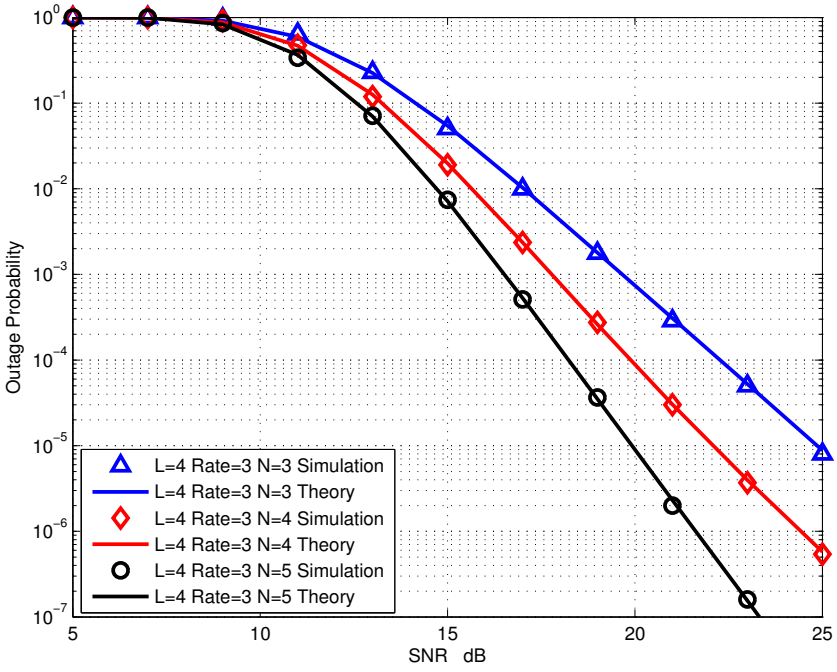

Figure 6.5. The outage probability for a simulation and theory of participating available antennas N=3, 4 and 5.

Chapter 7

CONCLUSIONS AND FUTURE WORK

The contributions of this thesis are summarised below and discussion on possible future work is also included.

7.1 Conclusions

Considering the chapters in detail:
In Chapter 2, a brief overview of space-time coding, including the Alamouti code and the Golden Code for use in a conventional MIMO system and MIMO-OFDM was presented. OFDM offers the advantage of lower implementation complexity in systems with a large bandwidth-delay spread product. To overcome the correlated path drawback of traditional MIMO, distributed MIMO with distributed space-time coding was introduced. Using all the relays was shown to have the disadvantage that it may not obtain the optimal performance in the relay network, and present practical problems such as asynchronism between the relays. Due to the high implementation cost of a multi-antenna system, antenna selection was described.

In Chapter 3, a simple offset transmission with FIC and OFDM scheme for a four path asynchronous cooperative relay system was proposed. In order to achieve asymptotically full data rate the source and one group of relays transmits on even transmission steps, whilst on odd transmission

steps, a different group of relays transmits and the first group receivers. The approach achieves the same diversity of 2 as a previously proposed half rate scheme. OFDM and CP were used at the source to combat timing errors from the source to the destination node. Moreover, through the use of time reversal in the destination node, CP removal is avoided at the relays in order to decrease the complexity of relay decoding. In order to mitigate the potential reduction in diversity gain due to dependent channel matrix elements in distributed Golden Code transmission, and the rate penalty of multihop transmission, relay selection based on two-way transmission is proposed. Simulation studies were used to evaluate the relative end-to-end BER performance of uncoded, coded, one-way and two-way networks with fixed and selected relays. The maximum-mean relay selection policy was shown to outperform the maximum-minimum approach by 1 to 1.5 dB SNR with given BER.

In Chapter 4, distributed transmission using the Golden Code in wireless relay networks, and a new multiple relay selection strategy, were proposed. Through end-to-end BER simulations, the maximum of the channel parameter means selection was shown to achieve the best performance. The improvement was because this approach performs an overall channel strength tradeoff at every relay node to select the best two relays. Therefore, this new maximum-mean policy appears valuable for cooperative diversity systems based on the Golden Code. The Golden Code was also implemented in an asynchronous wireless relay network over frequency flat and selective channels, and a simple approach to overcome asynchronism was proposed. As in synchronous wireless relay networks, the maximum of the channel parameter means selection was shown to still have the advantage of 0.5 -1 dB SNR when given BER for the relay selection through BER simulations with computationally efficient SD in flat fading channel environment. The improvement was because this approach performs an overall channel strength

tradeoff at every relay node to select the best two relays. In the frequency selective channel case, however, the advantage of the maximum-mean selection was lost.

Chapter 5 examined the best two transmit antenna selection for the Golden Code in a MIMO system with instantaneous channel conditions by using maximum-minimum and maximum-sum selection. Mathematical derivation and analysis of the PDF and CDF of end-to-end SNR were performed for Rayleigh fading channels. The numerical results presented the outage probability, based on the different participating transmit antennas, and the outage events of antenna selection for a MIMO system using maximum-sum selection which was shown to outperform the maximum-minimum selection. If the measurement of outage probability is 10^{-1} for 6 participating antennas, simulation results have shown that maximum-sum selection is better than maximum-minimum by 1 dB in terms of target SNR. The other superiority is that the maximum-sum selection be able to achieve accurate outage probability while maximum-minimum selection just determined the upper bound of outage probability. The PEP analysis was performed for maximum-sum transmit antenna selection within the Golden Code and the diversity order was obtained. The results confirmed that full diversity can be achieved by the full rank Golden Code.

In Chapter 6, fibre-connected distributed multi-antenna selection with finite buffers for cooperative wireless networks was realised. Max-sum antenna selection was used within a DF scheme over Rayleigh fading channels. The buffer states were described by a Markov Chain. The stationary state property of which was used to analyse the outage probability performance of the system. Given participating number of antennas N, the performance can be derived in closed form. Numerical results were presented and verified the outage probability, based on different target rates, variation of buffer size and increasing the number of participating antennas. The target rate R was

increased from 1 to 3 bits/sec/Hz and the system capacity was unchanged, the outage probability significantly increases from 10^{-6} to 1 at 15 dB channel SNR for 3 participating antennas and buffer size $L = 4$. When changing the buffer size, the outage probability curve decreased to a limitation about $L = 50$ with increasing the buffer size. For the effect of different the number of participating antennas at relay, the total number of available antennas increased from 3 to 4, the channel SNR of the best two antenna selection is decreased from approximately 20 dB to 22.5 dB when the probability is 10^{-4}.

7.2 Future Work

There are several directions in which the research presented in this thesis could be extended.

The solutions presented in this thesis were for Rayleigh channels but a wider class of fading channel conditions, modelled by for example the Nakagami-m distribution could be considered. In Chapter 5, the closed form of outage probability for multi-antenna selection still can not be obtained. In future work, mutual information could play an important roll in performance analysis.

The system performance measurement could extent to other sides, such as system throughput. In future, BLAST and space-time trellis codes could be used in the systems of this thesis. To compare the Golden Code, BLAST is the simplest transmitted code. The concept of space-time trellis code was first introduced by [7]. It became extremely popular because space-time trellis codes can simultaneously offer coding gain with spectral efficiency and full diversity over fading channels.

Recently, multi-antenna selection is implemented to enhance security with reduced hardware complexity [90] and [91]. On the other hand, the

idea of multi-antenna selection of a multi-source and multi-destination system could be considered, which may have application in 5G systems. The outstanding characteristic of 5G is the high peak transmit rate which should achieve 10Gbps (4G:100Mbps). The end-to-end time delay will also be decreased 5-10 times. Larger MIMO systems will play an important roll. Before 5G, the antenna array was two dimensional while three dimensional MIMO technique will be researched. This will decrease the interference so that the performance of wireless signal coverage will be improved. Therefore, decreasing the cost reduction of antenna hardwares will be more and more attractive for researchers.

References

[1] J. Mietzner, R. Schober, L. Lampe, W. H. Gerstacker, and P. A. Hoeher, "Multiple-antenna techniques for wireless communications - a comprehensive literature survey," *IEEE Commun. Surveys Tuts.*, vol. 11, no. 2, pp. 87 – 105, Jun. 2009.

[2] S. M. Alamouti, "A simple transmit diversity technique for wireless communications," *IEEE J. Sel. Areas Commun.*, vol. 16, no. 8, pp. 1451 – 1458, Oct. 1998.

[3] S. Sanayei and A. Nosratinia, "Antenna selection in MIMO systems," *IEEE Commun. Mag.*, vol. 42, no. 10, pp. 68–73, Oct. 2004.

[4] A. Nosratinia, T. E. Hunter, and A. Hedayat, "Cooperative communication in wireless networks," *IEEE Commun. Mag.*, vol. 42, no. 10, pp. 74–80, Oct. 2004.

[5] Y. Jing and H. Jafarkhani, "Using orthogonal and quasi-orthogonal designs in wireless relay networks," *IEEE Trans. Inf. Theory*, vol. 53, no. 11, pp. 4106 – 4118, Nov. 2007.

[6] A. F. Molisch, M. Z. Win, Y.-S. Choi, and J. H. Winters, "Capacity of MIMO systems with antenna selection," *IEEE Trans. Wireless Commun.*, vol. 4, no. 4, pp. 1759 – 1772, Jul. 2005.

[7] N. S. V. Tarokh and A. R. Calderbank, "Space-time codes for high data

rate wireless communication: Performance criterion and code construction," *IEEE Trans. Inf. Theory.*, vol. 44, no. 2, pp. 744–765, Mar. 1998.

[8] P. W. Wolniansky, G. J. Foschini, G. Golden, and R. Valenzuela, "V-BLAST: An architecture for realizing very high data rates over the rich-scattering wireless channel," *Signals, Systems, and Electronics, 1998 URSI International Symposium on*, pp. 295–300, Sep.-Oct. 1998.

[9] B. Sergio, *Multiantenna wireless communication systems.* Artech house, inc, 2005.

[10] M. Dohler and Y. H. Li, *Cooperative Communications Hardware, Channel* PHY. Wiley, New York, 2010.

[11] J. N. Laneman and G. W. Wornell, "Distributed space-time-coded protocols for exploiting cooperative diversity in wiesless networks," *IEEE Trans. Inf. Theory.*, vol. 49, no. 10, pp. 2415 – 2425, Oct. 2003.

[12] D. Tse and P. Viswanath, *Fundamentals of Wireless Communication.* Cambridge University Press, 2005.

[13] L. Zheng and D. N. C. Tse, "Diversity and multiplexing: A fundamental tradeoff in multiple antenna channels," *IEEE Trans. Inf. Theory*, vol. 49, no. 5, pp. 1073–1096, May, 2003.

[14] J. G. Proakis, *Digital Communication.* 3rd edition. McGraw-Hill, 1995.

[15] H. Yao and G. W. Wornell, "Achieving the full MIMO diversity-multiplexing frontier with rotation-based space-time codes," *in Proc. Allerton Conf. Communication, Control, and Computing*, Monticello, Oct. 2003.

[16] K. Azarian, H. E. Gamal, and P. Schniter, "On the achievable diversity multiplexing tradeoff in half-duplex cooperative channel," *IEEE Trans. Inf. Theory*, vol. 51, no. 12, pp. 4152–4172, Dec. 2005.

[17] R. W. Heath and A. Paulraj, "Antenna selection for spatial multiplexing systems based on minimum error rate," *Proc. ICC*, vol. 7, pp. 2276 – 2280, Jun. 2001.

[18] A. F. Coskun and O. Kucur, "Performance analysis of joint single transmit and receive antenna selection in Nakagami-m fading channels," *IEEE Commun. Lett.*, vol. 15, no. 2, pp. 211–213, Feb. 2011.

[19] J. MinChul, S. Hyoung-Kyu, and K. Il-Min, "Joint relay-and-antenna selection in multi-antenna relay networks," *IEEE Trans. Commun.*, vol. 58, no. 12, pp. 3417 – 3422, Dec. 2010.

[20] Y. Jing and H. Jafarkhani, "Single and multiple relay selection schemes and their achievable diversity orders," *IEEE Trans. Wireless Commun.*, vol. 8, no. 3, pp. 1414–1423, Mar. 2009.

[21] M. Uysal, "Cooperative communications for improved wireless network transmission: Framework for virtual antenna array applications," *IGI Global Snippet*, 2010.

[22] D. Gesbert, M. Shafi, D. shan Shiu, P. J. Smith, and A. Naguib, "From theory to practice: An overview of MIMO space-time coded wireless systems," *IEEE J. Sel. Areas Commun.*, vol. 21, no. 3, pp. 281–302, 2003.

[23] J.-C. Belfiore, G. Rekaya, and E. Viterbo, "The Golden Code: A 2×2 full-rate space-time code with nonvanishing determinants," *IEEE Trans. Inf. Theory*, vol. 51, pp. 1432–1436, Apr. 2005.

[24] A. Bannour, M. Ammari, and R. Bouallegue, "Adaptation of Golden Codes with a correlated Rayleigh frequency-selective channel in OFDM system with imperfect channel estimation," *in Wireless Communication Systems (ISWCS), 2010 7th International Symposium on*, pp. 159 – 163, Sept. 2010.

[25] O. Damen, A. Chkeif, and J.-C. Belfiore, "Lattice code decoder for space-time codes," *IEEE Commun. Lett.*, vol. 4, no. 5, pp. 161 – 163, May, 2000.

[26] Y. S. Cho, J. Kim, W. Y. Yang, and C. G. Kang, MIMO-OFDM *wireless communications with* M*atlab*. Wiley, 2010.

[27] H. Rohling, T. May, K. Bruninghaus, and R. Grunheid, "Broadband OFDM radio trasmission for multimedia applications," *Proc. IEEE*, vol. 87, no. 10, pp. 1778 – 1789, Oct. 1999.

[28] H. Bolcskei, D. Gesbert, C. B. Papadias, and A. V. D. Veen, *Space-time wireless systems − from array processing to* MIMO *communications*. Cambridge University Press., 2006.

[29] D. A. GORE and A. J. Paulraj, "MIMO antenna subset selection with space-time coding," *IEEE Trans. Signal Process.*, vol. 50, no. 10, pp. 2580 – 2588, Oct. 2002.

[30] G. Tsoulos, MIMO *System Technology for Wireless Communication*. CRC Press, Inc., 2006.

[31] G. Zhang, W. Zhan, and J. Qin, "Transmit antenna selection in the Alamouti-coded MIMO relay systems," *Wireless Pers. Commun.*, vol. 64, no. 4, pp. 879–891, Feb. 2012.

[32] Z. Zhendong, V. Branka, D. Mischa, and L. Yonghui, "MIMO systems with adaptive modulation," *IEEE Trans. Veh. Technol.*, vol. 54, no. 5, pp. 1828–1842, Sep. 2005.

[33] N. Yang, P. L. Yeoh, M. Elkashlan, R. Schober, and I. B. Collings, "Transmit antenna selection for security enhancement in MIMO wiretap channels," *IEEE Trans. Commun.*, vol. 61, no. 1, pp. 144–154, Jan. 2013.

[34] H. Frank and D. Marcos, *Cooperation in wireless networks:* P*rinciples and applications*. Springer, 2006.

[35] W. Shuangqing, D. L. Goeckel, and M. C. Valenti, "Asynchronous cooperative diversity," *IEEE Trans. Wireless Commun.*, vol. 5, no. 6, pp. 1547–1557, Jun. 2006.

[36] L. Zheng and X. Xiang-Gen, "A simple Alamouti space-time transmission scheme for asynchonous cooperative system," *IEEE Signal Process. Lett.*, vol. 14, no. 11, pp. 804 – 807, Nov. 2007.

[37] L. Xiaohua, "Space-time coded multi-transmission among distributed transmitters without perfect synchronization," *IEEE Signal Process. Lett.*, vol. 11, no. 12, pp. 948–951, Dec. 2004.

[38] Z. Xi, W. Jiangzhou, and Q. Yi, "Advances in cooperative wireless networking: Part i [Guest Editorial]," *IEEE Commun. Mag.*, vol. 49, no. 5, pp. 54–55, May. 2011.

[39] M. Shichuan, Y. Yaoqing, and S. Hamid, "Distributed MIMO technologies in cooperative wireless networks," *IEEE Commun. Mag.*, vol. 49, no. 5, pp. 78–82, May. 2011.

[40] L. Yonghui, "Distributed coding for cooperative wireless networks: An overview and recent advances," *IEEE Commun. Mag.*, vol. 47, no. 8, pp. 71–77, Aug. 2009.

[41] N. Balakrishnan and A. C. Cohen, *Order statistics and inference: estimation methods.* London : Academic Press, 1991.

[42] Y. Jing and B. Hassibi, "Distributed space-time coding in wireless relay networks," *IEEE Trans. Wireless. Commun.*, vol. 5, no. 12, pp. 3524–3536, Dec. 2006.

[43] A. Goldsmith, *Wireless Communications.* Cambridge University Press, 2005.

[44] M. Chiani, D. Dardari, and M. K. Simon, "New exponential bounds and approximations for the computation of error probability in fading channels," *IEEE Trans. Wireless Commun.*, vol. 2, no. 4, pp. 840–845, Jul. 2003.

[45] S.-H. Chang, P. C. Cosman, and L. B. Milstein, "Chernoff-type bounds for the Gaussian error function," *IEEE Trans. Commun.*, vol. 59, no. 11, pp. 2939–2944, Nov. 2011.

[46] M. K. Simon and M.-S. Alouini, "Exponential-type bounds on the generalized marcum Q-function with application to error probability analysis over fading channels," *IEEE Trans. Commun.*, vol. 48, no. 2, pp. 359–366, Mar. 2000.

[47] J. N. Laneman, D. N. C. Tse, and G. W. Wornell, "Cooperative diversity in wireless networks: Efficient protocol and outage behavior," *IEEE Trans. Inf. Theory*, vol. 50, no. 12, pp. 3062–3080, Dec. 2004.

[48] Y. Li and X. G. Xia, "Full diversity distributed space-time trellis codes for asynchronous cooperative communications," *Proc. IEEE Int. Symp. Information Theory (ISIT), Adelaide, Australia*, pp. 911 – 915, Sep. 2005.

[49] C. E. Shannon, "Two-way communication channels," *in Proc. 4th Berkeley Symp. Math. Stat. Prob.*, vol. 1, pp. 611–644, 1961.

[50] T. Cui, F. Gao, T. Ho, and A. Nallanathan, "Distributed space-time coding for two-way wireless relay networks," *IEEE Trans. Signal Process.*, vol. 57, no. 2, pp. 658–671, Feb. 2009.

[51] B. D. V. Veen and K. M. Buckley, "Beamforming: a versatile approach to spatial filtering," *IEEE ASSP Magazine*, vol. 5, no. 2, pp. 5–24, April. 1988.

[52] Z. Li, X. G. Xia, and B. Li, "Achieving full diversity and fast ML decoding via simple analog network coding for asynchronous two-way relay

networks," *IEEE Trans. Commun.*, vol. 57, no. 12, pp. 3672–3681, Dec. 2009.

[53] C. Luo, Y. Gong, and F. Zheng, "Full interference cancellation for two-path cooperative communications," *Proc. IEEE WCNC.*, 2009.

[54] E. Viterbo and Y. Hong, "Applications of the Golden Code," *in Proc. of Information Theory and Applications Workshop*, pp. 393 – 400, Jan-Feb, 2007.

[55] L. Ge, G. J. Chen, and J. A. Chambers, "Relay selection in distributed transmission based on the Golden Code in wireless networks," *2011 5th International Conference on Next Generation Mobile Applications, Services and Technologies (NGMAST)*, vol. 14, pp. 196–199, Sep.2011.

[56] A. Bletsas, A. Khisti, D. P. Reed, and A. Lippman, "A simple cooperative diversity method based on network path selection," *IEEE J. Sel. Areas Commun.*, vol. 24, no. 3, pp. 659–672, Mar. 2006.

[57] H. Jafarkhani, *Space-Time Coding – Theory and Practice.* Cambridge University Press, 2005.

[58] W.-J. Choi, R. Negi, and J. M. Cioffi, "Combined ML and DFE decoding for the V-BLAST system," *Proc. ICC*, vol. 3, pp. 1243 – 1248, 2000.

[59] V. Tarokh, H. Jafarkhani, and A. R. Calderbank, "Space-time block codes from orthogonal designs," *IEEE Trans. Inf. Theory*, vol. 45, no. 5, pp. 1456–1467, Jul. 1999.

[60] P. Michael, "On the computation of lattice vectors of minimal length, successive minima and reduced bases with applications," *SIGSAM Bull.*, vol. 15, no. 1, pp. 37–44, Feb. 1981.

[61] N. Wu and H. Gharavi, "Asynchronous cooperative mimo systems using

a linear dispersion structure," *IEEE Trans. Veh. Technol.*, vol. 59, no. 2, pp. 779 – 787, Feb. 2010.

[62] M. Sarkiss, M. O. Damen, and J.-C. Belfiore, "2 × 2 delay-tolerant distributed space-time codes with non-vanishing determinants," *in Proc. IEEE Personal, Indoor and Mobile Radio Communications*, pp. 1–5, Sept. 2008.

[63] M. Nahas, A. Saadani, and G. R.-B. Othman, "Bounded delay-tolerant space time block codes for asynchronous cooperative networks," *IEEE Trans. Wireless Commun.*, vol. 10, no. 10, pp. 3288 – 3297, Oct. 2011.

[64] M. El-Khamy, H. Vikalo, B. Hassibi, and R. J. McEliece, "Performance of sphere decoding of block codes," *IEEE Trans. Commun.*, vol. 57, no. 10, pp. 2940 – 2950, Oct. 2009.

[65] E. Viterbo and J. Boutros, "A universal lattice code decoder for fading channel," *IEEE Trans. Inf. Theory*, vol. 45, no. 5, pp. 1639 – 1642, Jul 1999.

[66] M. O. Damen, H. E. Gamal, and G. Caire, "On maximum-likelihood detection and the search for the closest lattice point," *IEEE Trans. Inf. Theory*, vol. 49, no. 10, pp. 2389 – 2402, Oct. 2003.

[67] L. Zhang, B. Li, T. Yuan, X. Zhang, and D. Yang, "Golden Code with low complexity sphere decoder," pp. 1 – 5, Athen, Sept. 2007.

[68] P. Elias, "Error free coding," *IRE Trans. on Inf. Theory*, vol. PFIT-4, no. 4, 1954.

[69] S. Sanayei and A. Nosratinia, "Asymptotic capacity gain of transmit antenna selection," in *Proc. WNCG Symposium*, Oct. 2003.

[70] A. Ghrayeb and T. M. Duman, "Performance analysis of MIMO systems with antenna selection over quasi-static fading channels," *IEEE Trans. Veh. Technol.*, vol. 52, no. 2, pp. 281–288, Mar. 2003.

[71] I. Bahceci, T. M. Duman, and Y. Altunbasak, "Antenna selection for multiple-antenna transmission systems: Performance analysis and antenna selection for multiple-antenna transmission systems: Performance analysis and code construction," *IEEE Trans. Inf. Theory*, vol. 49, no. 10, pp. 2669–2681, Oct. 2003.

[72] C.-Y. Chen, A. Sezgin, J. M. Cioffi, and A. Paulraj, "Antenna selection in space-time block coded systems: Performance analysis and low-complexity algorithm," *IEEE Trans. Signal Process.*, vol. 56, no. 7, pp. 3303 – 3314, Jul. 2008.

[73] C.-C. Hung, C.-T. Chiang, N.-Y. Yen, and R.-C. Wu, "Outage probability of multiuser transmit antenna selection/maximal-ratio combining systems over arbitrary Nakagami-m fading channels," *IET Commun.*, vol. 4, no. 1, pp. 63–68, Jan. 2010.

[74] G. Amarasuriya, C. Tellambura, and M. Ardakani, "Two-way amplify-and-forward multiple-input multiple-output relay networks with antenna selection," *IEEE J. Sel. Areas Commun.*, vol. 30, no. 8, pp. 1513 – 1529, Sep. 2012.

[75] P. L. Yeoh, M. Elkashlan, N. Yang, D. B. da Costa, and T. Q. Duong, "Unified analysis of transmit antenna selection in MIMO multirelay networks," *IEEE Trans. Veh. Technol.*, vol. 62, no. 2, pp. 933–939, Feb. 2013.

[76] A. Gilat and V. Subramaniam, *Numerical methods for engineers and scientists:* A*n introduction with applications using* M*atlab.* John Wiley Sons Ltd, 2011.

[77] A. F. Molisch and M. Win, "MIMO systems with antenna selection," *IEEE Microwave Mag.*, vol. 5, no. 1, pp. 46–56, Mar. 2004.

[78] C. Zhuo, Y. Jinhong, and B. Vucetic, "Analysis of transmit antenna

selection/maximal-ratio combining in Rayleigh fading channels," *IEEE Trans. Veh. Technol.*, vol. 54, no. 4, pp. 1312–1321, Jul. 2005.

[79] M. Yuksel and E. Erkip, "Multiple-antenna cooperative wireless systems: a diversity-multiplexing tradeoff perspective," *IEEE Trans. Inf. Theory*, vol. 53, no. 10, pp. 3371–3393, Oct. 2007.

[80] J. Xianglan, N. Jong-Seon, and S. Dong-Joon, "Source transmit antenna selection for mimo decode-and-forward relay networks," *IEEE Trans. Siganl Process.*, vol. 61, no. 7, pp. 1657–1662, Apr. 2013.

[81] A. A. M. Saleh, A. J. Rustako, and R. Roman, "Distributed antennas for indoor radio communications," *IEEE Trans. Commun.*, vol. 35, no. 12, pp. 1245 – 1251, Dec. 1987.

[82] H. Ding, J. Ge, D. B. da Costa, and T. Tsiftsis, "A novel distributed antenna selection scheme for fixed-gain amplify-and-forward relaying systems," *IEEE Trans. Veh. Technol.*, vol. 61, no. 6, pp. 2836–2842, Jul. 2012.

[83] J. Du, M. Xiao, and M. Skoglund, "Cooperative network coding strategies for wireless relay networks with backhaul," *IEEE Trans. Commun.*, vol. 59, no. 9, Sep. 2011.

[84] H. Jin and V. C. M. Leung, "Performance analysis of full-duplex relaying employing fiber-connected distributed antennas," *IEEE Trans. Veh. Technol.*, vol. 63, no. 1, pp. 146–160, Jan. 2014.

[85] B. Xia, Y. Fan, J. Thompson, and H. V. Poor, "Buffering in a three-node relay network," *IEEE Trans. Wireless Commun.*, vol. 7, no. 11, pp. 4492–4496, Nov. 2008.

[86] W. Rui, V. K. N. Lau, and H. Huang, "Opportunistic buffered decode-wait-and-forward (OBDWF) protocol for mobile wireless relay networks," *IEEE Trans. Wireless Commun.*, vol. 10, no. 4, pp. 1224–1231, Apr. 2011.

[87] A. Ikhlef, D. S. Michalopoulos, and R. Schober, "Max-max relay selection for relays with buffers," *IEEE Trans. Wireless Commun.*, vol. 11, no. 3, pp. 1124–1135, Mar. 2012.

[88] I. Krikidis, T. Charalambous, and J. S. Thompson, "Buffer-aided relay selection for cooperative diversity systems without delay constraints," *IEEE Trans. Wireless Commun.*, vol. 11, no. 5, pp. 1957–1967, May. 2012.

[89] J. R. Norris, *Markov Chains.* Cambridge University Press., 1998.

[90] H. Alves, R. D. Souza, and M. Debbah, "Enhanced physical layer security through transmit antenna selection," *in Proc. 2011 IEEE GlobeCOM Workshops*, pp. 879–883, Dec. 2011.

[91] H. Alves, R. D. Souza, M. Debbah, and M. Bennis, "Performance of transmit antenna selection physical layer security schemes," *IEEE Signal Process. Lett.*, vol. 19, no. 6, pp. 372–375, Jun. 2012.